BioMed Research International

Hypoglycaemic Proteins and Peptides from Plants to Treat Diabetes Mellitus

Guest Editors: Ghulam Mustafa, Sibtain Ahmed, and Muhammad Irfan

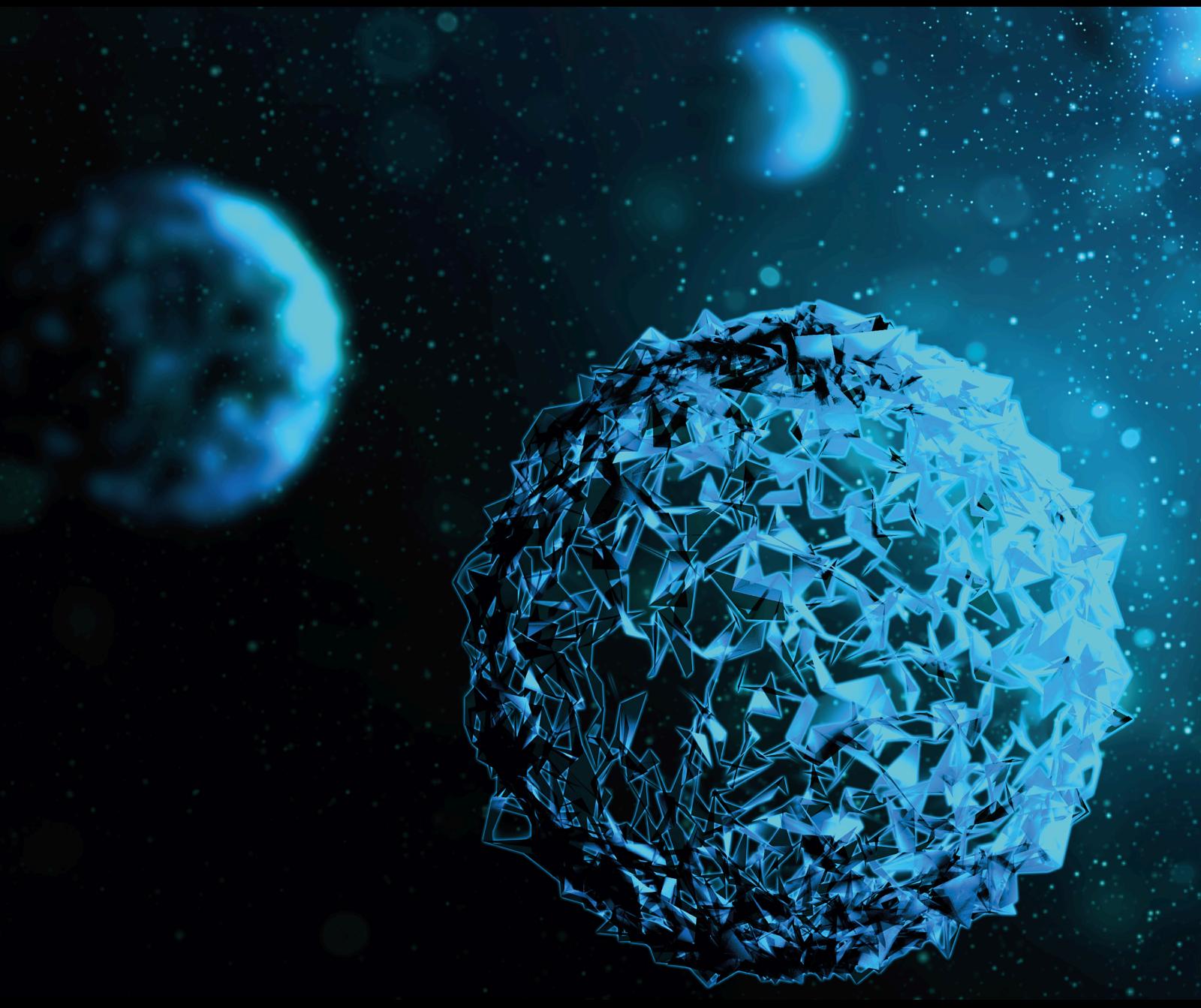

Hypoglycaemic Proteins and Peptides from Plants to Treat Diabetes Mellitus

BioMed Research International

Hypoglycaemic Proteins and Peptides from Plants to Treat Diabetes Mellitus

Guest Editors: Ghulam Mustafa, Sibtain Ahmed, and Muhammad Irfan

Section Editors

Penny A. Asbell, USA
David Bernardo, Spain
Gerald Brandacher, USA
Kim Bridle, Australia
Laura Chronopoulou, Italy
Gerald A. Colvin, USA
Aaron S. Dumont, USA
Pierfrancesco Franco, Italy
Raj P. Kandpal, USA
Fabrizio Montecucco, Italy
Mangesh S. Pednekar, India
Letterio S. Politi, USA
Jinsong Ren, China
William B. Rodgers, USA
Harry W. Schroeder, USA
Andrea Scribante, Italy
Germán Vicente-Rodriguez, Spain
Momiao Xiong, USA
Hui Zhang, China

Academic Editors

Biochemistry

Contents

Investigation of Hypoglycemic Peptides Derived from Conserved Regions of adMc1 to Reveal Their Antidiabetic Activities

Hafiza Salaha Mahrosh, Rizwan Mehmood, Shazia Anwer Bukhari, Gulnaz Afzal, and Rawaba Arif

Research Article (8 pages), Article ID 5550180, Volume 2021 (2021)

Hindawi
BioMed Research International
Volume 2024, Article ID 9876404, 1 page
https://doi.org/10.1155/2024/9876404

Retraction

Retracted: Use of Medicinal Plants for Respiratory Diseases in Bahawalpur, Pakistan

BioMed Research International

Received 12 March 2024; Accepted 12 March 2024; Published 20 March 2024

This article has been retracted by Hindawi following an investigation undertaken by the publisher [1]. This investigation has uncovered evidence of one or more of the following indicators of systematic manipulation of the publication process:

(1) Discrepancies in scope

(2) Discrepancies in the description of the research reported

(3) Discrepancies between the availability of data and the research described

(4) Inappropriate citations

(5) Incoherent, meaningless and/or irrelevant content included in the article

(6) Manipulated or compromised peer review

The presence of these indicators undermines our confidence in the integrity of the article's content and we cannot, therefore, vouch for its reliability. Please note that this notice is intended solely to alert readers that the content of this article is unreliable. We have not investigated whether authors were aware of or involved in the systematic manipulation of the publication process.

Wiley and Hindawi regrets that the usual quality checks did not identify these issues before publication and have since put additional measures in place to safeguard research integrity.

We wish to credit our own Research Integrity and Research Publishing teams and anonymous and named external researchers and research integrity experts for contributing to this investigation.

The corresponding author, as the representative of all authors, has been given the opportunity to register their agreement or disagreement to this retraction. We have kept a record of any response received.

References

[1] S. Afzal, H. I. Ahmad, A. Jabbar et al., "Use of Medicinal Plants for Respiratory Diseases in Bahawalpur, Pakistan," *BioMed Research International*, vol. 2021, Article ID 5578914, 10 pages, 2021.

Hindawi
BioMed Research International
Volume 2024, Article ID 9834546, 1 page
https://doi.org/10.1155/2024/9834546

Retraction

Retracted: *In Silico* Structural, Functional, and Phylogenetic Analysis of Cytochrome (CYPD) Protein Family

BioMed Research International

Received 12 March 2024; Accepted 12 March 2024; Published 20 March 2024

This article has been retracted by Hindawi following an investigation undertaken by the publisher [1]. This investigation has uncovered evidence of one or more of the following indicators of systematic manipulation of the publication process:

(1) Discrepancies in scope

(2) Discrepancies in the description of the research reported

(3) Discrepancies between the availability of data and the research described

(4) Inappropriate citations

(5) Incoherent, meaningless and/or irrelevant content included in the article

(6) Manipulated or compromised peer review

The presence of these indicators undermines our confidence in the integrity of the article's content and we cannot, therefore, vouch for its reliability. Please note that this notice is intended solely to alert readers that the content of this article is unreliable. We have not investigated whether authors were aware of or involved in the systematic manipulation of the publication process.

Wiley and Hindawi regrets that the usual quality checks did not identify these issues before publication and have since put additional measures in place to safeguard research integrity.

We wish to credit our own Research Integrity and Research Publishing teams and anonymous and named external researchers and research integrity experts for contributing to this investigation.

The corresponding author, as the representative of all authors, has been given the opportunity to register their agreement or disagreement to this retraction. We have kept a record of any response received.

References

[1] H. I. Ahmad, G. Afzal, A. Jamal et al., "*In Silico* Structural, Functional, and Phylogenetic Analysis of Cytochrome (CYPD) Protein Family," *BioMed Research International*, vol. 2021, Article ID 5574789, 13 pages, 2021.

Hindawi
BioMed Research International
Volume 2024, Article ID 9808946, 1 page
https://doi.org/10.1155/2024/9808946

Retraction

Retracted: *Mangifera indica* Extracts as Novel PKM2 Inhibitors for Treatment of Triple Negative Breast Cancer

BioMed Research International

Received 12 March 2024; Accepted 12 March 2024; Published 20 March 2024

This article has been retracted by Hindawi following an investigation undertaken by the publisher [1]. This investigation has uncovered evidence of one or more of the following indicators of systematic manipulation of the publication process:

(1) Discrepancies in scope

(2) Discrepancies in the description of the research reported

(3) Discrepancies between the availability of data and the research described

(4) Inappropriate citations

(5) Incoherent, meaningless and/or irrelevant content included in the article

(6) Manipulated or compromised peer review

The presence of these indicators undermines our confidence in the integrity of the article's content and we cannot, therefore, vouch for its reliability. Please note that this notice is intended solely to alert readers that the content of this article is unreliable. We have not investigated whether authors were aware of or involved in the systematic manipulation of the publication process.

Wiley and Hindawi regrets that the usual quality checks did not identify these issues before publication and have since put additional measures in place to safeguard research integrity.

We wish to credit our own Research Integrity and Research Publishing teams and anonymous and named external researchers and research integrity experts for contributing to this investigation.

The corresponding author, as the representative of all authors, has been given the opportunity to register their agreement or disagreement to this retraction. We have kept a record of any response received.

References

[1] A. Rasul, A. Riaz, W. Wei et al., "*Mangifera indica* Extracts as Novel PKM2 Inhibitors for Treatment of Triple Negative Breast Cancer," *BioMed Research International*, vol. 2021, Article ID 5514669, 11 pages, 2021.

Hindawi
BioMed Research International
Volume 2021, Article ID 3094571, 8 pages
https://doi.org/10.1155/2021/3094571

Research Article

Therapeutic Role of Mango Peels in Management of Dyslipidemia and Oxidative Stress in Obese Females

Farkhanda Arshad,[1] Huma Umbreen,[2] Iqra Aslam,[3] Arruje Hameed,[1] Kiran Aftab,[4] Wahidah H. Al-Qahtani,[5] Nighat Aslam,[6] and Razia Noreen[1]

[1]*Department of Biochemistry, Government College University, Faisalabad-, Pakistan*
[2]*Department of Nutritional Sciences, Government College University, Faisalabad-, Pakistan*
[3]*Department of Biochemistry, University of Management and Technology, Sialkot Campus, Sialkot-, Pakistan*
[4]*Department of Chemistry, Government College University, Faisalabad-, Pakistan*
[5]*Department of Food Science and Nutrition, College of Food and Agriculture Sciences, King Saud University, Riyadh 11451, Saudi Arabia*
[6]*Department of Biochemistry, Independent Medical College, Faisalabad-, Pakistan*

Correspondence should be addressed to Razia Noreen; itsrazia@yahoo.com

Received 18 May 2021; Accepted 29 September 2021; Published 23 October 2021

Academic Editor: Andrei Surguchov

Obesity is a chronic metabolic and noncommunicable disease that affects 50% of world population. Reactive oxygen species and oxidative stress are interconnected with the obesity and several metabolic disorders, gaining the attention of scientific community to combat this problem naturally. Among various fruits, mango as a yellow fruit is rich in polyphenols, carotenoids, terpenes, and flavonoids that act as antioxidants to protect against free radicals produced in the body. The present study was performed to explore *in vivo* antioxidant potential of mango peels against dyslipidemia and oxidative stress in overweight subjects. The female volunteers ($n = 31$) between 25 and 45 years of age having a body mass index (BMI) of 25.0-29.9 (overweight) were included in this study, while participants with complications as diabetes, hypertension, cardiovascular, and liver diseases were excluded. The treatment group consumed 1 g mango peel powder for 84 days. The subjects were analyzed for biochemical analysis, antioxidant status, and anthropometric measurements at baseline and end of the study period. Further, at the end of study, the safety evaluation tests were also performed. The results showed that upon consumption of mango peel powder, low-density lipoproteins (LDL), cholesterol, triglyceride, urea, and creatinine levels were decreased and high-density lipoprotein (HDL) level was increased ($P \leq 0.05$), while thiobarbituric acid reactive substances (TBARS) showed increased antioxidant status ($P \leq 0.05$) which suggests that mango peels have a strong management potential against oxidative stress and dyslipidemia in obese subjects.

1. Introduction

Obesity is a chronic disease characterized by accumulation of fat in adipose tissues resulting in increased body weight [1, 2]. It is considered a frequent metabolic disease, having 50% prevalence among adult masses throughout the world [3]. It is as common as is expected to be affecting 38% of adult women and 36.9% of adult men around the globe [4]. Obesity is the major causative agent for oxidative stress, which in return worsens the situation by changing the metabolite functions and stimulating the process of inflammation through cytokines [1, 5]. Furthermore, due to increased oxidative stress, innate immunity is triggered which gives rise to increased inflammation and lipid peroxidation that is ultimate route cause for different degenerative diseases [6, 7]. It is proposed that a cycle runs between obesity and oxidative stress which has threatening effects on cells and tissues, further depriving them of antioxidants [8]. Adipose tissues act as the gland which produces hormones, i.e., resistin, estrogen, and leptin as well as signaling

protein such as cytokines. In response to increased adipocytes, unchecked adipokines are secreted which show increased immune response by producing reactive oxygen species (ROS) and free radicles, further enhancing the oxidative stress [9]. Moreover, oxidative stress damages pancreatic β cells and affects the production and release of insulin leading to altered transportation of glucose to the tissues, which may result in the development of metabolic syndrome [10]. Fruits and vegetables have biologically active compounds including carotenoids, anthocyanins, and polyphenols, which show prospective antioxidant action and can also strengthens defense against metabolic risk factors [11, 12]. Mango peel is an important part of the fruit considered inedible, rich in flavonoids, polyphenols, and carotenoids as antioxidants. It is about 15–20% of the fruit weight and is a major waste material of fruit processing sector [13]. Mango peel powders protect against fatty liver disease and impairment of renal and liver function as caused by medicines. Treatments of chronic diseases using the natural components as present in mango peels provide a better alternate of conventional medicines.

Keeping in view the potent health benefits of this by product, the present study was designed to probe its functional effect against most prevalent issue of society, i.e., dyslipidemia and oxidative stress related to obesity. Although there are few earlier research findings available showing the reduction in oxidative stress in rats, there are insufficient evidences available to address oxidative stress in human subjects using such an economical and natural resource.

2. Materials and Methods

2.1. Preparation of Raw Materials. Mangoes (*Mangifera indica*) variety Chaunsa were procured from the local market of Faisalabad, Pakistan, and washed and peeled. Afterwards, the separated peels were washed with warm water to deplete any sugars and dried at 60°C in a dehydrator (NESCO®/American Harvest). The dried peels were ground using a grinder (Panasonic MX AC 400 Mixer Grinder) and sieved to get even sized particles of 500–600 μm size; then, the powder was stored in glass jars at 18°C and kept in the dry place [14].

2.2. HPLC Analysis. The mango peel extract was prepared from mango peel powder (MPP) according to the method followed by Tunchaiyaphum et al. [15]. The extract of MPP was prepared using 40% methanol in the ratio of 1 : 1, shaken gently for 5 minutes, and then added with 10 mL HCl (6 M). The prepared solution was kept for 2 hours in an oven at 50°C and filtered through microfilters of 0.2-0.4 microns, and the resulted sample was analyzed through gradient HPLC (Model LC-10; 32KARAT SOS, Shimazdu Japan) [16]. The mobile phase consisted of freshly prepared acetonitrile, dichloromethane, and methanol (ratio 60 : 20 : 20, respectively) and flow rate of sample (injection volume 15 μL) was set at 0.8 mL/min [17].

2.3. Experimental Study Design. The nonprobability sampling technique (convenience sampling method) was used to select the sample. The participants were selected from Allied Hospital and Civil Hospital Faisalabad, Pakistan. The inclusion criteria was comprised of female subjects between 25 and 45 years of age having a BMI of 25.0-29.9 (overweight), while participants having any other complication as diabetes, hypertension, cardiovascular, and liver diseases were excluded. Out of a total 120 volunteers at the preliminary stage, 77 were excluded on the basis of diabetes and hypertension, and 12 were suffering from some sort of heart ailments. A total of 31 overweight subjects were divided in two groups: one treatment (21 subjects, taking selected doses of mango peels powder)and the other as control (10 subjects), which received no treatment but dietary guidelines were provided to both groups. All participants were requested to complete questionnaires about informed consent, physical examination, medical history, anthropometric measurements, and the food frequency questionnaire [18]. The dose was optimized and selected for all experiments and was provided in sachet (1 g MPP) that had to be taken twice a day half an hour before meal with one glass of water. The control group was advised to take one glass of water half an hour before meal for equivalence. High-fat and high-carbohydrate diets were restricted in all groups. The study was continued for 84 days after which the blood sample was taken again and BMI was calculated.

"Informed consent was obtained from all individual participants included in the study."

2.4. Ethical Approval. The study was approved by the ethical review committee of the University for human and animal studies (ERC/GCUF/1966-IRB-566), and all studies were performed in accordance with the ethical standards of the 1964 Helsinki declaration and ethical principles of WHO (2008) and its later amendments or comparable ethical standards.

2.5. Blood Biochemistry and Antioxidant Analysis. The venous blood was processed to obtain plasma and serum under sterilized conditions at base line and at end of the study. A 4 mL blood was taken in the tube and let it stand for an hour to clot at room temperature. After clotting, centrifugation was performed for 10 minutes at 1000 rpm and serum containing aliquots were stored in a freezer at -4°C. For separation of plasma, blood was taken in EDTA tubes and kept at room temperature. After that, centrifugation was performed at 2000 rpm for 10 minutes and the supernatant (plasma) was separated and stored in a freezer at -4°C.

To measure complete blood count (CBC), the plasma was taken in a test tube and blood cells were analyzed through CBC autohaematology analyzer (NIPRO LE 1000 JAPAN). The serum was evaluated to find out the status of lipid profile using enzymatic colorimetric methods [19, 20]. Further, the serum was investigated for antioxidant status using thiobarbituric acid reactive substances (TBARS) by respective methods [21].

2.6. Safety Evaluation. For safety purpose, a discomfort questionnaire was filled up by the participants to report any disturbance after consumption of the MPP extract.

Furthermore, to perform liver function test (LFT) and renal function test (RFT), colorimetric kit protocol [22] was adopted. The concentrations of bilirubin, urea, creatinine, etc. were determined through respective methods [23, 24].

2.7. Statistical Analysis. Analysis of variance (ANOVA) was used for data analysis [25] to know the significant difference. The least significant difference (LSD) was calculated to find the difference between means using SPSS (Version 17, USA). The results were declared to be significant at $P \leq 0.05$.

3. Results and Discussion

3.1. HPLC Profiling. The gradient HPLC method was used for identification of polyphenolic compounds and antioxidants in the mango peel extract. The results of bioactive compounds showed a significant difference ($P \leq 0.05$) among different parameters (Table 1). The mango peel extract showed the highest amount of caffeic acid while querecetin was observed to be the lowest. It was also observed that mango peel extract contained an effective amount of vitamin C (49.52 ppm) along with a significant amount of kaempherol, chlorogenic acid, and gallic acid. The HPLC chromatogram (Figure 1) showed peaks for retention times which were comparable with a known standard to identify the unknown phenolic compounds.

HPLC analyses have revealed that the methanolic extract of mango peel provided a higher concentration of phenolic compounds which is in accordance with other studies [26, 27]. The presence of major bioactive compounds, e.g., caffeic acid kaempherol gallic acid etc. in mango peels (Table 1) may not only lower the lipid level of plasma, cause inhibition of lipoprotein secretion, and result in removal of extra cholesterol from blood through bile acids but also are responsible in obesity reduction [28]. Yellow-colored fruits as orange, lemon, and mango are higher in flavonoids, polyphenols, terpenes, and carotenoids, which act as antioxidants to scavenge free radicals and reactive oxygen species [29, 30]. During this research, antioxidant concentration in the mango peel extract was found to be higher than the study conducted by Carvalho et al. [31]. The difference may be due to the varied climate situation, mango cultivars, and harvesting factors.

3.2. Anthropometric Data. A total of 31 obese female volunteers (10 control and 21 treatment subjects) were between the ages of 25 and 45 belonging to nearly similar BMIs (Table 2). The results showed that the BMI value decreased nonsignificantly with time (0^{th} -84^{th} day) in both groups. However, this reduction was more pronounced (from 29 to 28.4 kg/m^2) in case of subjects in a group treated with mango peel extract (Figure 2).

The mango peel extract decreased weight gain in the treatment group compared to the control group. Previous studies have proved that due to consumption of mango peel, the body weight decreases and the antioxidant level increases [32]. Moreover, a nonsignificant reduction in BMI for treatment as compared to the control group at the end of experimental period may be attributed to the combined effect of bioactive compounds responsible for weight management including caffeic acid and kaempherol [33, 34].

3.3. Efficacy Study. All the subjects were analyzed for blood biochemistry. The results showed that hemoglobin, eosinophils, ESR (erythrocyte sedimentation rate), monocytes, polymorphs, and TLC (total leukocyte count) did not change significantly ($P \leq 0.05$) among the control and treatment groups, while lymphocytes were found to be increased significantly in the MPP-treated group compared to the control group (Table 3).

Moreover, the data showed a significant difference ($P \leq 0.05$) for the lipid profile test among the control and treatment groups of obese subjects (Table 3). After consumption of MPP, significant reduction in triglyceride (-4.63%), TC (-13.12%), and LDL (-9.04%), while 9.97% increase in the HDL level in the treatment group compared to the control group were observed.

There was a significant difference ($P \leq 0.05$) between the groups for thiobarbituric acid reactive substance (TBARS) values (Figure 3). The antioxidant status in the treatment group was significantly increased after the intake of mango peel powder (MPP) due to decrease in the TBARS value with increasing number of treatment days (0^{th}-84^{th}).

The biochemical profile showed that lymphocytes were increased in the concentration while count of other blood cells was decreased after intervention. In a review conducted by Moler and Soft [35], it was described that antioxidants affect the blood cell count over a longer period of time; therefore, during a short time as in the case of the present study, the results are not much pronounced.

Furthermore, the results showed the management of dyslipidemia with reduced plasma triglyceride and cholesterol levels in obese subjects treated with mango peel powder. Thus, it showed protective effects against vascular damage caused by oxidation of LDL. These findings are in accordance with those found by Duttaroy and Jørgensen [36]. The reduction in the concentration of LDL cholesterol may be accredited to bioactive compounds with higher antioxidant potential present in mango peels. They cause downregulation of proteins involved in lipogenesis; therefore, lipogenesis is repressed, whereas energy utilization is enhanced that give positive correlation to the adiposity. In the present study, HDL concentration was increased in the treatment group consuming MPP, which is important in the transport of extra cholesterol from cells and tissues to the liver for ultimate degradation. These findings are in accordance with the research work of Muruganandan et al. [37], which also showed an increase in the concentration of HDL in diabetic rats. With treatment of MPP, the antioxidant status was improved in subjects and TBARS values were decreased. TBARS are byproducts of lipid peroxidation and comprise of aldehydes and lipid hydroperoxides which are enhanced during oxidative stress. It describes lipid peroxidation in terms of MDA and is indicative of antioxidant status. Therefore, the consumption of mango peel powder not only controls the lipid level but also is effective against lipid peroxidation [38].

Table 1: HPLC profile of mango peel extract.

Compounds	Retention time (Rt)	Amount (ppm)	Area (mv·S)	Area (%)
Kaempherol	2.35 ± 0.02^{g}	187.7 ± 0.04^{b}	2813.37 ± 3.4^{d}	93.5 ± 1.2^{a}
Quercetin	3.07 ± 0.01^{f}	11.87 ± 0.01^{f}	224.82 ± 1.2^{g}	0.2 ± 0.2^{g}
Gallic acid	4.83 ± 0.01^{e}	95.90 ± 0.02^{c}	26641.69 ± 3.5^{b}	22.2 ± 0.1^{c}
Caffeic acid	12.68 ± 0.03^{d}	247.39 ± 0.59^{a}	53782.26 ± 3.3^{a}	44.8 ± 3.5^{b}
Chlorogenic acid	15.30 ± 0.04^{a}	95.52 ± 0.04^{c}	12250.82 ± 2.7^{c}	10.2 ± 0.09^{d}
Vitamin C	23.56 ± 0.1^{b}	49.52 ± 0.04^{d}	2476.19 ± 1.3^{e}	2.1 ± 0.03^{e}
Sinapic acid	26.61 ± 0.7^{a}	14.76 ± 0.04^{e}	1136.40 ± 1.4^{f}	0.9 ± 0.01^{f}

[a–g]Different letters in columns show a significant difference at $P \leq 0.05$.

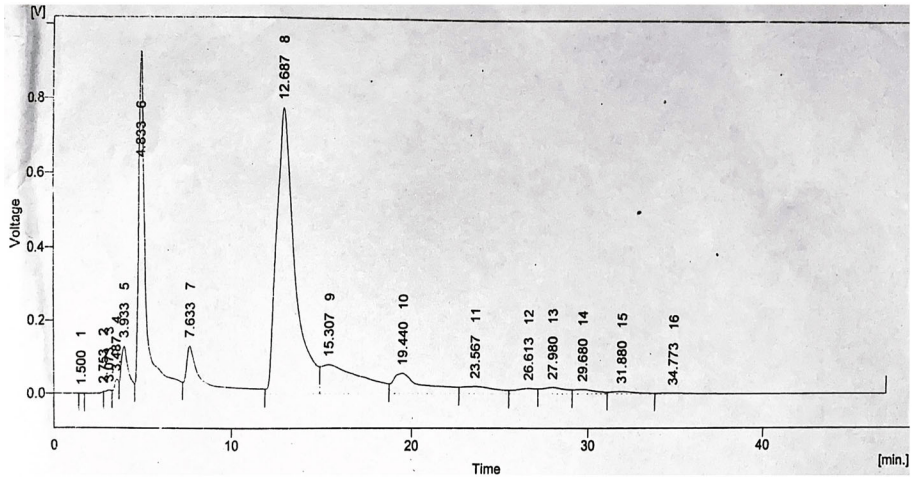

Figure 1: HPLC chromatogram of phenolic compounds of the mango peel extract. Peak identification of mango peel extract: 2, kaempherol; 3, quercetin; 6, gallic acid; 8, caffeic acid; 9, chlorogenic acid; 11, vitamin C; and 12, sinapicacid.

Table 2: Average baseline anthropometric measurement of volunteers.

Parameters	Groups		Probability values*
	Control ($n = 10$)	Treatment ($n = 21$)	
Age (years)	33.7 ± 1.31	34.1 ± 0.92	0.15
BMI (kg/m^2)	29.2 ± 0.46	29.0 ± 0.46	0.12

Data is presented as the means ± SE of control and treatment group. * Probability values ($P \leq 0.05$) show significant differences between the groups.

3.4. Safety Evaluation. Both groups were also evaluated for safety test including discomfort questionnaire to find out any adverse effect on the subjects. The discomfort questionnaire showed no significant disturbance except reduction in appetite in the treatment group as compared to the control group. For liver function test (LFT) and renal function test (RFT), serum bilirubin, alkaline phosphate (ALP), alanine aminotransferase (ALT), aspartate aminotransferase (AST), blood urea, and creatinine, respectively, showed significant difference at $P \leq 0.05$ (Table 4).

Bilirubin concentration is an indicator of liver and bile disorders. Moreover, bilirubin results in decreased blood cholesterol concentration through increased HDL and decreased LDL levels. The present study showed an increased bilirubin concentration in the treatment group that may be due to an increased antioxidant status of the patient and reduced inflammatory condition [39]. Furthermore, the consumption of MPP reduced alkaline phosphatase (ALP) concentration and had required effects on adipocytes and fatty deposits. The ALP isozyme was reported to be expressed in adipocytes which ultimately raise the fat deposits during the enhanced adipogenesis in obesity [40]. As the ALP level is an indicator of obesity so reduction of the ALP level by MPP showed safety of mango peel doses to reduce the fatty deposits. The degenerative changes in the liver and heart cause the increase concentration of ALT and AST which are used as biomarker for diagnostic purpose of liver damage [41]. Moreover, the nonalcoholic fatty liver diseases (NAFLD) are most common metabolic syndrome related to obesity in which the increased level of hepatic enzymes leads towards the sever obesity. The ALT and AST are released into the blood circulation in response to the cell deterioration process due to high peroxidation of lipids, and in this condition, the antioxidant level of the body is much decreased. This increase in enzyme concentrations is due to the high-fat diet during the intervention period so mango peel powder serves to reduce these enzyme concentrations [42]. However, mango peel supplementation is also

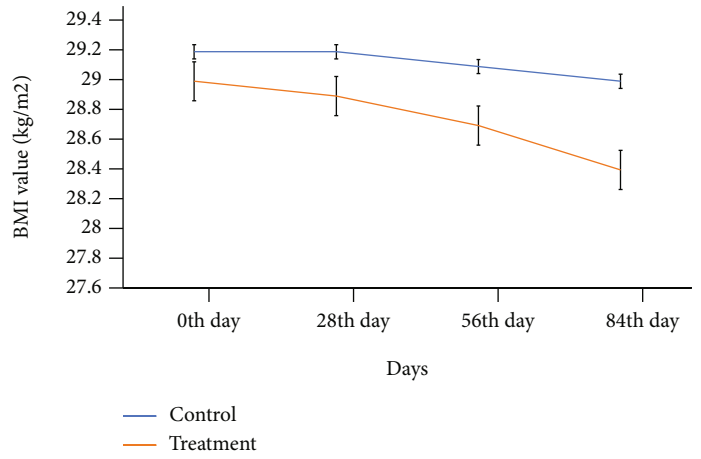

Figure 2: Effect of treatment days on the BMI value of obese subjects in the control and MPP-treated groups.

Table 3: Blood biochemistry of the control and treatment groups of obese subjects.

Parameters	Groups		Probability values*
	Control ($n = 10$)	Treatment ($n = 21$)	
Complete blood count (g/dL)			
Hemoglobin	12.44 ± 0.94	12.38 ± 0.84	0.96
Eosinophils	0.14 ± 0.024	0.14 ± 0.024	1
ESR	17.80 ± 0.80	16.60 ± 0.67	0.28
Lymphocytes	36.60 ± 0.40[b]	39.20 ± 0.91[a]	0.03
Monocytes	0.24 ± 0.024	0.24 ± 0.024	1
Polymorphs	60 ± 0.04	54.60 ± 2.46	0.59
TLC	7720 ± 185.47	7660.0 ± 60.0	0.76
Lipid profile (mg/dL)			
Triglycerides	146.80 ± 1.73[a]	140.30 ± 2.48[b]	0.02
Total cholesterol	188.90 ± 3.06[a]	164.10 ± 3.35[b]	0.01
HDL	46.10 ± 1.73[b]	50.70 ± 1.35[a]	0.05
LDL	134.90 ± 3.51[a]	122.70 ± 2.55[b]	0.01
TBARS (μmol)	6.08 ± 0.07[a]	5.66 ± 0.05[b]	0.001

Data are presented as the means ± SEM of the control and treatment groups. *Probability values ($P \leq 0.05$) show significant differences between the groups. [a,b]Different letters in rows show a significant difference at $P \leq 0.05$. TC: total cholesterol; HDL: high-density lipoprotein; LDL: low-density lipoprotein; Hb: hemoglobin; ESR: erythrocyte sedimentation rate; TLC: total leukocyte count.

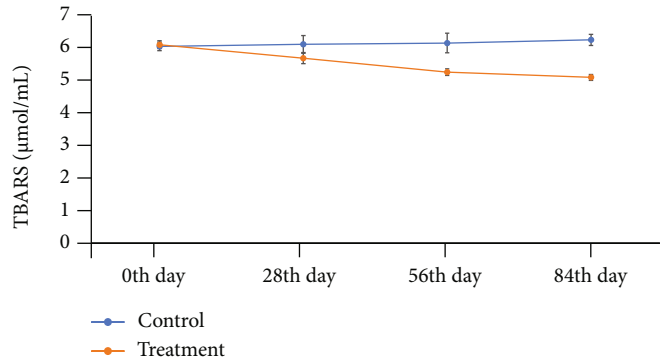

Figure 3: Reduction in the TBARS (μmol/mL ±SEM) value with increase in treatment days.

Table 4: Safety analysis for the control and treatment groups of obese subjects.

Parameters	Groups		Probability values*
	Control ($n = 10$)	Treatment ($n = 21$)	
Liver function test			
Bilirubin direct (mg/dL)	0.40 ± 0.05	0.41 ± 0.05	0.90
Bilirubin indirect (mg/dL)	0.23 ± 0.012^{b}	0.38 ± 0.05^{a}	0.03
Bilirubin total (mg/dL)	0.64 ± 0.048	0.48 ± 0.15	0.35
ALP (U/L)	244.0 ± 12.88^{a}	188.40 ± 0.40^{b}	0.002
ALT (U/L)	53.200 ± 3.30	44.00 ± 3.67	0.09
AST (U/L)	39.00 ± 2.19^{a}	30.40 ± 0.40^{b}	0.004
Renal function test (mg/dL)			
Blood urea	39.60 ± 1.50^{a}	34.6 ± 0.74^{b}	0.02
Creatinine	0.80 ± 0.06^{a}	0.74 ± 0.05^{b}	0.02

*Probability values $P \leq 0.05$ show significant differences between the groups. Different letters (ab) in the column show significant difference at $P \leq 0.05$. Data is presented as the means ± SEM of the control and treatment groups. ALP: Alkaline phosphatase; ALT: alanine aminotransferase; AST: aspartate aminotransferase.

reported to improve the concentration of these enzymes in treated obese subjects due to higher polyphenolic content with appreciable antioxidant power [43]. In the current research, urea and creatinine were decreased in the treatment group compared to the control group and showed the efficiency of MPP against any deterioration in kidney function. Creatinine is actually a metabolic product of muscle which is transported to the kidney through renal glomeruli for filtration and some dispose in urine. Creatinine concentration increases with age, gender, and BMI [44], and these results are in accordance with the results demonstrated by Morsi et al. [45].

4. Conclusion

Obesity is increasing at an alarming rate which becomes further dangerous due to production of reactive oxygen species (ROS). Based upon the present research results, it can be concluded that bioactive compounds from agricultural waste (mango peels) present a comprehensive remedy to fight against the ROS produced in the body. Thus, these are helpful in preventing damages caused, using economical resources that otherwise go waste and become a source of pollution.

Data Availability

All types of data are included in the research manuscript.

Conflicts of Interest

The authors declare no conflict of interest.

Acknowledgments

The authors are thankful to the participants (Volunteers) and Hospitals of Faisalabad, for their kind cooperation. The authors are thankful to the Government College University, Faisalabad, for providing funds and the research facilities. The authors extend their appreciation to the researchers supporting project number (RSP-2020/293) King Saud University, Riyadh, Saudi Arabia.

References

[1] L. Marseglia, S. Manti, G. D'Angelo et al., "Oxidative stress in obesity: a critical component in human diseases," *International Journal of Molecular Sciences*, vol. 16, no. 1, pp. 378–400, 2015.

[2] J. Vekic, A. Zeljkovic, A. Stefanovic, Z. Jelic-Ivanovic, and V. Spasojevic-Kalimanovska, "Obesity and dyslipidemia," *Metabolism*, vol. 92, pp. 71–81, 2019.

[3] J. I. Mechanick, A. Youdim, D. B. Jones et al., "Clinical practice guidelines for the perioperative nutritional, metabolic, and nonsurgical support of the bariatric surgery patient—2013 update: cosponsored by American Association of Clinical Endocrinologists, the Obesity Society, and American Society for Metabolic & Bariatric Surgery," *Obesity*, vol. 21, no. S1, pp. S1–S27, 2013.

[4] M. Ng, T. Fleming, M. Robinson et al., "Global, regional, and national prevalence of overweight and obesity in children and adults during 1980-2013: a systematic analysis for the Global Burden of Disease Study 2013," *The Lancet*, vol. 384, no. 9945, pp. 766–781, 2014.

[5] C. N. Lumeng and A. R. Saltiel, "Inflammatory links between obesity and metabolic disease," *The Journal of Clinical Investigation*, vol. 121, no. 6, pp. 2111–2117, 2011.

[6] Y. Zhang, K. E. Fischer, V. Soto et al., "Obesity-induced oxidative stress, accelerated functional decline with age and increased mortality in mice," *Archives of Biochemistry and Biophysics*, vol. 576, pp. 39–48, 2015.

[7] P. V. Dludla, B. B. Nkambule, B. Jack et al., "Inflammation and oxidative stress in an obese state and the protective effects of gallic acid," *Nutrients*, vol. 11, no. 1, p. 23, 2019.

[8] S. A. Noeman, H. E. Hamooda, and A. A. Baalash, "Biochemical study of oxidative stress markers in the liver, kidney and heart of high fat diet induced obesity in rats," *Diabetology and Metabolic Syndrome*, vol. 3, no. 1, p. 17, 2011.

[9] A. Fernández-Sánchez, E. Madrigal-Santillán, M. Bautista et al., "Inflammation, oxidative stress, and obesity," *International Journal of Molecular Sciences*, vol. 12, no. 5, pp. 3117–3132, 2011.

[10] T. M. Avelar, A. S. Storch, L. A. Castro, G. V. Azevedo, L. Ferraz, and P. F. Lopes, "Oxidative stress in the pathophysiology of metabolic syndrome: which mechanisms are involved?," *Jornal Brasileiro de Patologia e Medicina Laboratorial*, vol. 51, no. 4, pp. 231–239, 2015.

[11] C. Ajila, K. Naidu, S. Bhat, and U. P. Rao, "Bioactive compounds and antioxidant potential of mango peel extract," *Food Chemistry*, vol. 105, no. 3, pp. 982–988, 2007.

[12] H.-E. Khoo, K. N. Prasad, K.-W. Kong, Y. Jiang, and A. Ismail, "Carotenoids and their isomers: color pigments in fruits and vegetables," *Molecules*, vol. 16, no. 2, pp. 1710–1738, 2011.

[13] C. Ajila and U. P. Rao, "Mango peel dietary fibre: composition and associated bound phenolics," *Journal of Functional Foods*, vol. 5, no. 1, pp. 444–450, 2013.

[14] H. Umbreen, M. U. Arshad, F. Saeed, N. Bhatty, and A. I. Hussain, "Probing the functional potential of agro-industrial wastes in dietary interventions," *Journal of Food Processing and Preservation*, vol. 39, no. 6, pp. 1665–1671, 2015.

[15] S. Tunchaiyaphum, M. Eshtiaghi, and N. Yoswathana, "Extraction of bioactive compounds from mango peels using green technology," *International Journal of Chemical Engineering and Applications*, vol. 4, no. 4, pp. 194–198, 2013.

[16] M. S. Pak-Dek, A. Osman, N. G. Sahib et al., "Effects of extraction techniques on phenolic components and antioxidant activity of Mengkudu (Morinda citrifolia L.) leaf extracts," *Journal of Medicinal Plants Research*, vol. 5, no. 20, pp. 5050–5057, 2011.

[17] B. Sultana, F. Anwar, M. Rafique Asi, and S. Ali Shahid Chatha, "Antioxidant potential of extracts from different agro wastes: stabilization of corn oil," *Grasas y Aceites*, vol. 59, no. 3, pp. 205–217, 2008.

[18] A. L. Romero, J. E. Romero, S. Galaviz, and M. L. Fernandez, "Cookies enriched with psyllium or oat bran lower plasma LDL cholesterol in normal and hypercholesterolemic men from northern Mexico," *Journal of the American College of Nutrition*, vol. 17, no. 6, pp. 601–608, 1998.

[19] H. Khan, S. Sobki, and S. Khan, "Association between glycaemic control and serum lipids profile in type 2 diabetic patients: HbA1c predicts dyslipidaemia," *Clinical and Experimental Medicine*, vol. 7, no. 1, pp. 24–29, 2007.

[20] H. Stockbridge, R. I. Hardy, and C. J. Glueck, "Public cholesterol screening: motivation for participation, follow-up outcome, self-knowledge, and coronary heart disease risk factor intervention," *The Journal of Laboratory and Clinical Medicine*, vol. 114, no. 2, pp. 142–151, 1989.

[21] E. Dorta, M. G. Lobo, and M. González, "Using drying treatments to stabilise mango peel and seed: effect on antioxidant activity," *LWT-Food Science and Technology*, vol. 45, no. 2, pp. 261–268, 2012.

[22] E. I. Etim, E. E. Essien, O. A. Eseyin, and I. E. Udoh, "Effect of some artemisinin and combination therapy regimens with and without concomitant administration of phospholipids on the levels of plasma aminotransferases and bilirubin in Nigerian male subjects," *African Journal of Pharmacology and Therapeutics*, vol. 2, no. 1, pp. 17–25, 2013.

[23] P. Ugwu Okechukwu, F. Nwodo Okwesili, J. Parker, E. Odo Christian, C. Ossai Emmanuel, and B. Aburbakar, "Ameliorative effects of ethanol leaf extract of Moringa oleifera on the liver and kidney markers of malaria infected mice," *International Journal of Life Sciences Biotechnology and Pharma Research*, vol. 2, pp. 43–52, 2013.

[24] S. Eruke, M. M. Okechukwu, and E. E. Bassey, "Effects of consumption of yaji (clove, ginger, garlic and red pepper) on some haematological parameters of wistar albino rats," *Journal of Engineering and Applied Science*, vol. 2, no. 2, pp. 120–125, 2013.

[25] R. G. Steel and J. H. Dickey, "Analysis of variance II: multiway classifications," *Principles and procedures of statistics: A biometrical approach*, vol. 519, pp. 352–358, 1997.

[26] J. S. Boeing, É. O. Barizão, B. C. Silva, P. F. Montanher, V. de Cinque Almeida, and J. V. Visentainer, "Evaluation of solvent effect on the extraction of phenolic compounds and antioxidant capacities from the berries: application of principal component analysis," *Chemistry Central Journal*, vol. 8, no. 1, pp. 1–48, 2014.

[27] N. Turkmen, F. Sari, and Y. S. Velioglu, "Effects of extraction solvents on concentration and antioxidant activity of black and black mate tea polyphenols determined by ferrous tartrate and Folin- Ciocalteu methods," *Food Chemistry*, vol. 99, no. 4, pp. 835–841, 2006.

[28] S. Baba, N. Osakabe, Y. Kato et al., "Continuous intake of polyphenolic compounds containing cocoa powder reduces LDL oxidative susceptibility and has beneficial effects on plasma HDL-cholesterol concentrations in humans," *The American Journal of Clinical Nutrition*, vol. 85, no. 3, pp. 709–717, 2007.

[29] L. R. Hai, "Health-promoting components of fruits and vegetables in the diet," *Advances in Nutrition*, vol. 4, no. 3, pp. 384S–392S, 2013.

[30] M. E. Maldonado-Celis, E. M. Yahia, B. Ramiro et al., "Chemical composition of mango (Mangifera indica L.) fruit: nutritional and phytochemical compounds," *Frontiers in Plant Science*, vol. 10, pp. 1–23, 2019.

[31] C. R. L. Carvalho, C. J. Rossetto, D. M. B. Mantovani, M. A. Morgano, J. V. Castro, and N. Bortoletto, "Avaliação de cultivares de mangueira selecionadas pelo Instituto Agronômico de Campinas comparadas a outras de importância comercial," *Revista Brasileira de Fruticultura*, vol. 26, no. 2, pp. 264–271, 2004.

[32] M. El-Ghany, M. Ramadan, and S. Hassanain, "Antioxidant activity of some agro-industrial peels on liver and kidney of rats exposed to oxidative stress," *World Journal of Dairy & Food Sciences*, vol. 6, no. 1, pp. 105–114, 2011.

[33] B. Bocco, G. Fernandes, F. Lorena et al., "Combined treatment with caffeic and ferulic acid from Baccharis uncinella C. DC.(Asteraceae) protects against metabolic syndrome in mice," *Brazilian Journal of Medical and Biological Research*, vol. 49, no. 3, p. e5003, 2016.

[34] A. De Lorenzo, S. Gratteri, P. Gualtieri, A. Cammarano, P. Bertucci, and L. Di Renzo, "Why primary obesity is a disease?," *Journal of Translational Medicine*, vol. 17, no. 1, p. 169, 2019.

[35] P. Møller and S. Loft, "Oxidative DNA damage in human white blood cells in dietary antioxidant intervention studies," *The American Journal of Clinical Nutrition*, vol. 76, no. 2, pp. 303–310, 2002.

[36] A. K. Duttaroy and A. Jørgensen, "Effects of kiwi fruit consumption on platelet aggregation and plasma lipids in healthy human volunteers," *Platelets*, vol. 15, no. 5, pp. 287–292, 2004.

[37] S. Muruganandan, K. Srinivasan, S. Gupta, P. Gupta, and J. Lal, "Effect of mangiferin on hyperglycemia and atherogenicity in streptozotocin diabetic rats," *Journal of Ethnopharmacology*, vol. 97, no. 3, pp. 497–501, 2005.

[38] B. Fuhrman, A. Lavy, and M. Aviram, "Consumption of red wine with meals reduces the susceptibility of human plasma and low-density lipoprotein to lipid peroxidation," *The American Journal of Clinical Nutrition*, vol. 61, no. 3, pp. 549–554, 1995.

[39] A.-C. Boon, C. L. Hawkins, K. Bisht et al., "Reduced circulating oxidized LDL is associated with hypocholesterolemia and enhanced thiol status in Gilbert syndrome," *Free Radical Biology and Medicine*, vol. 52, no. 10, pp. 2120–2127, 2012.

[40] I. Khan, S. J. A. Shah, S. A. Ejaz et al., "Investigation of quinoline-4-carboxylic acid as a highly potent scaffold for the development of alkaline phosphatase inhibitors: synthesis, SAR analysis and molecular modelling studies," *RSC Advances*, vol. 5, no. 79, pp. 64404–64413, 2015.

[41] S. Gowda, P. B. Desai, V. V. Hull, A. A. Math, S. N. Vernekar, and S. S. Kulkarni, "A review on laboratory liver function tests," *The Pan African Medical Journal*, vol. 3, p. 17, 2009.

[42] B. D. Nelson, "Hepatic lysosome and serum enzyme alterations in rats exposed to high altitude," *American Journal of Physiology Legacy Content*, vol. 211, no. 3, pp. 651–655, 1966.

[43] S. Li, H.-Y. Tan, N. Wang et al., "The role of oxidative stress and antioxidants in liver diseases," *International Journal of Molecular Sciences*, vol. 16, no. 11, pp. 26087–26124, 2015.

[44] O. Uemura, M. Honda, T. Matsuyama et al., "Age, gender, and body length effects on reference serum creatinine levels determined by an enzymatic method in Japanese children: a multicenter study," *Clinical and Experimental Nephrology*, vol. 15, no. 5, pp. 694–699, 2011.

[45] R. M. Morsi, N. El-Tahan, and A. M. El-Hadad, "Effect of aqueous extract Mangifera indica leaves, as functional foods," *Journal of Applied Sciences Research*, vol. 6, no. 6, pp. 712–721, 2010.

Hindawi
BioMed Research International
Volume 2021, Article ID 5561129, 15 pages
https://doi.org/10.1155/2021/5561129

Research Article

Molecular Docking and Simulation Studies of Antidiabetic Agents Devised from Hypoglycemic Polypeptide-P of *Momordica charantia*

Rawaba Arif,[1] **Sajjad Ahmad**,[2] **Ghulam Mustafa**,[1] **Hafiza Salaha Mahrosh**,[1] **Muhammad Ali**,[3] **Muhammad Tahir ul Qamar**,[4] **and Hafiza Rabia Dar**[5]

[1]*Department of Biochemistry, Government College University, Faisalabad 38000, Pakistan*
[2]*Department of Health and Biological Sciences, Abasyn University, Peshawar, Pakistan*
[3]*Department of Biotechnology, Akhuwat Faisalabad Institute of Research Science and Technology, Faisalabad 38000, Pakistan*
[4]*College of Life Science and Technology, Guangxi University, Nanning, China*
[5]*Department of Biochemistry, University of Agriculture, Faisalabad 38040, Pakistan*

Correspondence should be addressed to Ghulam Mustafa; gmustafa_uaf@yahoo.com

Received 25 February 2021; Revised 30 August 2021; Accepted 4 September 2021; Published 20 September 2021

Academic Editor: Dorota Formanowicz

Diabetes mellitus termed as metabolic disorder is a collection of interlinked diseases and mainly body's inability to manage glucose level which leads to cardiovascular diseases, renal failure, neurological disorders, and many others. The drugs contemporarily used for diabetes have many inevitable side effects, and many of them have become less responsive to this multifactorial disorder. *Momordica charantia* commonly known as bitter gourd has many bioactive compounds with antidiabetic properties. The current study was designed to use computational methods to discover the best antidiabetic peptides devised from hypoglycemic polypeptide-P of *M. charantia*. The binding affinity and interaction patterns of peptides were evaluated against four receptor proteins (i.e., as agonists of insulin receptor and inhibitors of sodium-glucose cotransporter 1, dipeptidyl peptidase-IV, and glucose transporter 2) using molecular docking approach. A total of thirty-seven peptides were docked against these receptors. Out of which, top five peptides against each receptor were shortlisted based on their S-scores and binding affinities. Finally, the eight best ligands (i.e., LIVA, TSEP, EKAI, LKHA, EALF, VAEK, DFGAS, and EPGGGG) were selected as these ligands strictly followed Lipinski's rule of five and exhibited good ADMET profiling. One peptide EPGGGG showed activity towards insulin and SGLT1 receptor proteins. The top complex for both these targets was subjected to 50 ns of molecular dynamics simulations and MM-GBSA binding energy test that concluded both complexes as highly stable, and the intermolecular interactions were dominated by van der Waals and electrostatic energies. Overall, the selected ligands strongly fulfilled the drug-like evaluation criterion and proved to have good antidiabetic properties.

1. Introduction

Diabetes mellitus (DM) is widely known as a rising multifactorial disease reaching epidemic level. It has been affecting every age group without any discrimination [1]. It has been estimated by the International Diabetes Federation that almost 415 million people were suffering from diabetes in the year 2015, and by the year 2040, this will exceed to 640 million [2]. There are two main types of diabetes (i.e., type 1 and type 2). In type I DM, the body stops producing insulin, and in type II, there is a defect in insulin secretion and its action [3]. Diabetes can be treated by healthy dietary intake, regular exercise, and use of synthetic or natural drugs and maintaining a healthy lifestyle [4]. Present therapies are effective in managing diabetes but have many side effects. Limitations of current therapies are not just escalating the diabetes prevalence but also crossing the limits of economical budget. All these effects are demanding safer, efficient,

easy to administrate, and budget-friendly treatment [5]. The traditional approach of treatment involves antidiabetic compounds from different plant species, and it is catching more and more attention as natural drugs show fewer side effects compared to synthetic drugs [6]. It has been estimated that almost 1200 plant species have been identified which are comprised of compounds with promising hypoglycemic activity. Plant species with respective bioactivity have also been scrutinized to find exact lead compounds for desirable activity [7].

Momordica charantia is commonly known as bitter gourd. Its extract has been known for effectively lowering the blood glucose level [8]. There are many hypoglycemic compounds isolated from *M. charantia* including insulin-like peptides, vicine, polypeptide-P, alkaloids, charantin, sterol glycosides, mcIRBP, triterpenoids, cucurbutanoid compounds, flavonoids, and phenols, and all these compounds have hypoglycemic activity. Water-soluble proteins (MC1, MC6, MC6.1, MC6.2, and MC6.3 and MC2–1-5) and insulin receptor- (IR-) binding protein all have antidiabetic activity [9]. Due to antihyperglycemic activity of *M. charantia*, its consumption as a dietary source and use in traditional medicines has made it more attractive for the advanced research [10]. In a study, Elekofehinti et al. [11] have reported that *M. charantia* have many bioactive compounds such as charantin, cucurbitacin, and momordicoside D which have antidiabetic properties, and all these compounds belong to saponin class. Similarly, Shivanagoudra et al. [12] isolated 3β,7β,25-trihydroxycucurbita-5,23(E)-dien-19-al, charantal, charantoside XI, and 25ξ-isopropenylchole 5,6-ene-3-O-D-glucopyranoside from the fruit of *M. charantia* and used in molecular docking studies. The compounds were found to have antidiabetic properties.

DM is a complicated disease because it can be caused by defects in many organs, proteins, and enzymes [13]. Due to complex nature of this disease, one cannot rely on a single experimental model and also single treatment cannot circumvent this multifactorial disease. The experimental models are the protein receptors which are involved in the regulation of glucose throughout the body such as insulin receptor and sodium-glucose cotransporter 1 and 2 [14]. Insulin receptor (IR) is a member of the protein tyrosine kinase family and a transmembrane signaling protein. IR has many crucial regulatory activities regarding cell growth, differentiation, and metabolism. Its role in the regulation of glucose homeostasis discriminates it from other members of the family [15]. Inactivation of insulin receptor by knocking out its gene leads towards the loss of insulin secretion and glucose tolerance. The studies have clearly defined the role of IR in glucose homeostasis and showed its importance in the treatment of DM [15]. Studies also reported that an altered insulin receptor activity has been indicated in type I and type II DM [16]. Sodium-glucose cotransporter 1 (SGLT1) plays a very important role in the reabsorption of glucose by facilitated diffusion from the kidney and intestine [17]. It has been reported that alteration in SGLT1 leads towards the defects in reabsorption of glucose from the kidney and intestine. Such studies have indicated that inhibition of SGLT1 might be effective in the treatment of DM [18].

In the current study, four proteins were used as target receptors including IR, SGLT1, DPP-IV, and GLUT2 proteins. The aim of the study was to explore hypoglycemic peptides devised from polypeptide-P of *M. charantia* using in silico approaches. The selected peptides were scrutinized through Lipinski's rule of five and ADMET profiling. Finally, the ligands which fulfilled all these criteria are referred as potential antihyperglycemic agents. It is hypothesized that the selected peptides as antidiabetic agents would be better and safe alternate of currently available treatments of DM. The findings of this study would be employed as a novel approach for screening of antidiabetic drugs.

2. Materials and Methods

Molecular docking has accelerated the drug discovery by providing the structure-based interactions between ligand and receptor protein. A total of thirty-seven peptides from polypeptide-P of *M. charantia* were prepared including tetra-, penta-, and hexapeptides. These receptor proteins were selected based on their key roles in DM and in the maintenance of glucose homeostatic. This study involves the docking of thirty-seven peptides devised from polypeptide-P of *M. charantia* against IR as agonists and against SGLT1, DPP-IV, and GLUT2 as inhibitors. The docking analysis was performed using Molecular Operating Environment (MOE) software [19].

2.1. Retrieval of 3D Structures of Receptor Proteins. The three-dimensional (3D) structures of IR (PDB ID: 1IR3) [20], SGLT1 (PDB ID: 3DH4) [21], and human dipeptidyl peptidase-IV (PDB ID: 4A5S) [22] as receptor proteins were retrieved from the RCSB Protein Data Bank (https://www.rcsb.org/) in .pdb format [23] while the 3D structure of GLUT2 which was predicted in our previous study [24] was also used as a target protein.

2.2. Refinement of Receptor Proteins. Protein structures of receptor proteins were refined using MOE software before docking studies. The receptor proteins were prepared and optimized by removing ligands and water molecules. The receptor proteins were also energy minimized, and 3D protonation was done using parameter force field gradient: 0.05.

2.3. Ligand Selection and Database Preparation. The protein sequence of polypeptide-P from *M. charantia* was retrieved from NCBI's Entrez Protein under accession No. ADO14327.1. Tetra-, penta-, and hexapeptides were devised from the polypeptide-P, and their 3D structures were prepared using the ChemSketch software in MOL format [25]. The peptides were energy minimized using MOE.

2.4. Molecular Docking. Molecular docking analysis was carried out to identify the best agonists of IR and inhibitors of SGLT1, DPP-IV, and GLUT2. The site finder tool of MOE was used to predict the active sites of both receptor proteins. The docking analysis was done using default parameters (i.e., rescoring 1: London dG; retain: 10; refinement: force field; rescoring 1: London dG; retain: 10). The most appropriate protein-ligand interactions were selected on the basis

of best S-scores and binding interactions. MOE docking algorithm poses peptides within the catalytic pocket of the receptor protein with various orientations and conformational degrees of freedom. The docking analysis predicts suitable structural interactions of ligand and receptor protein based on combined scoring functions (i.e., ligand shape, electrostatic compatibility with the target, solvation effects, binding energies, and enthalpy and entropic effects, most stable binding mode with minimum energy, number of hydrogen bonds, values of root mean square deviation (RMSD), and S-scores) [26].

2.5. Molecular Dynamics Simulations. MD simulations were conducted using the AMBER20 suite of molecular dynamics program with the force filed FF14SB [27, 28]. AMBER force field (GAFF) using the Antechamber program was used to generate force-field parameters for the ligand molecules [29, 30]. The studied systems were then solvated by immersing each complex in a cubic box of TIP3P water molecules with a 10 Å solute-wall distance. The net charge on the complex protein was neutralized by the addition of Na^+ ions. The energies of the solvated systems were minimized before undergoing molecular dynamics simulations. All the systems were subjected to 1,500 steps of the steepest descent algorithm and 1,000 steps of the conjugate gradient algorithm with a nonbonded cutoff of 8 Å. Standard MD simulation protocol was followed consisting of an initial heating period of 100 ps starting slowly from 0 K to a temperature of 300 K and pressure of 1 atm. Following the heating procedure, each complex system underwent 100 ps equilibration at a constant temperature of 300 K. Equilibration was followed by a production run of 5 ns for the undocked protein and 12 ns each for all the docked complexes. The Ewald summation method was applied to treat long-range electrostatic interactions. PTRAJ module of AMBER was utilized to generate output files for analysis [31]. The conformational entropy evaluation (normal mode analysis) requires large amounts of CPU resources. Therefore, the approximation of the calculation of the binding free energy by removing this term from the MM-GBSA equation has been widely used, including in this study, as the removal of the entropic evaluation can be considered for the analysis and comparison of structurally similar compounds. All the trajectories were used for the calculation. The Molecular Mechanics Generalized Born Surface Area (MM-GBSA) method [32] with the MMPBSA.py script was used to calculate the complex binding energy [33]. The MM-GBSA energy values of the 50 ns period were calculated from the representative 100 frames. All structures were visualized by UCSF Chimera [34]. The solvent-accessible surface area (SASA) was performed using a visual molecular dynamics tool [35].

2.6. Drug Scan and ADMET Profiling. The best selected ligands must fulfill the criteria of drug scan through Lipinski's rule of five (Ro5) [36]. The peptides selected on the basis of Ro5 are considered safe. admetSAR is an online available webserver. It is used to check ADMET-related properties of selected ligands including pharmacokinetics of drugs in the human body including absorption, distribution, metabolism, excretion, and toxicity. Ligands that accomplished all these parameters are accepted as potential drug candidates [37].

3. Results

The docking analysis was carried by the MOE algorithm using devised peptides against IR, SGLT1, DPP-IV, and GLUT2. The top five peptides were selected in each analysis based on their interaction patterns and energy validations.

3.1. Interaction Analysis. For insulin receptor, the top five ligands were selected based on their S-scores and interaction patterns. Results have pointed out that all the five ligands have the efficiency to bind with IR. Amino acids that were unanimous to interact with at least three peptides were referred as interacting amino acids. The peptide KDDGHL showed the best interactions (binding score: -18.56) with the IR receptor, and Ser1270, Asp1143, Glu1108, Glu1115, and His1058 were found to be the leading interactive residues in these interactions (Figure 1(a)). The binding mode of the KDDGHL peptide within the binding pocket of IR is shown in Figure 1(b). Chaetochromin was also docked against IR as a positive control because chaetochromin has been reported for its antidiabetic activity [38]. The chaetochromin showed interactions with Arg*B*1061, Ser*A*151, and Cys*B*1056. The interactions and binding pattern of chaetochromin have been shown in Figure S1. The chaetochromin showed an S-score of -19.11 and RMSD of 1.89 which is comparable with the best selected peptide in this study.

The S-scores, RMSD values, and interacting amino acids of the top five peptides with IR are given in Table 1. All selected ligands showed strong interactions with Ser1270, Asp1143, Glu1108, Glu1115, His1057, Thr1345, and Thr1145. These interactions play a vital role in the determination of stability of the ligand-receptor complex in terms of hydrogen bond and hydrophobic and electrostatic interactions. All these interacting amino acids are present in the catalytic site of the receptor protein. Following KDDGHL, the interactions and binding patterns of the next three best peptides have been shown in Figures S2 to S4 of the Supplementary file.

The binding pocket of SGLT1 receptor protein contains Asn267, Tyr138, Tyr263, Ser368, and Thr431 as main interacting amino acids. In the current study, out of 37 docked ligands, the top five ligands with the best S-scores and interactions with these active amino acids are given in Table 1. The peptide ESIRD showed best interactions (binding score: -23.81) with the SGLT1 receptor, and Thr431, ser368, Gln428, Asn142, Ser364, Ser66, Lys294, Gln69, and Glu88 were found to be the leading interactive residues in these interactions (Figure 2(a)). The binding mode of the ESIRD peptide within the binding pocket of SGLT1 is shown in Figure 2(b). The other four peptides DSRHR, RRKKV, and PTRHM with docking scores of -23.64, -20.64, and -19.60 showed best interactions with active amino acids of the binding pocket of SGLT1 (Figures S5-S7 of the Supplementary file). Phlorizin has been reported as an inhibitor of SGLT1 [39] and therefore selected as a positive

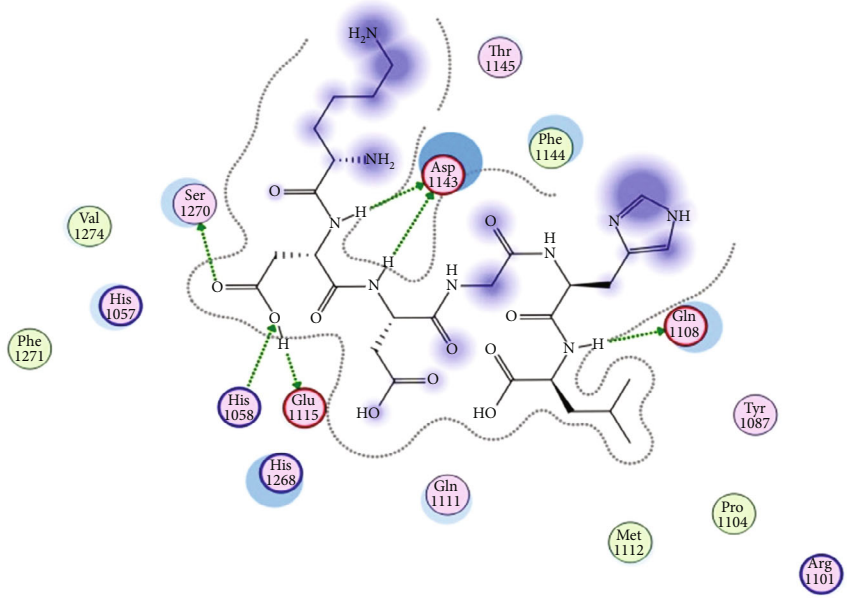

(a)

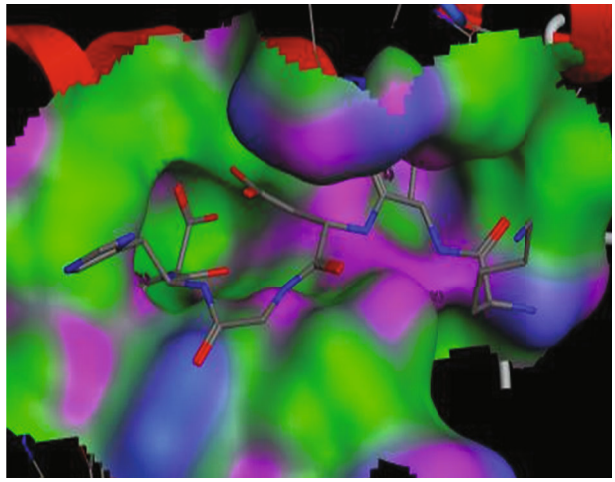

(b)

Figure 1: Docking of KDDGHL peptide with insulin receptor. (a) Interactions of peptide with IR. In these interactions, His1058 is a basic amino acid and acting as a sidechain donor. Glu1108, Glu1115, and Asp1143 are acidic amino acids and acting as sidechain acceptors. (b) Binding pattern of KDDGHL with the binding pocket of IR.

control in this study. The peptides reported in this study showed better S-scores compared to the reported drug phlorizin (i.e., S-score of -18.25, RMSD of 1.42). The phlorizin showed interactions with amino acids Asn267, Ser68, Tyr263, Gln69, and Asn142. The interactions and binding patterns of phlorizin with SGLT1 have been shown in Figure S8 of the Supplementary file.

Similarly, the library of devised peptides was also docked against DPP-IV and GLUT2 receptor proteins. The peptide PTRHM interacted with Gln268, Thr375, and Asn371 amino acids of DPP-IV with an S-score of -10.11 (Figure S9). The interactions and binding patterns of the other two peptides, i.e., RRKKV and KDDGHL with DPP-IV, have been shown in Figures S10 and S11. The peptide RRKKV interacted with Met174, Glu361, and Arg432 amino acids of GLUT2 receptor protein and exhibited the S-score of -10.60 (Figure S12). The interactions and binding patterns of the other two peptides, i.e., RSIHEP and ERFDSG with GLUT2, have been shown in Figures S13 and S14. The detail of interactions (i.e., interacting amino acids, S-scores, and RMSD values) of the top five peptides against DPP-IV and GLUT2 as receptor proteins has been given in Table 1.

The interactions and binding patterns of peptides LIVA with IR and DFGAS with SGLT1 receptor proteins are shown in Figures 3 and 4, respectively. Both peptides were found best among all selected peptides on the basis of their pharmacokinetic parameters which are important for the bioavailability of compounds as drugs.

Table 1: Property profile of selected peptides against five selected receptor proteins.

Sr. No.	Peptide	Receptor	S-score	RMSD	Interacting amino acids
1	KDDGHL	IR	-18.56	2.75	Ser1270, Asp1143, Glu1108, Glu1115, His1057
2	EPGGGG	IR	-16.71	1.85	Arg B1026. Glu A186, Asp B1343, His B1057, Lys B1147, Ala B1050, Ser A187
3	TSEP	IR	-15.66	1.21	Asp1143, Thr1145, Glu1115, Arg1101, Glu1108
4	VAEK	IR	-15.53	2.29	Glu1115, His1058, Ser1270, Asp1143, Phe1144, Glu1108
5	LIVA	IR	-14.00	1.73	Thr A178, His B1057, Cys B1056, Val B1059, Glu B1077, Lys B1147
6	ESIRD	SGLT1	-23.81	2.86	Thr431, ser368, Gln428, Asn142, Ser364, Ser66, Lys294, Gln69, Glu88
7	DSRHR	SGLT1	-23.64	2.46	Thr431, Ser368. Gln428. Ser91, Lys294, Ser365, Gln268, Asn267, Asn64, Ser66
8	RRKKV	SGLT1	-20.64	2.92	Thr431, Asn260, Asn267, Tyr263, Asn64, Ser435
9	PTRHM	SGLT1	-19.60	1.83	Tyr263, Gln68, Ala63, Ser365
10	DFGAS	SGLT1	-9.3259	1.5980	Asp189, Tyr176
11	PTRHM	DPP-IV	-10.1067	2.5395	Gln268, Thr375, Asn371
12	RRKKV	DPP-IV	-9.9189	1.7598	Val185, Asn267, Tyr269
13	KDDGHL	DPP-IV	-9.4991	1.4528	Ser368, Asn267, Val185
14	RSIHEP	DPP-IV	-9.0877	1.7136	Asn371, Val185
15	VAEK	DPP-IV	-8.1677	2.3228	Ser59, Ala63, Ser368
16	RRKKV	GLUT2	-10.5970	1.3552	Met174, Glu361, Arg432
17	RSIHEP	GLUT2	-10.5171	2.4307	Met174, Glu361
18	ERFDSG	GLUT2	-9.6986	1.7398	Gln429, Phe421
19	KDDGHL	GLUT2	-9.5645	1.5598	Glu282
20	PTRHM	GLUT2	-9.2187	1.4949	Arg432

3.2. Molecular Dynamics Simulation Study. The dynamics stability of the receptors (i.e., IR and SGLT1) in the presence of the filtered peptides was investigated by running 50 ns of molecular dynamics simulations. The structural stability of receptors was evaluated first by calculating root mean square deviation (RMSD) analysis, which computes structural deviations by overlapping simulation snapshots over docking reference snapshot based on carbon alpha atoms. Both complexes were revealed stable as the RMSD was in good acceptable range (Figure 5(a)). The RMSD plot of both complexes was found very consistent, and no major deviations were reported. The maximum RMSD touched by DFGAS-SGLT1 is around 2.2 or 2.3 Å whereas for LIVA-Insulin receptor, the maximum RMSD noticed is 3 Å. Next, root mean square fluctuations (RMSFs) were calculated for the docked receptors. Consistent with the RMSD analysis, RMSF results indicated the stable nature of complexes (Figure 5(b)). The RMSF for complexes is within 3 Å though some residues fluctuation was observed. The RMSFs correspond to the receptor loop regions and have no significant impact on the peptide bonding. Also, radius of gyration (RoG) analysis was performed to check the compactness of the complexes (Figure 5(c)). The RoG results are in coherence with the RMSD; the systems are highly compact with exception of few minor deviations. Both RoG systems fluctuated around 45 Å. The systems were seen in good equilibrium towards the end of simulation time.

Further, binding free energies of complexes were estimated as tabulated in Table 2. As can be seen in the table, both electrostatic and van der Waals energy are contributing significantly to overall system stabilization. The van der Waals seems to be playing a major role in the ligand stability at the docked site. Opposed, the solvation energy is noncontributing majorly because of polar solvation energy. The nonpolar energy term though plays a favorable part in the complex formation. Overall, both the systems acquired highly significant net binding energy values, i.e., LIVA-Insulin (-93.38 kcal/mol) and DFGAS-SGLT1 (-62.85 kcal/-mol). The individual contribution of each interacting residue of the receptor to ligand was further determined by decomposing the net MM-GBSA binding free energy into residues of the receptor molecules. It was revealed that most of the residues near the binding site of the ligands contributed significantly in stabilizing the ligands as can be seen by lower binding energy value. The ligand interacting residue binding energy value is given in Table 3. The SASA analysis was performed to investigate the surface of the system accessible to the solvent (Figure S15 of the Supplementary file).

3.3. Drugability and ADMET Profiling. Lipinski's rule of five indicates drug-like characteristics or drug potency of proposed compounds based on parameters such as molecular mass (<500 Dalton), molar refractive index (40-130), partition coefficient (Log$P \leq 5$), hydrogen bond donors ($\leq$5), and hydrogen bond acceptors ($\leq$10). This rule basically distinguishes the compounds based on drug-like and non-drug-like properties. Only those compounds that fulfill these criteria are considered as good drug candidates. In this study, a total of twenty ligands were selected based on their best interaction patterns with active amino acids of the target proteins, S-scores, and energy validations. Out of twenty selected ligands, only eight peptides fulfilled the criteria of

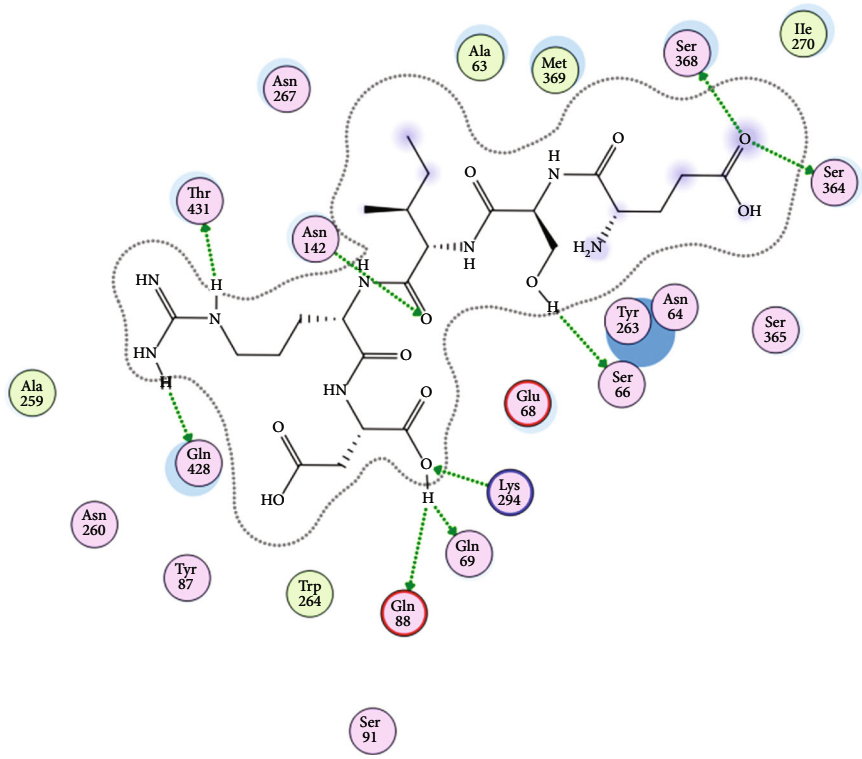

(a)

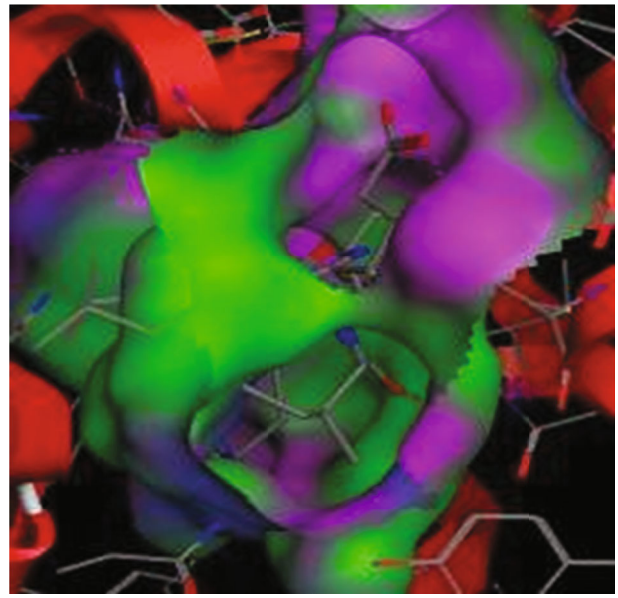

(b)

Figure 2: Docking of ESIRD peptide with SGLT1 receptor. (a) Interactions of peptide with SGLT1. In these interactions, Ser66, Gln69, Ser364, Ser368, Gln428, and Thr431 are polar amino acids and acting as sidechain acceptors. Asn142 is also a polar amino acid but acting as a sidechain donor. Lys294 and Glu88 are basic and acidic amino acids and acting as sidechain donor and acceptor, respectively. (b) Binding pattern of ESIRD with the binding pocket of SGLT1.

being good drug candidates according to Lipinski's Ro5 (Table 4). Six tetrapeptides, one pentapeptide, and one hexapeptide were revealed to be good agonists of IR. The hexapeptide EPGGGG has shown good binding affinity with both IR and SGLT1 receptors. The peptide (VAEK) showed good binding affinity with IR and DPP-IV. Similarly, the peptide (DFGAS) showed good binding affinity with IR, SGLT1, and DPP-IV. Out of eight, seven peptides violated only one parameter of Lipinski's rule of five but one peptide (LIVA) did not violate any rule and therefore revealed as a

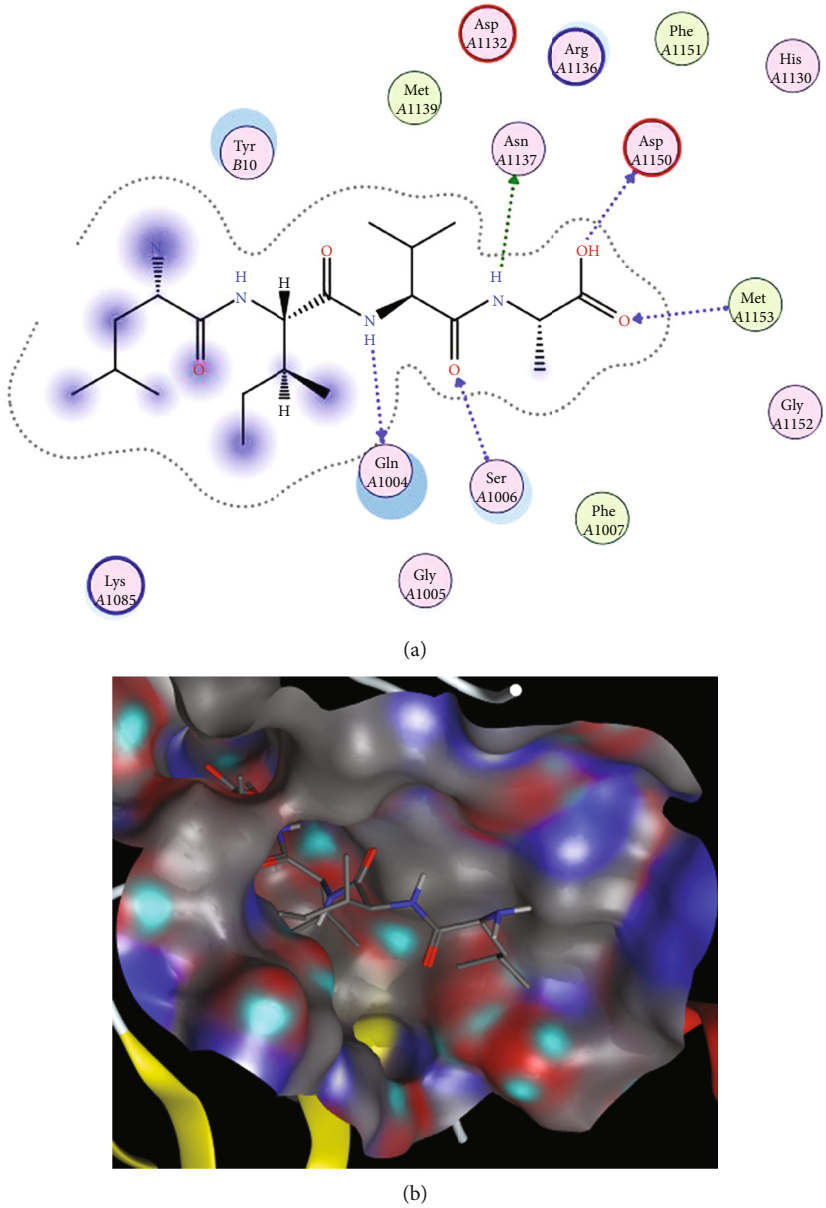

Figure 3: Docking of LIVA peptide with insulin receptor. (a) Interactions of LIVA with IR. In these interactions, Gln*A*1004 and Ser*A*1006 are polar amino acids and acting as backbone acceptor and backbone donor, respectively. Asn*A*1137 is a polar amino acid and acting as a sidechain acceptor. The amino acid Asp*A*1150 is acidic in nature and acting as backbone acceptor while Met*A*1153 (greasy in nature) is acting as backbone donor. (b) Binding pattern of LIVA with the binding pocket of IR.

best potential agonist of IR. The structures of these eight peptides are given in Figure 6. On the basis of Lipinski's Ro5, these peptides could be accepted for their reasonable oral bioavailability.

The best selected peptides were further evaluated through admetSAR server to check their pharmacokinetics or ADMET (absorption, distribution, metabolism, excretion, and toxicity) profiling. The results of admetSAR have suggested that all the selected ligands are non-Ames toxic and noncarcinogens (Table 5). The evaluation of ADMET profiling of these peptides has predicted that they are tolerable and safe, and therefore, these peptides could be referred as efficient drug candidates against selected receptor proteins.

4. Discussion

In silico screening of natural compounds for drug designing has become the need of the hour due to expensive, tiresome, and laborious screening methods. A giant amount is wasted due to directionless laboratory procedures which lack structural understanding of drugs and target molecules. On the other hand, computational biology reduces the risk of late-stage failure of a drug [40]. In the current study, *M. charantia* was selected as a source of antidiabetic agent. It has been reported that a series of fractions from the fruit of *M. charantia* have been used to treat the diabetic rats. Consequently, those fractions improved the insulin signaling in diabetic

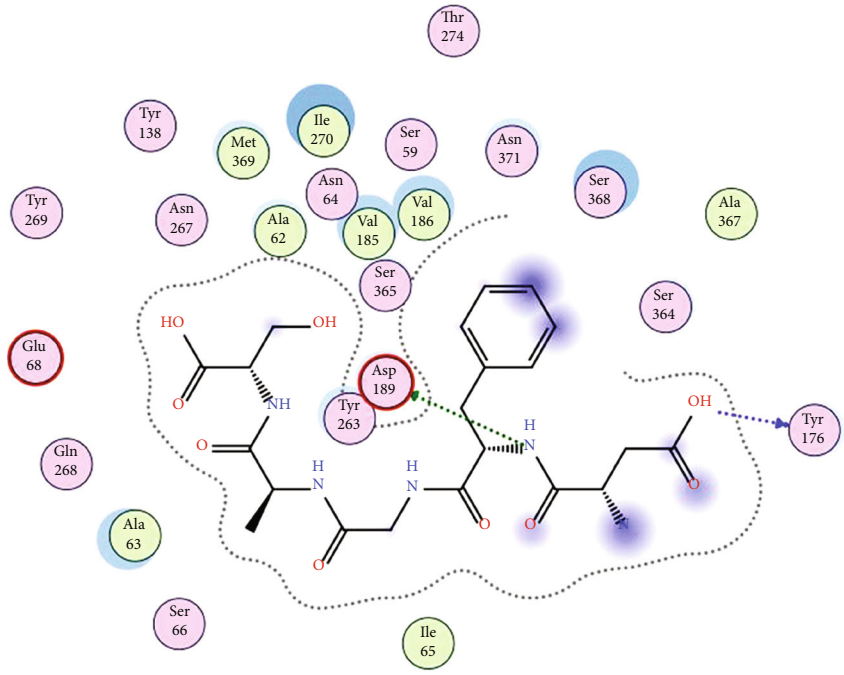

(a)

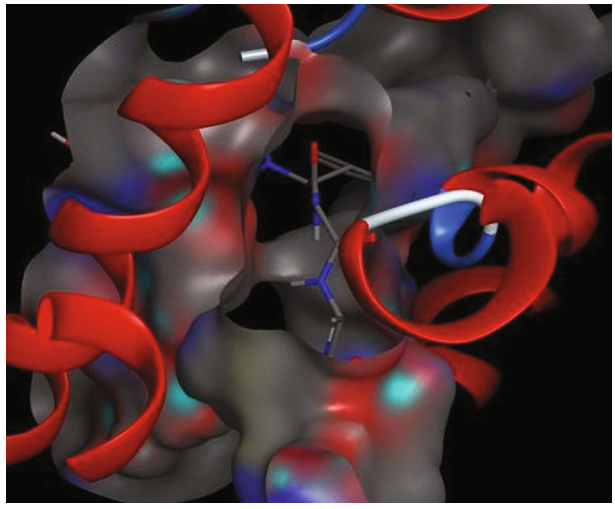

(b)

Figure 4: Docking of DFGAS peptide with SGLT1. (a) Interactions of DFGAS with SGLT1. In these interactions, the amino acids Tyr176 and Asp189 are polar and acidic amino acids and acting as backbone and sidechain acceptors, respectively. (b) Binding pattern of DFGAS with SGLT1.

rats [41]. In the current study, four target receptors were selected (i.e., IR, SGLT1, DPP-IV, and GLUT2) due to their crucial roles in maintaining the glucose level in the body [42]. Interestingly, the finding of small molecules which can elicit the IR signaling pathway and inhibit SGLT1, DPP-IV, and GLUT2 would be great alternative of insulin to treat DM.

The docking analysis of thirty-seven peptides devised from polypeptide-P of *M. charantia* was performed against IR, and the top five peptides were selected based on their scoring and binding patterns. The amino acids that were unanimously involved in structural interactions of peptides and receptors were found to be Ser1270, Asp1143, Glu1108, Glu1115, His1057, Tyr1087, and Thr1145. These amino acids are repeatedly involved in the binding interaction of each peptide with receptor protein and therefore adapted as active amino acids of the catalytic cleft. In a similar study, the antidiabetic potential of cowpea peptides was determined which can act as agonists of insulin and the peptides were proved to activate the IR signaling pathway [43]. Many previous studies have proved that *M. charantia* contains many peptides which are involved in the lowering of blood glucose level, and these studies support our findings [44].

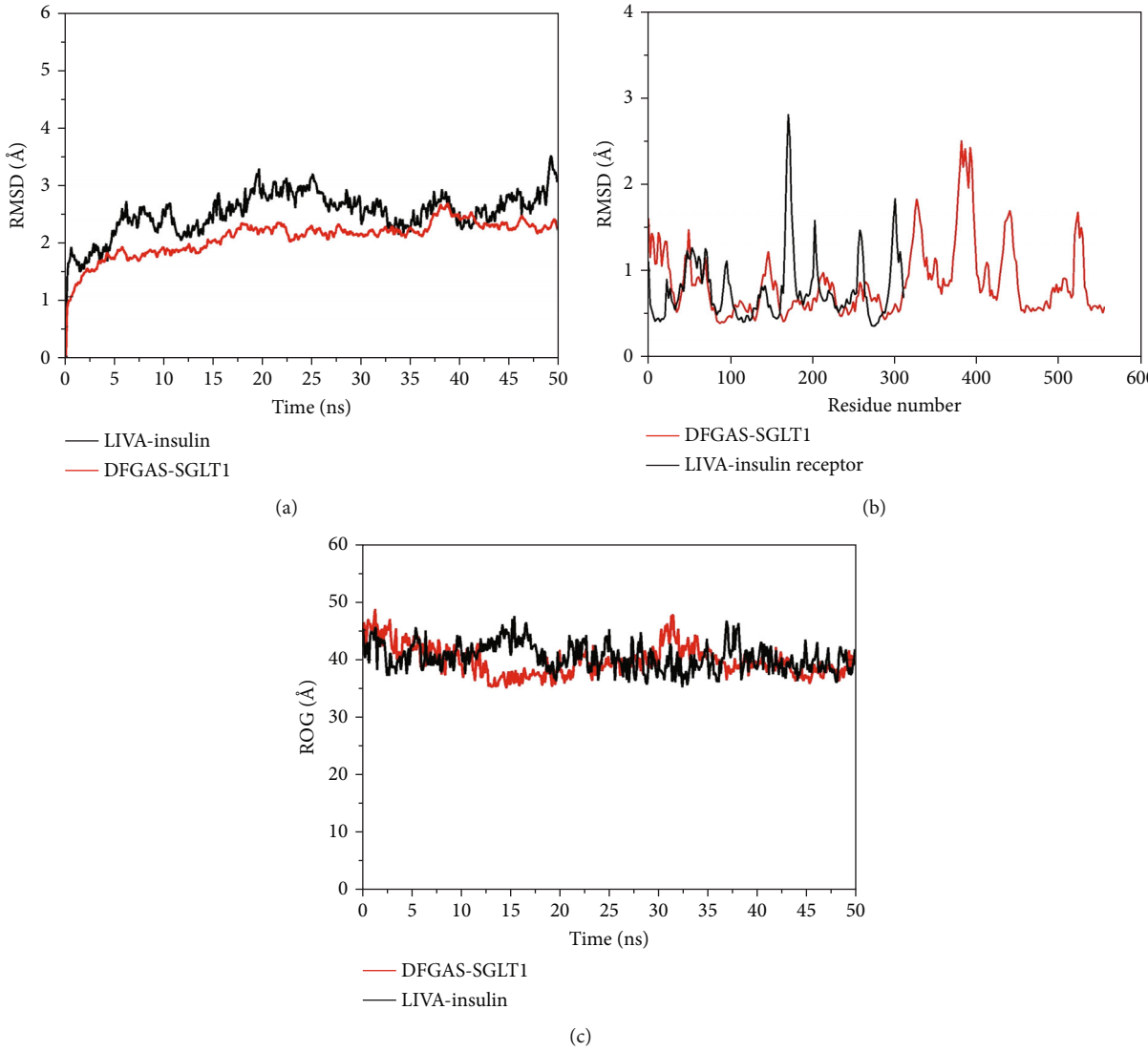

Figure 5: Structural stability evaluation of complexes based on carbon alpha atoms. (a) RMSD, (b) RMSF, and (c) RoG. The residue numbering is adjusted from 1 to the end.

Table 2: MM-GBSA binding free energy estimation (all the values are described in kcal/mol).

Energy component	LIVA-Insulin	DFGAS-SGLT1
van der Waals	-66.15	-50.27
Electrostatic	-52.45	-45.12
Polar solvation	35.69	39.41
Nonpolar solvation	-10.47	-6.87
Net gas phase	-118.6	-95.39
Net solvation	25.22	32.54
Net complex energy	-93.38	-62.85

Similarly, molecular docking of thirty-seven peptides was also performed against SGLT1 and the top five peptides were selected as potential ligands based on their interactions with active amino acids on the basis of their S-scores. From the docking analysis, Asn267, Tyr138, Tyr263, Ser368, and Thr431 were found to be active amino acids in the binding patterns with SGLT1. Previously, the interaction with Ser368 has been reported, and in the present study, Ser368 is repeatedly and actively involved in the binding patterns between receptor and selected ligands [45, 46]. Similarly, the SGLT1 inhibitor LX4211 ((2S,3R,4R,5S,6R)-2-(4-chloro-3-(4-ethoxybenzyl)phenyl)-6-(methylthio)tetrahydro-2H-pyran-3,4,5-triol) has been found to be involved in the inhibition of SGLT1 and consequently reduces the glucose absorption from the intestine. The results of these studies are in accordance with current findings. A number of antidiabetic peptides also have been reported from soy protein [47]. A great number of bioactive compounds from different parts of *M. charantia* have been found effective to treat diabetes. Shivanagoudra et al. [48] isolated two compounds (i.e., momordicoside G and gentisic acid 5-O-β-D-xyloside) and docked against α-amylase and α-glucosidase as receptor proteins. The momordicoside G showed the highest inhibition of

Table 3: Net MM-GBSA binding free energy decomposition into residues of the receptors. The values are provided in kcal/mol.

Residue	LIVA-Insulin	Residue	DFGAS-SGLT1
Gln1004	-2.54	Ala62	-1.51
Gly1005	-1..85	Ala63	0.47
Ser1006	1.58	Asn64	1.47
Phe1007	-1.64	Ile65	1.02
Lys1085	-1.36	Ser66	-2.48
Ser1086	-1.00	Gly68	-1.35
Asp1083	-3.45	Tyr138	-1.23
His1130	0.25	Tyr176	-1.00
Asp1132	-0.89	Val185	-1.85
Arg1136	-1.65	Asp189	-2.58
Asn1137	0.05	Tyr263	-1.55
Met1139	1.63	Asn267	-1.27
Asp1150	-2.54	Gln268	-1.20
Phe1151	-1.02	Tyr269	-2.04
Gly1152	-1.50	Ile270	-0.87
		Thr274	0.68
		Ser365	0.12
Met1153	-2.54	Ser364	-1.08
		Ala367	-1.36
		Met369	-1.54
		Asn371	1.02

Table 4: Pharmacokinetic parameters important for bioavailability of compound drug-likeness properties of selected peptides.

Peptides	Target	Molecular properties[†]						
		MW	HBD	HBA	nrotb	Log*P*	*A*	Violations
LIVA	IR	414.54	5	6	12	0.51	111.74	0
TSEP	IR	432.43	7	10	14	-3.21	103.31	1
EKAI	IR	459.54	7	7	16	-1.09	116.22	1
LKHA	IR	467.57	7	7	15	-0.99	121.46	1
EALF	IR	478.55	6	6	14	0.03	123.58	1
VAEK	IR/DPP-IV	445.51	7	7	15	-1.48	111.41	1
DFGAS	IR/SGLT1/DPP-IV	495.48	8	8	15	-3.30	118.13	1
EPGGGG	IR/SGLT1	472.45	7	10	18	-3.34	111.79	1
GDVEC	SGLT1	521.55	9	9	16	-3.11	121.41	2
DDPTG	SGLT1	503.47	8	9	17	-4.19	116.53	2
PTRHM	DPP-IV/GLUT2	640.77	11	10	19	-2.87	165.54	3
RRKKV	DPP-IV/GLUT2	685.88	14	10	26	-3.22	181.62	3
DTDEL	DPP-IV	591.57	10	10	19	-3.42	135.64	3

[†]Molecular properties were calculated using SwissADME, an online tool. MW: molecular weight; HBD: number of hydrogen bond donors; HBA: number of hydrogen bond acceptors; nrotb: number of rotatable bonds; Log*P*: the logarithm of octanol/water partition coefficient; *A*: molar refractivity.

α-amylase (70.5%), and gentisic acid 5-O-β-D-xyloside showed the highest inhibition of α-glucosidase (56.4%). In another study [49], the docking analysis of the compound nerolidol from *M. charantia* showed the best binding interactions with the diabetic enzyme glucokinase which is responsible to cause diabetes in humans.

The effectiveness and safety are the primary objectives for hunting a new drug as all drugs can help to combat diseases as well as cause harmful effects [50]. *In silico* analysis has played an increasingly significant part in the drug research and discovery by providing an effective way to assess multiple pharmacokinetics properties [51]. In this study, by taking into account all drug-like characteristics, only eight peptides were shortlisted (i.e., LIVA, TSEP, EKAI, LKHA, EALF, VAEK, DFGAS, and EPGGGG) followed by Lipinski's rule of five (Ro5). The peptide EPGGGG showed good binding affinity and efficacy for both IR and SGLT1 receptors. Some of the remaining ligands did not fulfill the

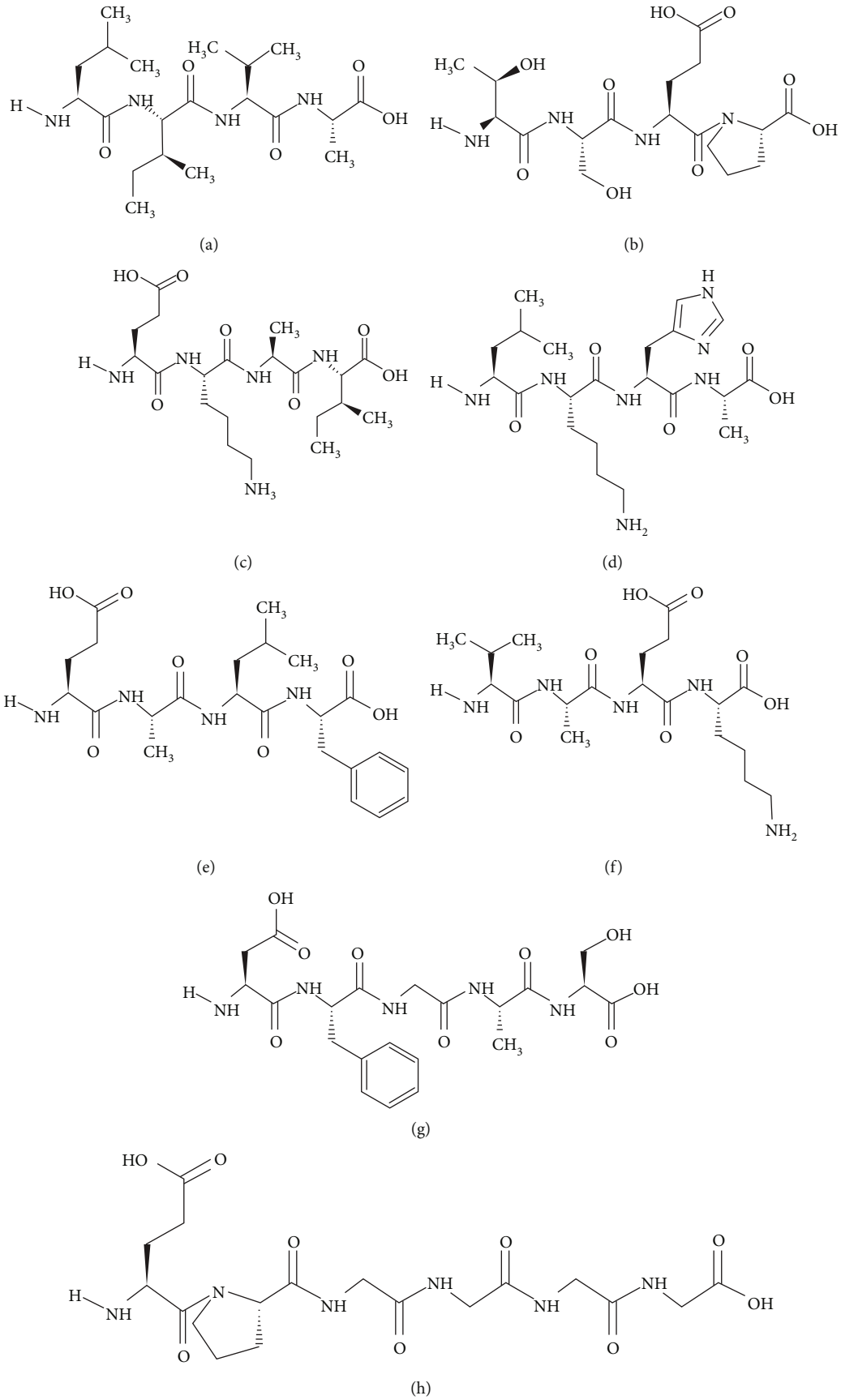

Figure 6: Structures of best selected peptides: (a) LIVA, (b) TSEP, (c) EKAI, (d) LKHA, (e) EALF, (f) VAEK, (g) DFGAS, and (h) EPGGGG.

Table 5: ADMET profiling enlisting absorption, metabolism, and toxicity-related drug-like parameters of best selected peptides.

	Peptides							
	LIVA	TSEP	EKAI	LKHA	EALF	VAEK	DFGAS	EPGGGG
Absorption								
BBB	+	+	+	+	−	+	+	+
HIA	−	−	−	+	+	−	−	+
Caco-2 permeability	Caco-2-Substrate	Caco-2-NS	Caco-2-Substrate	Caco-2-Substrate	Caco-2-Substrate	Caco-2-NS	Caco-2-NS	Caco-2-Substrate
PGS	NI	NI	NI	NI	NI	NI	NI	NI
PGI	NI	NI	NI	NI	NI	NI	NI	NI
ROCT	NI	NI	NI	NI	NI	NI	NI	NI
Metabolism								
CYP3A4 substrate	Substrate	NS	Substrate	Substrate	NS	NS	NS	Substrate
CYP2C9 substrate	NS	NS	Substrate	NS	NS	NS	NS	Substrate
CYP2D6 substrate	NS	NS	NS	NS	NS	NS	NS	NS
CYP3A4 inhibition	NI	NI	NI	NI	NI	NI	NI	NI
CYP2C9 inhibition	NI	NI	NI	NI	NI	NI	NI	NI
CYP2C19 inhibition	NI	NI	NI	NI	NI	NI	NI	NI
CYP2D6 inhibition	NI	NI	NI	NI	NI	NI	NI	NI
CYP1A2 inhibition	NI	NI	NI	NI	NI	NI	NI	NI
Toxicity								
Ames toxicity	NAT	NAT	NAT	NAT	NAT	NAT	NAT	NAT
Carcinogens	NC	NC	NC	NC	NC	NC	NC	NC

BBB: blood-brain barrier; HIA: human intestinal absorption; PGS: P-glycoprotein substrate; PGI: P-glycoprotein inhibitor; ROCT: renal organic cation transporter; NS: nonsubstrate; NI: noninhibitor; NAT: non-Ames toxic; NC: noncarcinogenic.

drug-like criteria as they violated two or more rules of Ro5. The eight selected ligands also passed the evaluation through ADMET drug profiling to predict the capability or incapability of these peptides as potential drugs DM.

Among the parameters predicted by admetSAR, the Log*P* value tells about the permeability of a compound through a lipid membrane, and for a potential drug, it should be ≤5. The number of hydrogen bond acceptors and hydrogen bond donors of a drug describes its ability to bind with other compound(s) that consequently define its solubility and permeability. Nonrotatable bonds explain the molecular flexibility and permeation rate of a drug candidate. CYP450 is a superfamily of heme-containing enzymes that facilitate the metabolism of drugs. There are five different isoforms of CYP450 (CYP 3A4, 2D6, 1A2, 2C9, and 2C19). The oxidation of a drug is necessary for its proper functioning and excretion from the body, and for this reason, the consideration of action of drugs against these enzymes is necessary [52]. All the top eight ligands shortlisted in this study are noninhibitors of CYP50 family enzymes which is good for their metabolism. The Ames test predicts whether a selected ligand causes DNA mutation(s) or not. All the top eight peptides were predicted as non-Ames toxic. Structural alerts (SAs) are the main components which are the mastermind behind certain toxicities and carcinogenic behaviors. For the first time, it was reported that there is strong connection between some structural alters and chemical mutagenicity in *Salmonella* sp. [53]. Therefore, admetSAR predicts toxicity and carcinogenicity of ligands based on SAs. In our current findings, all top eight ligands are non-Ames toxic and noncarcinogenic and, therefore, they are safe and tolerable. Finally, all the eight peptides were predicted as having potential drug-like characters by successfully fulfilling the ADMET profiling criteria. The selected ligands have good affinity for receptors and efficacy to active receptors and acting as agonists of IR and inhibitors of SGLT1, DPP-IV, and GLUT2.

The foremost goal of the current study was to target those proteins that act as receptors in the regulation of glucose level in the body. Any insertion, deletion, and/or substitution in the amino acid sequence of these receptor proteins can lead to a deleterious effect in the maintenance of glucose level. Currently, many antidiabetic drugs have been excessively used but their disastrous outcomes make them undesirable and unsafe to use. This alarming situation requires the discovery of antihyperglycemic compounds with minimal side effects and maximal efficacy, and therefore, in the current study, we have explored natural peptides with great affinity for receptors involved in glucose regulation. *In silico* drug discovery is expected hunting the drugs quicker, cheaper, and more effective, but in spite of all these pros, the computational biology techniques have some limitations as various tools give different results for the same analyses, and therefore, one cannot fully rely on the results without wet lab investigation and validation [54].

5. Conclusion

Diabetes mellitus is an inevitable disorder, and in spite of all the available treatments, its consequences are rapidly

enhancing epidemiologically. Protein-ligand docking and simulation approaches have greatly accelerated the discovery of novel antidiabetic agents. In the current study, using an in silico approach, we have discovered, designed, and proposed novel antidiabetic peptides for oral administration. Upon investigating dynamics stability, it was found that both complexes (i.e., LIVA-IR and DFGAS-SGLT1) were revealed to be stable as the RMSD values of both complexes were in good acceptable range. These ligands might reduce dependency on painful subcutaneous administration of insulin and on other drugs with a number of side effects. Out of thirty-seven peptides, the peptides LIVA, TSEP, EKAI, LKHA, EALF, VAEK, DFGAS, and EPGGGG were found to be the best ones as potential antidiabetic agents based on their interaction studies through molecular docking. These ligands were strictly evaluated through Lipinski's rule of five and ADMET profiling which strongly supported their antihyperglycemic properties, and therefore, these natural bioactive compounds would act as agonist of IR and inhibitors of SGLT1, DPP-IV, and GLUT2 and may lead to design potential drugs to combat diabetes with fewer or no side effects. A wet lab procedure has to be performed to further evaluate their activity as antidiabetic agents.

Data Availability

The data used to support the findings of this study are available from the corresponding author upon request.

Conflicts of Interest

The authors declare that they have no conflict of interest.

Acknowledgments

The authors would like to gratefully acknowledge the Department of Biochemistry, Government College University Faisalabad for providing space and facilities to accomplish this study.

Supplementary Materials

Figure S1: interactions (a) and binding pattern (b) of chaetochromin with IR as a positive control. Figures S2–S4: interactions and binding patterns of EPGGGG, TSEP, and VAEK peptides with IR. Figures S5–S7: interactions and binding patterns of DSRHR, RRKKV, and PTRHM peptides with SGLT1 receptor. Figure S8: interactions (a) and binding patterns (b) of phlorizin with SGLT1 receptor as a positive control. Figures S9–S11: interactions and binding patterns of PTRHM, RRKKV, and KDDGHL peptides with DPP-IV receptor. Figures S12–S14: interactions and binding patterns of RRKKV, RSIHEP, and ERFDSG peptides with GLUT2 receptor. Figure S15: SASA analysis of the systems. *(Supplementary Materials)*

References

[1] A. Misra, H. Gopalan, R. Jayawardena et al., "Diabetes in developing countries," *Journal of Diabetes*, vol. 11, no. 7, pp. 522–539, 2019.

[2] K. Papatheodorou, M. Banach, E. Bekiari, M. Rizzo, and M. Edmonds, "Complications of diabetes 2017," *Journal of Diabetes Research*, vol. 2018, Article ID 3086167, 4 pages, 2018.

[3] R. H. Houtkooper and J. Auwerx, "New life for antidiabetic drugs," *Nature*, vol. 466, no. 7305, pp. 443-444, 2010.

[4] D. LeRoith, G. J. Biessels, S. S. Braithwaite et al., "Treatment of diabetes in older adults: an endocrine society clinical practice guideline," *The Journal of Clinical Endocrinology & Metabolism*, vol. 104, no. 5, pp. 1520–1574, 2019.

[5] J. J. Gout-Zwart, L. A. de Jong, L. Saptenno, and M. J. Postma, "Budget impact analysis of metformin sustained release for the treatment of type 2 diabetes in the Netherlands," *PharmacoEconomics - Open*, vol. 4, no. 2, pp. 321–330, 2020.

[6] S. Marella and N. V. K. V. P. Tollamadugu, "Nanotechnological approaches for the development of herbal drugs in treatment of diabetes mellitus–a critical review," *IET Nanobiotechnology*, vol. 12, no. 5, pp. 549–556, 2018.

[7] C. Lankatillake, T. Huynh, and D. A. Dias, "Understanding glycaemic control and current approaches for screening antidiabetic natural products from evidence-based medicinal plants," *Plant Methods*, vol. 15, no. 1, pp. 1–35, 2019.

[8] E. L. Peter, F. M. Kasali, S. Deyno et al., "*Momordica charantia* L. lowers elevated glycaemia in type 2 diabetes mellitus patients: Systematic review and meta-analysis," *Journal of Ethnopharmacology*, vol. 231, pp. 311–324, 2019.

[9] Z. J. Li, J. C. Chen, Y. Y. Deng et al., "Two new cucurbitane triterpenoids from immature fruits ofMomordica charantia," *Helvetica Chimica Acta*, vol. 98, no. 10, pp. 1456–1461, 2015.

[10] Z. Li, A. Xia, S. Li et al., "The pharmacological properties and therapeutic use of bitter melon (Momordica charantia L.)," *Current Pharmacology Reports*, vol. 6, no. 3, pp. 103–109, 2020.

[11] O. O. Elekofehinti, E. O. Ariyo, M. O. Akinjiyan et al., "Potential use of bitter melon (*Momordica charantia*) derived compounds as antidiabetics: In silico and in vivo studies," *Pathophysiology*, vol. 25, no. 4, pp. 327–333, 2018.

[12] S. R. Shivanagoudra, W. H. Perera, J. L. Perez et al., "Cucurbitane-type compounds from *Momordica charantia*: Isolation, *in vitro* antidiabetic, anti-inflammatory activities and _in silico_ modeling approaches," *Bioorganic Chemistry*, vol. 87, pp. 31–42, 2019.

[13] J. Huang, Y. Xiao, P. Zheng et al., "Distinct neutrophil counts and functions in newly diagnosed type 1 diabetes, latent autoimmune diabetes in adults, and type 2 diabetes," *Diabetes/Metabolism Research and Reviews*, vol. 35, no. 1, article e3064, 2019.

[14] A. Soumyanath and S. Srijayanta, *In Vitro Models for Assessing Antidiabetic Activity*, CRC Press, Taylor & Francis, Boca Raton, FL, USA, 2005.

[15] R. A. Haeusler, T. E. McGraw, and D. Accili, "Biochemical and cellular properties of insulin receptor signalling," *Nature Reviews Molecular Cell Biology*, vol. 19, no. 1, pp. 31–44, 2018.

[16] C. R. Kahn and M. White, "The insulin receptor and the molecular mechanism of insulin action," *The Journal of Clinical Investigation*, vol. 82, no. 4, pp. 1151–1156, 1988.

[17] H. M. Salah, S. J. al'Aref, M. S. Khan et al., "Effects of sodium-glucose cotransporter 1 and 2 inhibitors on cardiovascular and kidney outcomes in type 2 diabetes: a meta-analysis update," *American Heart Journal*, vol. 233, pp. 86–91, 2021.

[18] J. A. Dominguez Rieg and T. Rieg, "What does sodium-glucose co-transporter 1 inhibition add: prospects for dual inhibition," *Obesity and Metabolism*, vol. 21, no. S2, pp. 43–52, 2019.

[19] S. Vilar, G. Cozza, and S. Moro, "Medicinal chemistry and the molecular operating environment (MOE): application of QSAR and molecular docking to drug discovery," *Current Topics in Medicinal Chemistry*, vol. 8, no. 18, pp. 1555–1572, 2008.

[20] S. R. Hubbard, "Crystal structure of the activated insulin receptor tyrosine kinase in complex with peptide substrate and ATP analog," *The EMBO Journal*, vol. 16, no. 18, pp. 5572–5581, 1997.

[21] S. Faham, A. Watanabe, G. M. Besserer et al., "The crystal structure of a sodium galactose transporter reveals mechanistic insights into Na+/sugar symport," *Science*, vol. 321, no. 5890, pp. 810–814, 2008.

[22] J. M. Sutton, D. E. Clark, S. J. Dunsdon et al., "Novel heterocyclic DPP-4 inhibitors for the treatment of type 2 diabetes," *Bioorganic & Medicinal Chemistry Letters*, vol. 22, no. 3, pp. 1464–1468, 2012.

[23] S. K. Burley, H. M. Berman, C. Bhikadiya et al., "Protein Data Bank: the single global archive for 3D macromolecular structure data," *Nucleic Acids Research*, vol. 47, no. D1, pp. D520–D528, 2019.

[24] H. S. Mahrosh, R. Mehmood, S. A. Bukhari, G. Afzal, and R. Arif, "Investigation of hypoglycemic peptides derived from conserved regions of adMc1 to reveal their antidiabetic activities," *BioMed Research International*, vol. 2021, Article ID 5550180, 8 pages, 2021.

[25] Z. Li, H. Wan, Y. Shi, and P. Ouyang, "Personal experience with four kinds of chemical structure drawing software: review on ChemDraw, ChemWindow, ISIS/Draw, and ChemSketch," *Journal of Chemical Information and Computer Sciences*, vol. 44, no. 5, pp. 1886–1890, 2004.

[26] H. S. Mahrosh, M. Tanveer, R. Arif, and G. Mustafa, "Computer-aided prediction and identification of phytochemicals as potential drug candidates against MERS-CoV," *BioMed Research International*, vol. 2021, Article ID 5578689, 7 pages, 2021.

[27] J. A. Maier, C. Martinez, K. Kasavajhala, L. Wickstrom, K. E. Hauser, and C. Simmerling, "ff14SB: improving the accuracy of protein side chain and backbone parameters from ff99SB," *Journal of Chemical Theory and Computation*, vol. 11, no. 8, pp. 3696–3713, 2015.

[28] J. Wang, R. M. Wolf, J. W. Caldwell, P. A. Kollman, and D. A. Case, "Development and testing of a general amber force field," *Journal of Computational Chemistry*, vol. 25, no. 9, pp. 1157–1174, 2004.

[29] M. Suleman, M. Tahir ul Qamar, S. Saleem et al., "Mutational landscape of Pirin and elucidation of the impact of most detrimental missense variants that accelerate the breast cancer pathways: a computational modelling study," *Frontiers in Molecular Biosciences*, vol. 8, 2021.

[30] M. A. Alamri, M. Tahir ul Qamar, O. Afzal, A. B. Alabbas, Y. Riadi, and S. M. Alqahtani, "Discovery of anti-MERS-CoV small covalent inhibitors through pharmacophore modeling, covalent docking and molecular dynamics simulation," *Journal of Molecular Liquids*, vol. 330, article 115699, 2021.

[31] D. R. Roe and T. E. Cheatham III, "PTRAJ and CPPTRAJ: software for processing and analysis of molecular dynamics trajectory data," *Journal of Chemical Theory and Computation*, vol. 9, no. 7, pp. 3084–3095, 2013.

[32] T. Hou, J. Wang, Y. Li, and W. Wang, "Assessing the performance of the MM/PBSA and MM/GBSA methods. 1. The accuracy of binding free energy calculations based on molecular dynamics simulations," *Journal of Chemical Information and Modeling*, vol. 51, no. 1, pp. 69–82, 2011.

[33] B. R. Miller III, T. D. McGee Jr., J. M. Swails, N. Homeyer, H. Gohlke, and A. E. Roitberg, "MMPBSA.py: an efficient program for end-state free energy calculations," *Journal of Chemical Theory and Computation*, vol. 8, no. 9, pp. 3314–3321, 2012.

[34] E. F. Pettersen, T. D. Goddard, C. C. Huang et al., "UCSF chimera—a visualization system for exploratory research and analysis," *Journal of Computational Chemistry*, vol. 25, no. 13, pp. 1605–1612, 2004.

[35] W. Humphrey, A. Dalke, and K. Schulten, "VMD: visual molecular dynamics," *Journal of Molecular Graphics*, vol. 14, no. 1, pp. 33–38, 1996.

[36] A. Daina, O. Michielin, and V. Zoete, "SwissADME: a free web tool to evaluate pharmacokinetics, drug-likeness and medicinal chemistry friendliness of small molecules," *Scientific Reports*, vol. 7, no. 1, pp. 1–13, 2017.

[37] F. Cheng, W. Li, Y. Zhou et al., "admetSAR: a comprehensive source and free tool for assessment of chemical ADMET properties," *Journal of Chemical Information and Modeling*, vol. 52, no. 11, pp. 3099–3105, 2012.

[38] G. Qiang, S. Xue, J. J. Yang et al., "Identification of a small molecular insulin receptor agonist with potent antidiabetes activity," *Diabetes*, vol. 63, no. 4, pp. 1394–1409, 2014.

[39] Y. Kashiwagi, T. Nagoshi, T. Yoshino et al., "Expression of SGLT1 in human hearts and impairment of cardiac glucose uptake by phlorizin during ischemia-reperfusion injury in mice," *PLoS One*, vol. 10, no. 6, article e0130605, 2015.

[40] A. S. Rifaioglu, H. Atas, M. J. Martin, R. Cetin-Atalay, V. Atalay, and T. Doğan, "Recent applications of deep learning and machine intelligence on in silico drug discovery: methods, tools and databases," *Briefings in Bioinformatics*, vol. 20, no. 5, pp. 1878–1912, 2019.

[41] M. Sridhar, R. Vinayagamoorthi, V. Arul Suyambunathan, Z. Bobby, and N. Selvaraj, "Bitter gourd (Momordica charantia) improves insulin sensitivity by increasing skeletal muscle insulin-stimulated IRS-1 tyrosine phosphorylation in high-fat-fed rats," *British Journal of Nutrition*, vol. 99, no. 4, pp. 806–812, 2008.

[42] N. Kerru, A. Singh-Pillay, P. Awolade, and P. Singh, "Current anti-diabetic agents and their molecular targets: a review," *European Journal of Medicinal Chemistry*, vol. 152, pp. 436–488, 2018.

[43] M. J. Barnes, F. Uruakpa, and C. Udenigwe, "Influence of cowpea (Vigna unguiculata) peptides on insulin resistance," *Journal of Nutritional Health and Food Science*, vol. 3, no. 2, pp. 1–3, 2015.

[44] L. D. Jones, P. Pangloli, H. B. Krishnan, and V. P. Dia, "BG-4, a novel bioactive peptide from _momordica charantia,_ inhibits lipopolysaccharide-induced inflammation in THP-1 human macrophages," *Phytomedicine*, vol. 42, pp. 226–232, 2018.

[45] R. Feng, L. Dong, L. Wang, Y. Xu, H. Lu, and J. Zhang, "Development of sodium glucose co-transporter 2 (SGLT2) inhibitors with novel structure by molecular docking and dynamics simulation," *Journal of Molecular Modeling*, vol. 25, no. 6, pp. 1–11, 2019.

[46] B. Zainab, Z. Ayaz, M. S. Alwahibi et al., "In-silico elucidation of _Moringa oleifera_ phytochemicals against diabetes mellitus," *Saudi Journal of Biological Sciences*, vol. 27, no. 9, pp. 2299–2307, 2020.

[47] R. Wang, H. Zhao, X. Pan, C. Orfila, W. Lu, and Y. Ma, "Preparation of bioactive peptides with antidiabetic, antihypertensive, and antioxidant activities and identification of α-glucosidase inhibitory peptides from soy protein," *Food Science & Nutrition*, vol. 7, no. 5, pp. 1848–1856, 2019.

[48] S. R. Shivanagoudra, W. H. Perera, J. L. Perez et al., "In vitro and in silico elucidation of antidiabetic and anti-inflammatory activities of bioactive compounds from Momordica charantia L," *Bioorganic & Medicinal Chemistry*, vol. 27, no. 14, pp. 3097–3109, 2019.

[49] J. Suganya, M. Radha, S. Manoharan, V. Vinoba, and A. Francis, "Virtual screening and analysis of bioactive compounds ofMomordica charantiaagainst diabetes using computational approaches," *Research Journal of Pharmacy and Technology*, vol. 10, no. 10, pp. 3353–3360, 2017.

[50] K. Cohen, A. Weizman, and A. Weinstein, "Positive and negative effects of cannabis and cannabinoids on health," *Clinical Pharmacology & Therapeutics*, vol. 105, no. 5, pp. 1139–1147, 2019.

[51] L. L. Ferreira and A. D. Andricopulo, "ADMET modeling approaches in drug discovery," *Drug Discovery Today*, vol. 24, no. 5, pp. 1157–1165, 2019.

[52] S. Fatima, P. Gupta, S. Sharma, A. Sharma, and S. M. Agarwal, "ADMET profiling of geographically diverse phytochemical using chemoinformatic tools," *Future Medicinal Chemistry*, vol. 12, no. 1, pp. 69–87, 2020.

[53] H. Yang, L. Sun, W. Li, G. Liu, and Y. Tang, "In silico prediction of chemical toxicity for drug design using machine learning methods and structural alerts," *Frontiers in Chemistry*, vol. 6, p. 30, 2018.

[54] S. Saeidnia, A. Manayi, and M. Abdollahi, "From in vitro experiments to in vivo and clinical studies; pros and cons," *Current Drug Discovery Technologies*, vol. 12, no. 4, pp. 218–224, 2016.

Hindawi
BioMed Research International
Volume 2024, Article ID 9808946, 1 page
https://doi.org/10.1155/2024/9808946

Retraction

Retracted: *Mangifera indica* Extracts as Novel PKM2 Inhibitors for Treatment of Triple Negative Breast Cancer

BioMed Research International

Received 12 March 2024; Accepted 12 March 2024; Published 20 March 2024

This article has been retracted by Hindawi following an investigation undertaken by the publisher [1]. This investigation has uncovered evidence of one or more of the following indicators of systematic manipulation of the publication process:

(1) Discrepancies in scope

(2) Discrepancies in the description of the research reported

(3) Discrepancies between the availability of data and the research described

(4) Inappropriate citations

(5) Incoherent, meaningless and/or irrelevant content included in the article

(6) Manipulated or compromised peer review

The presence of these indicators undermines our confidence in the integrity of the article's content and we cannot, therefore, vouch for its reliability. Please note that this notice is intended solely to alert readers that the content of this article is unreliable. We have not investigated whether authors were aware of or involved in the systematic manipulation of the publication process.

Wiley and Hindawi regrets that the usual quality checks did not identify these issues before publication and have since put additional measures in place to safeguard research integrity.

We wish to credit our own Research Integrity and Research Publishing teams and anonymous and named external researchers and research integrity experts for contributing to this investigation.

The corresponding author, as the representative of all authors, has been given the opportunity to register their agreement or disagreement to this retraction. We have kept a record of any response received.

References

[1] A. Rasul, A. Riaz, W. Wei et al., "*Mangifera indica* Extracts as Novel PKM2 Inhibitors for Treatment of Triple Negative Breast Cancer," *BioMed Research International*, vol. 2021, Article ID 5514669, 11 pages, 2021.

Hindawi
BioMed Research International
Volume 2021, Article ID 5514669, 11 pages
https://doi.org/10.1155/2021/5514669

Research Article

Mangifera indica Extracts as Novel PKM2 Inhibitors for Treatment of Triple Negative Breast Cancer

Azhar Rasul,[1,2] **Ammara Riaz**,[2] **Wei Wei**,[1] **Iqra Sarfraz**,[2] **Mudassir Hassan**,[2] **Jiang Li**,[3] **Faryal Asif**,[4] **Şevki Adem**,[5] **Shazia Anwer Bukhari**,[6] **Muhammad Asrar**,[2] **and Xiaomeng Li**[1]

[1]*The Key Laboratory of Molecular Epigenetics of MOE, Institute of Genetics and Cytology, Northeast Normal University (NENU), Changchun, China*
[2]*Cell and Molecular Biology Lab, Department of Zoology, Faculty of Life Sciences, Government College University Faisalabad, 38000 Faisalabad, Pakistan*
[3]*Affiliated Stomatology Hospital of Guangzhou Medical University, Guangzhou, China*
[4]*University of Agriculture Faisalabad (UAF), Faisalabad, Pakistan*
[5]*Department of Chemistry, Faculty of Science, Cankiri Karatekin University, 18100 Cankırı, Turkey*
[6]*Department of Biochemistry, Faculty of Life Sciences, Government College University Faisalabad, 38000 Faisalabad, Pakistan*

Correspondence should be addressed to Azhar Rasul; azharrasul@gcuf.edu.pk, Jiang Li; ljiang@gzhmu.edu.cn, and Xiaomeng Li; lixm441@nenu.edu.cn

Received 24 February 2021; Revised 3 April 2021; Accepted 29 April 2021; Published 27 May 2021

Academic Editor: Sibtain Ahmed

Pyruvate kinase (PK), a key enzyme that determines glycolytic activity, has been known to support the metabolic phenotype of tumor cells, and specific pyruvate kinase isoform M2 (PKM2) has been reported to fulfill divergent biosynthetic and energetic requirements of cancerous cells. PKM2 is overexpressed in several cancer types and is an emerging drug target for cancer during recent years. Therefore, this study was carried out to identify PKM2 inhibitors from natural products for cancer treatment. Based on the objectives of this study, firstly, plant extract library was established. In order to purify protein for the establishment of enzymatic assay system, pET-28a-HmPKM2 plasmid was transformed to *E. coli* BL21 (DE3) cells for protein expression and purification. After the validation of enzymatic assay system, plant extract library was screened for the identification of inhibitors of PKM2 protein. Out of 51 plant extracts screened, four extracts *Mangifera indica* (leaf, seed, and bark) and *Bombex ceiba* bark extracts were found to be inhibitors of PKM2. In the current study, *M. indica* (leaf, seed, and bark) extracts were further evaluated dose dependently against PKM2. These extracts showed different degrees of concentration-dependent inhibition against PKM2 at 90-360 μg/ml concentrations. We have also investigated the anticancer potential of these extracts against MDA-MB231 cells and generated dose-response curves for the evaluation of IC_{50} values. *M. indica* (bark and seed) extracts significantly halted the growth of MDA-MB231 cells with IC_{50} values of 108 μg/ml and 33 μg/ml, respectively. Literature-based phytochemical analysis of *M. indica* was carried out, and *M. indica*-derived 94 compounds were docked against three binding sites of PKM2 for the identification of PKM2 inhibitors. The results of *in silico* based screening have unveiled various PKM2 modulators; however, further studies are recommended to validate their PKM2 inhibitory potential via *in vitro* biochemical assay. The results of this study provide novel findings for possible mechanism of action of *M. indica* (bark and seed) extracts against TNBC via PKM2 inhibition suggesting that *M. indica* might be of therapeutic interest for the treatment of TNBC.

1. Introduction

Metabolic reprogramming has been reported as an emerging hallmark of cancer in recent years [1]. Reprogrammed tumor metabolism is characterized by enhanced aerobic glycolysis, upregulation of glutaminolysis, and lipid metabolism along with other different bioenergetics pathways which promote cellular growth and survival [2]. Among all these metabolic

pathways, glycolysis has been contemplated as the main source of energy for the growing tumor cells [3].

The pyruvate kinase (PK) is a key mediator of glycolytic pathway which codes for four different isoforms in mammalian cells. The oncofetal isoform is the M2 isoform of pyruvate kinase (PKM2) which differs from its M1 isoform by 22 amino acids. PKM1 isoform is expressed in normal cells; however, tumor cells as well as fetal tissues predominantly express the PKM2 isoform [4]. Multiple evidences demonstrate that PKM2 expression support energetic and macromolecular biosynthetic requirements of tumor cells by allowing the accumulation of glycolytic intermediates [5]. PKM2 is overexpressed in numerous kinds of human cancers mainly breast, prostate, lung, colorectal, and hepatocellular carcinoma. Previous studies have also demonstrated that PKM2-mediated glycolysis plays a critical role in tumor development, propagation, survival, and migration of cancer cells; thus, PKM2 inhibition has potential to inhibit growth of cancer cells selectively [6].

Given that PKM2 could serve as an ideal drug target for cancer [7], it is of immense interest to identify its natural inhibitors from natural products (NPs). Through long history of traditional medicinal applications, NPs have been well accepted by oncologists and pharmacologists as a worthwhile database for screening of bioactive extracts and compounds for novel drug discovery [8]. Previous studies have also demonstrated that NPs have promising ability to hit different metabolic targets in cancer cells. Thus, NP-mediated metabolic reprogramming is an emerging trend in the recent years for the development of novel anticancer therapies [9]. Although shikonin has been reported as a potent inhibitor of PKM2 [10], however, poor solubility and toxicity have limited its clinical applications [11]. The investigations on the identification and characterization of PKM2 inhibitors are ongoing, and the discovery of novel, potent, and safer inhibitors with good bioavailability and low toxicity has potential to provide great benefit to cancer patients. Based on this context, the aim of this work was to evaluate the potential of various plant extracts belonging to Pakistani flora against PKM2.

Based on the aims and objectives of this study, we have screened plant extract library using an *in vitro* enzymatic kinetic assay system for the identification of PKM2 inhibitors. Here, we present biochemical and cell-based evidences suggesting that *Mangifera indica* seed coat and bark extracts target PKM2 and possess anticancer activity against MDA-MB231 cells.

2. Materials and Methods

2.1. Preparation of Plant Extract Library. Various plants (35) belonging to different families were collected across the Punjab province of Pakistan. The specimens of plants were deposited at Herbarium for identification by Dr. Qasim, Assistant Professor, Department of Botany, GCUF. Plants were washed by water after collection and identification, followed by air drying at a shady place. After drying, the plant matter was subjected to grinding till a coarse powder was obtained. Plant extracts were prepared using Soxhlet apparatus. Methanolic extract was further concentrated using a rotary evaporator at reduced activity and solidified in the freeze drier.

2.2. Construction of pET-28a-PKM2 Plasmid. The amplification of coding region of full-length human PKM2 (accession number NM_002654.6) was done from human cells with the following primers: PKM2-Fw: 5′- GAC TCA GAT CTC GAG ATG TCG AAG CCC CAT AGT GAA GC -3′; PKM2-Rev: 5′- CGA CTG CAG AAT TCG CCG CAC AGG AAC AAC AC -3′. Agarose gel electrophoresis was done to fractionate the amplicon. This amplicon was then recovered by using a Qiagen Gel Purification column. Cloning of the coding region of PKM2 was done in expression vector pET28a. Sequence was validated by Sanger sequencing.

2.3. Expression and Purification of rPKM2 Protein. Transformation of recombinant plasmid pET-28a-PKM2 was done in the *E. coli* BL21 (DE3) cells. Transformed colony was transferred to 25 ml of LB medium supplemented with a suitable antibiotic, i.e., Kanamycin (50 μg/ml) for incubation. Inoculated culture medium was left for overnight at 37°C. After that, the cultured medium was centrifuged at 6000 rpm for 30 min. 5 ml from this suspension was again inoculated in LB medium (500 ml) with Kanamycin (50 μg/ml). This medium was allowed to grow at room temperature with shaking, till the OD_{600nm} that reached to 0.6. IPTG (0.1 mM) was added and cells were collected by centrifugation after the OD_{600nm} reached to 0.6 and was kept at -20°C for freezing purpose. Followed by freezing, further steps were performed at 4°C. The frozen cell paste was suspended in salt Lysis Buffer which contains the following chemicals: 30 mM NaCl, 50 mM NaH_2PO_4, 1M $NADP^+$, 1.4 mM β-mercaptoethanol, 0.5 mM PMSF, and 10 mM Imidazole. Protease inhibitor cocktail was added as supplementation. Egg white lysozyme was added in the quantity of 0.1 mg/ml, after half an hour. After two hours of incubation for this mixture, 1 h Benzonase treatment was performed. 3 M NaCl stock was added to adjust NaCl to 300 mM, and the lysate was incubated for one hour prior to its centrifugation at 14000 rpm for a time period of 30 min. The clear lysate obtained after centrifugation was subjected to Ni-NTA column which was preequilibrated with Lysis Buffer (10 ml). Lysis Buffer was prepared by adding 300 mM NaCl, 0.5 mM PMSF, 50 mM NaH_2PO_4, 1.4 mM β-mercaptoethanol, 10 mM Imidazole, and 1M $NADP^+$. Maximum binding was ensured for flow-through fraction by reloading it twice. Lysis Buffer (10 ml) and Wash Buffer which comprised of 300 mM NaCl, 50 mM NaH_2PO_4, 1M $NADP^+$, 20 mM Imidazole, 1.4 mM β-mercaptoethanol, and 0.5 mM PMSF was used for washing of Ni-NTA column. Then the recombinant PKM2 protein was exposed to elution buffer 1 (300 mM NaCl, 0.5 mM PMSF, 50 mM NaH_2PO_4, 250 mM Imidazole, 1.4 mM b-mercaptoethanol, and 1M $NADP^+$) followed by exposure to Elution Buffer 2 (50 mM NaH_2PO_4, 300 mM NaCl, 0.5 mM PMSF, 500 mM Imidazole, 1.4 mM b-mercaptoethanol, and 1M $NADP^+$). The two elutions were kept separated and treated with 1X PBS, 1M $NADP^+$, 0.5 mM PMSF, and 1.4 mM β-mercaptoethanol. The final elutions

were diluted by addition of glycerol (80%) and stored at -20°C in aliquots [12].

2.4. Establishment of PKM2 Enzymatic Assay System. LDH assay was established in order to investigate the PKM2 inhibitory activity of plant extracts. Plant extracts were dissolved in DMSO to 10 mg/ml, then diluted tenfold with pure water. At 25°C, 200 ng/μl of test extract was incubated for 1 hour in a solution containing 100 mM KCl, 50 mM HEPES, 0.2 mM NADH, 10 mM $MgCl_2$, 2 mM ADP, 2 mM phosphoenolpyruvate, and 8 units LDH/ml. With the help of compared change in absorbance at 340 nm, the relative pyruvate kinase activity was calculated.

2.5. Cell Culture. Human triple negative breast cancer (TNBC) cells, MDA-MB231, were cultured in DMEM supplemented with FBS (10%) and 100 IU/ml penicillin streptomycin. Cancerous cells were allowed to grow in a CO_2 incubator at 37°C with the supply of 5% CO_2 [13].

2.6. MTT Cytotoxic Assay. The anticancer activity of plant extracts was assessed by MTT assay. For this purpose, MDA-MB231cells were seeded in 96-well plates. After 12-18 hours, cancerous cells were treated with the various doses of plant extracts for 48 hours. Further, 10 μl of MTT (5 mg/ml) was added and cells were then incubated for 4 hours at 37°C. Then, media was aspirated and 150 μl of DMSO was added. As the last step, absorbance was checked at 490 nm on an ELISA plate reader (Thermo Scientific) [14]. Percentage cell viability was calculated by following formula:

$$\text{Percentage cellular viability} = \frac{\text{Absorbance of treated cells}}{\text{Absorbance of control}} \times 100. \quad (1)$$

2.7. Docking Studies. The X-ray crystallography structure of the human pyruvate kinase M2 (PKM2) was obtained from the https://www.rcsb.org/structure6V74 [15]. Proteins were imported to a Molegro Virtual Docker [16] and prepared for docking. Water molecules at crystal structure were removed; protein structure errors were checked. The binding regions of 1,6-di-O-phosphono-beta-D-fructofuranose (FBP), amino acids (AA), and oxalate ion/phosphoenolpyruvate (PEP) were determined to docking. Results were reported as MolDock Score. Each docking cavity was defined 16 Å radiuses by selecting the reference ligand center. Binding poses were analyzed by Discovery Studio Visualizer 2021software. The phytochemicals were searched at PubChem database, and their 3D SDF Conformers were downloaded from ZİNC database with InChI Key Codes. They were prepared for docking using UCSF Chimera Software.

3. Results

3.1. Construction of pET28a-PKM2 Recombinant Plasmid. The recombinant pEGFP-C1-PKM2 plasmid was digested by restriction enzymes, and retrieved DNA fragment was subcloned into a histidine-tagged pET28a vector to generate pET28a-PKM2 recombinant plasmid. Figure 1(a) shows successfully subcloned PKM2 cDNA into pET28a vector. The double digestion of the recombinant expression plasmid with these restriction enzymes resulted in the generation of two fragments which stand for PKM2 and pET28a backbone, respectively. Sequencing of the plasmid confirmed the correct orientation of insert (PKM2) in the vector (data is not shown).

3.2. Expression and Purification of Recombinant PKM2 Protein. Recombinant 6×his-PKM2 plasmid was expressed in BL21-DE3 *E. coli* cells. The recombinant N histidine-tagged protein was purified from *E. coli* cells by using Ni-NTA affinity chromatography. The purified recombinant protein was analyzed on SDS-PAGE. The approximate 58 kDa band on SDS PAGE (Figure 1(b)) represents the successful expression of PKM2 recombinant protein in BL21-DE3 *E. coli* clones.

3.3. Establishment and Validation of PKM2 Enzymatic Assay. Using the purified rPKM2 protein, PKM2 enzymatic assay was established based on the principle that the product of PKM2-catalyzed reaction is converted to lactate by LDH with concomitant conversion of NADH to NAD+ which can be monitored spectrophotometrically. The first enzymatic reaction is coupled with another in order to make PKM2 enzymatic activity easily detectable by monitoring NADH (Figure 1(c)). PKM2 enzymatic activity is spectrophotometrically monitored by measuring the decreased NADH at 340 nm. The reaction conditions were optimized using different concentrations of protein and substrate. The PKM2 enzymatic activity was determined at varying concentrations of PEP (Figure 1(d)). Based on our obtained results, 0.5 mM concentration of substrate was selected for further experimentations.

3.4. Screening of Crude Plant Extract Library by In Vitro PKM2 Enzymatic Assay. Our established coupled PKM2 enzymatic assay was used to determine the inhibitory potential of 51 extracts from various parts of 35 plants covering over 20 families of the Pakistani flora. In this preliminary screening, the PKM2 inhibiting activities of 51 extracts were investigated at 400 μg/ml, and the obtained results are presented in Table 1. From these screened plant extracts, 7.8% (four plant extracts) were identified as active against PKM2 (>70% inhibition), 9.8% exhibited moderate inhibitory activity against PKM2 (41-70% inhibition), and 82.3% displayed insignificant or low activity (0-40% inhibition).

To find the most potent plant extracts at lower concentrations, we further proceeded with screening of hits at lower concentrations. From these highly active plant extracts, *M. indica* (leaf, bark, and seed coat) extracts were tested dose dependently at varying concentrations (90, 180, and 360 μg/ml) in the reconfirmation assay and dose-response curves were obtained (Figure 2).

The obtained results show that *M. indica* extracts could serve as a starting point for the further identification and isolation of PKM2 inhibitory compounds or development of anticancer functional foods. Thus, these plant extracts were selected for further testing of cytotoxicity against breast cancer.

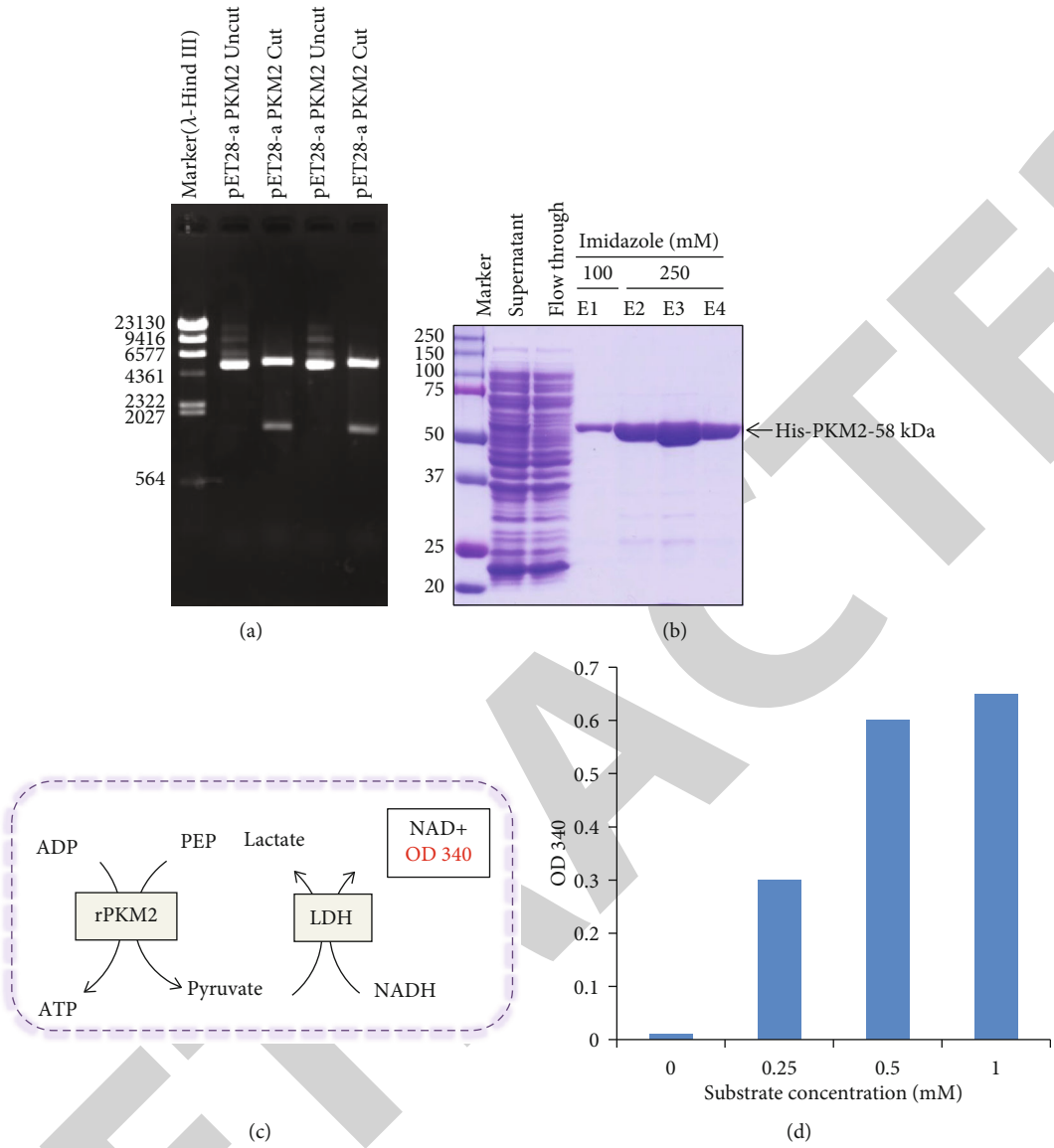

Figure 1: Protein expression, purification, and establishment of enzymatic activity assay. (a) Double enzyme digestion for checking of insert. (b) Purity check of the purified recombinant PKM2 protein. (c) Principle of PKM2 enzymatic activity assay. (d) Optimization of substrate concentration (PEP) for PKM2 enzymatic assay.

3.5. Evaluation of Cytotoxicity of M. indica (Leaf, Bark, and Seed Coat) Extracts and Calculation of IC_{50} Values. In order to evaluate the antiproliferative potential of positive hits obtained after screening of plant extract library against PKM2, MTT assay was performed. *M. indica* leaf, bark, and seed coat extracts were found to be cytotoxic towards MDA-MB231 cells. The dose-response curves were generated to calculate the inhibitory concentrations (IC_{50}). *M. indica* (bark, leaf, and seed) extracts have potential to inhibit the growth of MDA-MB231 cells significantly with IC_{50} values of 108 μg/ml, 67 μg/ml, and 33 μg/ml, respectively (Figure 3). Thus, the results of this study provide a novel finding about possible mechanism of action of *M. indica* (bark and seed) extracts against TNBC.

3.6. Identification of PKM2 Inhibitors from M. indica via In Silico Based Screening. In order to identify the PKM2 inhibitor compounds from *M. indica* extract, phytochemical analysis was done through database searching and a list of *M. indica*-derived compounds reported in literature was prepared. The structures of these phytochemicals (ligands) were retrieved from PubChem database, and screening was performed by molecular docking against PKM2 binding sites. *M. indica*-derived 94 compounds were docked against 3 binding sites of PKM2 (PDB ID: 6V74). A comparative analysis of docking against 3 binding sites of PKM2 is provided in Table 2.

As for binding affinities, 15 compounds exhibit good binding energies (MolDock Score of >-145) to one or more of PKM2 binding sites. Three out of 15 compounds exhibit

Table 1: Preliminary screening of crude plant extract library for the identification of PKM2 inhibitors.

Sr. no.	Plant name	Family	Common name	Part used	Extract no.	PKM2 activity
1	*Cyamopsis tetragonoloba* (L.) Taub	Fabaceae	Guar gum	Seeds	1	–
2	*Calotropis procera* (Aiton) Dryand.	Apocynaceae	Sodom apple	Leaves	2	–
3	*Azadirachta indica* A. Juss.	Meliaceae	Indian lilac	Leaves	3	–
4	*Ageratum conyzoides* L.	Asteraceae	Goat weed	Whole plant	4	–
5	*Dalbergia sissoo* sensu Miq.	Fabaceae	Indian rosewood	Seeds	5	–
				Bark	6	–
6	*Albizia lebbeck* (L.) Benth.	Fabaceae	Lebbeck	Flowers	7	–
				Seeds	8	–
				Seed coat	9	–
				Leaves	10	+
7	*Momordica charantia* L.	Cucurbitaceae	Bitter melon	Vegetable	11	–
				Seeds	12	–
8	*Oxalis corniculata* L.	Oxalidaceae	Creeping woodsorrel	Whole plant	13	–
9	*Cassia fistula* L.	Fabaceae	Golden shower	Leaves	14	+
				Fruit	15	+
10	*Aloe barbadensis* Mill.	Asphodelaceae	Aloe vera	Whole plant	16	–
11	*Nerium oleander* L.	Apocynaceae	Oleander	Leaves	17	–
12	*Chenopodium album* L.	Amaranthaceae	Lamb's quarters	Whole plant	18	–
13	*Bombax ceiba* L.	Malvaceae	Cotton tree	Leaves	19	–
				Bark	20	++
14	*Cicer arietinum* L.	Fabaceae	Chickpea (white)	Seed	21	–
			Chick pea (black)	Seed	22	–
15	*Smilax china* L.	Smilacaceae	China root	Roots	23	–
16	*Eucalyptus camaldulensis* Dehnh.	Myrtaceae	Himalayan poplar	Bark	24	–
17	*Helianthus annuus* L.	Asteraceae	Sun flower	Seeds	25	–
18	*Artemisia absinthium* L.	Asteraceae	Common wormwood	Whole plant	26	+
19	*Litchi chinensis* Sonn.	Sapindaceae	Lychee	Seeds	27	–
				Bark	28	+
				Leaves	29	–
20	*Lawsonia inermis*	Lythraceae	Henna	Leaves	30	–
21	*Cyperus esculentus* L.	Cyperaceae	Water grass	Flowers	31	–
22	*Fagonia arabica* L.	Zygophyllaceae	Dhamasa	Whole plant	32	–
23	*Cucumis melo agrestis* Naudin	Cucurbitaceae	Wild melon	Leaves	33	–
				Stem	34	–
24	*Asphodelus tenuifolius* Cav.	Asphodelaceae	Wild onion	Whole plant	35	–
25	*Solanum nigrum* L.	Solanaceae	Black nightshade	Whole plant	36	–
26	*Mangifera indica* L.	Anacardiaceae	Mango	Fruit pulp	37	–
				Peel	38	–
				Bark	39	++
				Seed coat	40	++
				Leaves	41	++
27	*Trachyspermum ammi* (L.) Sprague	Apiaceae	Carom seeds	Seeds	42	–
28	*Ferula assa-foetida* L.	Umbelliferae	Heng	Resin	43	–
29	*Linum usitatissimum* L.	Linaceae	Flax seeds	Seeds	44	–
30	*Citrullus colocynthis* (L.) Schrad.	Cucurbitaceae	Desert bitter gourd	Fruit	45	–
31	*Trigonella foenum-graecum* L.	Fabaceae	Fenugreek	Seeds	46	–
32	*Punica granatum* L.	Lythraceae	Pomegranate	Fruit peel	47	–
				Seeds	48	–

Table 1: Continued.

Sr. no.	Plant name	Family	Common name	Part used	Extract no.	PKM2 activity
33	*Acacia farnesiana* (L.) Willd.	Fabaceae	Thorn Mimosa	Seeds	49	–
34	*Coriandrum sativum* L.	Apiaceae	Coriander	Seeds	50	–
35	*Citrus maxima* (Burm.) Merr.	Rutaceae	Chinese grapefruit	Peel	51	–

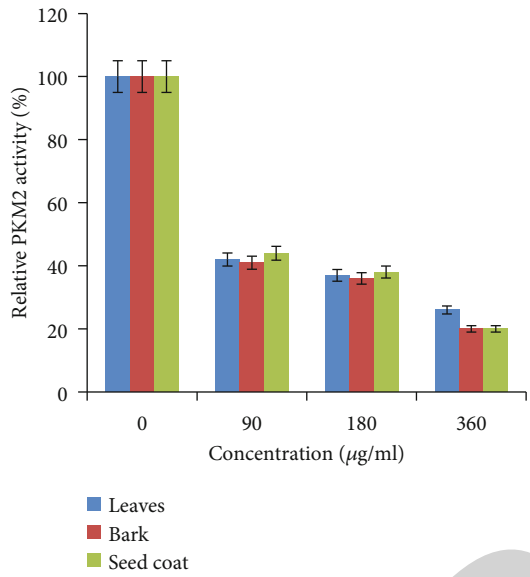

Figure 2: Relative (%) PKM2 activity by varying concentration of *M. indica* leaf, bark, and seed coat extracts.

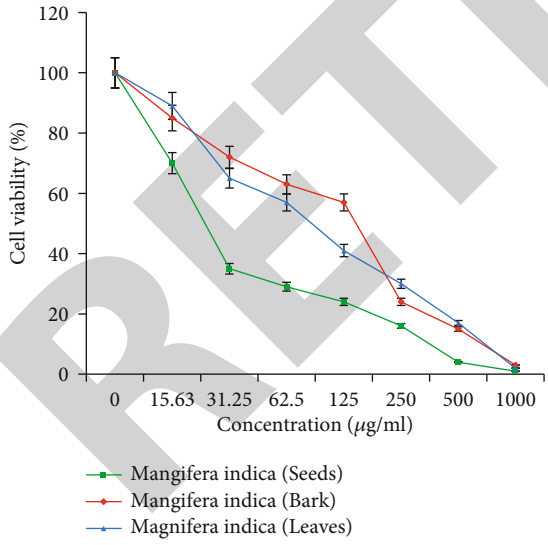

Figure 3: Dose-dependent growth inhibitions of MDA-MB231 cells by *M. indica* bark, leaf, and seed extracts.

good binding affinities to all the 3 binding sites of PKM2. The top 3 common hits are Lupeollinoleate, Neochrome, and Maclurin 3-C-(6″-O-phydroxybenzoyl)β-Dglucoside. Docking interaction patterns of the top three hit compounds against FBP binding site of PKM2 are presented in Figure 4. These compounds possess good theoretical binding affinity with the target protein by mainly forming hydrogen bond and Van der Waals forces. Docking complexes of the best three *M. indica*-derived compounds against AA and PEP binding sites of PKM2 are presented in Figures 5 and 6, respectively.

The summary of enzymatic assay-based screening and virtual screening against PKM2 is provided in Figure 7.

4. Discussion

Targeting tumor metabolism has emerged as a novel and selective strategy for cancer therapy. A major metabolic difference associated with cancer is alteration in glucose metabolism. PK, a key enzyme that determines glycolytic activity, plays a critical role in cancer development [17]. Cancer cells express the specific M2 isoform (PKM2), and multiple evidences demonstrate that PKM2 expression support divergent biosynthetic and energetic requirements of cells in tumors. Unlike cancer cells, most of the normal tissues express another isoform of PK (PKM1). As PKM2 provides selective growth advantages to cancer cells over its counterpart PKM1, thus, targeting PKM2 provides an excellent opportunity for cancer therapies and drug development [18].

PKM2 silencing has been known to induce apoptosis in cancer cells by recent studies [19]. PKM2 has also been reported to be highly expressed in various TNBC cell lines which provide further rationale for targeting PKM2 as novel anti-TNBC therapy [7].

Given that PKM2 inhibition has no effects on normal human breast tissues, PKM2 could serve as an ideal therapeutic target for TNBC [7] and it is of immense interest to identify and develop its inhibitors from natural products.

After screening of plant extract library, we identified *M. indica* (leaf, bark, and seed coat) extracts as PKM2 activity inhibitors at a final dose of 90 μg/ml. Previous studies indicate that natural products from *Alkanna tinctoria* and *Arnebia* spp. exhibit PKM2 inhibitory activity. The extracts from these potentially active plants contain bioactive naphthoquinone compounds like alkannin, shikonin, and their derivatives [20]. Another natural compound lapachol has been found to be the potential inhibitor of PKM2 activity, leading to reduced ATP production and inhibition of cellular proliferation in human melanoma cells [4]. Berberine, isolated from *Coptis* and *Hydrastis canadensis*, has also been found to inhibit PKM2 activity leading to antitumor activity in HCT116 and HeLa cells [21]. Apigenin, naturally found in parsley, oranges, and onions, has been reported to block tumor glycolysis via inhibiting PKM2 expression and activity which in turn induced anticancer effects in colon cancer cells

Table 2: Docking results of *M. indica*-derived compounds against different binding site of PKM2.

Compound name	FBP binding site		AA binding site		PEP binding site	
	MolDock Score	HBond	MolDock Score	HBond	MolDock Score	HBond
Lupeollinoleate	-195.03	-5.03	-158.135	-3.14911	-183.99	-5.44131
Neochrome	-163.73	-5.31	-163.218	-8.04216	-142.153	-4.8914
Tetra-O-galloylglucose	-157.20	-35.16	-193.459	-19.630	-130.615	-28.8154
Neoxanthin	-155.84	-5.00	-120.848	-4.71265	-153.167	-6.0305
Luteoxanthin	-148.74	-3.55	-143.937	-3.779	-134.169	-4.93468
Gamma-tocopherol	-146.94	-4.99	-138.311	-6.75642	-108.115	-4.37926
β-Carotene	-145.99	0.00	-146.335	0	-129.354	0
Zeaxanthin	-144.59	-2.52	-144.795	0	-134.096	-0.798168
Beta-tocopherol	-142.54	-5.61	-125.241	-3.94614	-133.965	-1.92741
Mangiferic acid	-141.59	-4.79	-126.118	-1.45213	-129.938	-2.10352
Maclurin 3-C-(6″-O-phydroxybenzoyl)β-Dglucoside	-141.11	-19.75	-185.504	-30.6823	-152.56	-29.1472
Cryptoxanthin	-139.99	0.00	-144.965	0	-146.105	-1.91568
3-Methoxy-2-(4′-methyl benzoyl)-chromone	-132.76	-9.86	-120.813	-4.29266	-102.599	-4.55386
Apigenin 7-glucoside	-131.70	-27.05	-112.568	-6.71948	-100.576	-15.5694
Violaxanthin	-128.58	-0.49	-119.488	-1.81432	-88.3268	-7.52592
9-cis-Lutein (lutein)	-127.19	-2.35	-136.35	-2.5	-142.497	0
Mangiferin-6′-O-gallate	-125.08	-23.94	-112.949	-22.8972	-103.519	-26.8348
Rhamnetin	-124.29	-20.48	-110.02	-13.7748	-115.109	-10.6913
Epicatechin gallate	-123.03	-15.86	-103.822	-14.8456	-91.3209	-21.6137
Quercetin	-123.02	-22.78	-110.428	-12.0814	-110.252	-11.1415
Maclurin	-121.60	-15.94	-111.415	-8.34809	-97.7143	-14.8418
Rhamnetin hexoside	-120.91	-15.68	-110.437	-10.9705	-77.4519	-13.2685
Quercetin 3-O-rhamnoside	-120.80	-12.94	-115.172	-11.7603	-87.4993	-21.5166
Ellagic acid	-117.80	-15.43	-87.435	-9.7998	-72.6948	-11.7498
Ferulic acid	-117.17	-18.61	-105.778	-7.67901	-89.8163	-1.45049
Kaempferol	-115.78	-13.68	-107.609	-11.5349	-85.1987	-4.76716
γ-Sitosterol	-115.47	0.00	-90.502	-2.36888	-60.0014	-0.4356
Apigenin	-114.03	-14.49	-102.655	-10.3857	-108.222	-11.2041
α-Farnesene	-109.14	0.00	-102.741	0	-104.068	0
Syringic acid	-107.06	-10.80	-97.8327	-5.54318	-82.3703	-8.07737
Catechin	-106.29	-16.81	-85.0592	-8.07189	-72.7696	-15.0371
Quercetin carboxylic acid	-106.26	-31.53	-147.825	-24.6151	-131.161	-18.669
Caffeic acid	-104.79	-16.96	-100.104	-8.29169	-84.0058	-7.97793
Alpha-tocopherol	-104.68	0.00	-93.3105	0	-109.057	-2.5
Quercetin carboxylic acid	-101.33	-17.05	-78.7161	-16.5643	-61.109	-21.0371
Elemicin	-100.85	-1.95	-98.532	-3.63297	-80.2126	0
Campesterol	-100.76	0.00	-92.344	-2.5	-67.2379	-4.41775
p-Coumaric acid	-100.03	-15.79	-106.985	-5.2956	-88.197	-11.3534
Stigmasterol	-98.57	-2.50	-109.341	-3.17755	-79.599	-7.28574
Ethyl gallate	-98.32	-15.70	-91.6331	-11.2495	-95.4522	-17.0114
Mangiferin	-95.60	-23.65	-62.7887	-12.7153	-46.4801	-9.84916
Penta-O-gallose-glucose	-93.54	-16.92	-140.348	-27.0176		
α-Cubebene	-93.39	0.00	-73.0146	0	-80.0748	-1.51948
Methyleugenol	-92.76	0.00	-81.484	-1.37587	-78.2553	0
Gallic acid	-91.66	-18.00	-97.1975	-10.3128	-72.1728	-11.0514
Humulene	-90.71	0.00	-61.618	0	-63.6181	0
Theogallin	-90.31	-18.97	-68.6305	-19.8959	-79.8986	-21.7922

Table 2: Continued.

Compound name	FBP binding site		AA binding site		PEP binding site	
	MolDock Score	HBond	MolDock Score	HBond	MolDock Score	HBond
Iriflophenone-di-O-galloyl glucoside	-89.47	-20.70	-93.1958	-11.7291	-69.9375	-17.7076
Methyl gallate	-89.00	-15.10	-79.6082	-9.30537	-88.5411	-15.4398
α-Guaiene	-88.71	0.00	-69.7068	0	-63.3114	0
Dehydroascorbic acid	-87.17	-20.05	-75.4451	-15.0859	-77.1176	-13.908
Ascorbic acid	-87.12	-22.48	-84.9714	-13.4832	-70.4795	-16.0717
29-Hydroxymangiferonicacid	-86.95	-5.10	-80.1064	-5.24553	-50.0767	-12.6962
α-Sitosterol	-85.59	-0.78	-90.9633	-4.75248	-77.87	-3.2075
Protocatechuic acid	-85.59	-16.13	-93.325	-7.21244	-70.7263	-9.9475
Cinnamic acid	-84.63	-7.22	-93.9566	-4.03022	-76.26	-5.39073
Estragole	-83.21	-4.99	-79.9985	-0.38853	-80.1188	-0.484549
δ-Elemene	-81.71	0.00	-66.5298	0	-61.4269	0
Terpinyl acetate	-81.53	-2.98	-74.9132	-0.97568	-70.4852	-2.99327
Vanillin	-80.14	-11.30	-77.7569	-4.78744	-74.7439	-4.53428
Myrcene	-80.04	0.00	-77.3758	0	-86.4075	0
Linalool	-79.69	-5.37	-81.62	-5	-85.1614	-2.3688
Ocimene	-79.26	0.00	-81.2441	0	-84.1246	0
Mangiferonic acid	-79.13	-5.19	-77.262	-6.28465	-64.86	-8.29727
24-Methylenecycloartane-3β,26-diol	-78.22	-1.43	-78.4328	-2.93017	-64.4235	-9.29597
β-Bulnesene	-77.62	0.00	-72.542	0	-63.9464	0
Sabinene	-75.23	0.00	-81.1319	0	-73.5542	0
β-Elemene	-73.68	0.00	-61.4113	0	-54.1936	0
γ-Terpinene	-73.18	0.00	-74.3906	0	-65.0567	0
γ-Cadinene	-72.33	0.00	-48.6785	0	-50.5432	0
Dammarenediol II	-72.02	-5.26	-50.9481	-3.73546	-44.3381	-6.83216
Cycloartane-3,24,25-triol	-71.53	-8.76	-56.5961	-6.19957	-42.7277	-7.07424
Benzoic acid	-70.68	-7.57	-88.9444	-4.49511	-58.6953	-1.48964
Cymene	-70.26	0.00	-75.1263	0	-69.7851	0
α-Terpinolene	-68.95	0.00	-74.3397	0	-66.6623	0
α-Pinene	-67.71	0.00	-72.5574	0	-63.4011	0
Mangiferolate B	-66.67	-5.45	-54.2368	-4.18714	-49.3208	-3.97387
Limonene	-65.77	0.00	-72.9592	0	-63.0344	0
Pyrogallol	-64.60	-13.01	-68.5738	-9.57125	-63.477	-9.66407
Car3-ene	-63.20	0.00	-69.2717	0	-61.3925	0
Shikimic acid	-62.90	-15.54	-67.0134	-11.6281	-46.58	-12.5796
Resinol	-59.58	-9.91	-69.0014	-5	-60.3014	-7.5
β-Pinene	-59.12	0.00	-68.3213	0	-55.6667	0
Cycloartan-3β-30-diol cycloartan-3b	-59.10	-4.89	-70.9584	-7.08208	-33.8611	-1.92964
Camphene	-55.20	0.00	-66.3445	0	-52.2991	0
Eucalyptol	-53.56	-0.20	-63.9989	-2.39085	-48.9044	-0.155108
Quercetin pentoside	-47.75	-24.01	-77.8756	-11.9264	-87.2484	-29.9426
Manglupenone	-39.78	-5.75	-35.8728	-2.83316	-18.4948	-5
β-Sitosterol	-34.08	-0.99	-57.562	-3.78085	-43.5471	-4.42292
Lupeol	-33.19	-1.47	-32.275	-1.97739	-15.5679	-2.5
β-Amyrin	-28.02	-1.95	-28.957	-2.20045	-21.9474	0
Taraxerol	-27.67	0.00	-30.1279	-4.35048	-10.9574	-2.19296
Friedelin	-23.99	-4.34	-23.99	-4.34	-11.5989	-4.47101
α-Amyrin	-13.41	-1.86	-21.125	-0.17742	-8.75428	-1.11693

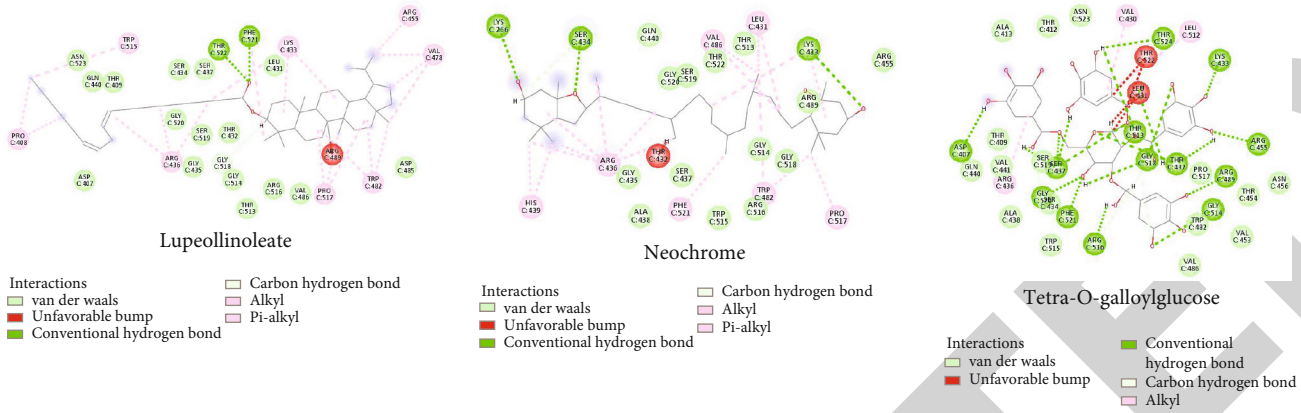

Figure 4: Docking complexes of the best three *M. indica* compounds within the FBP binding site of PKM2.

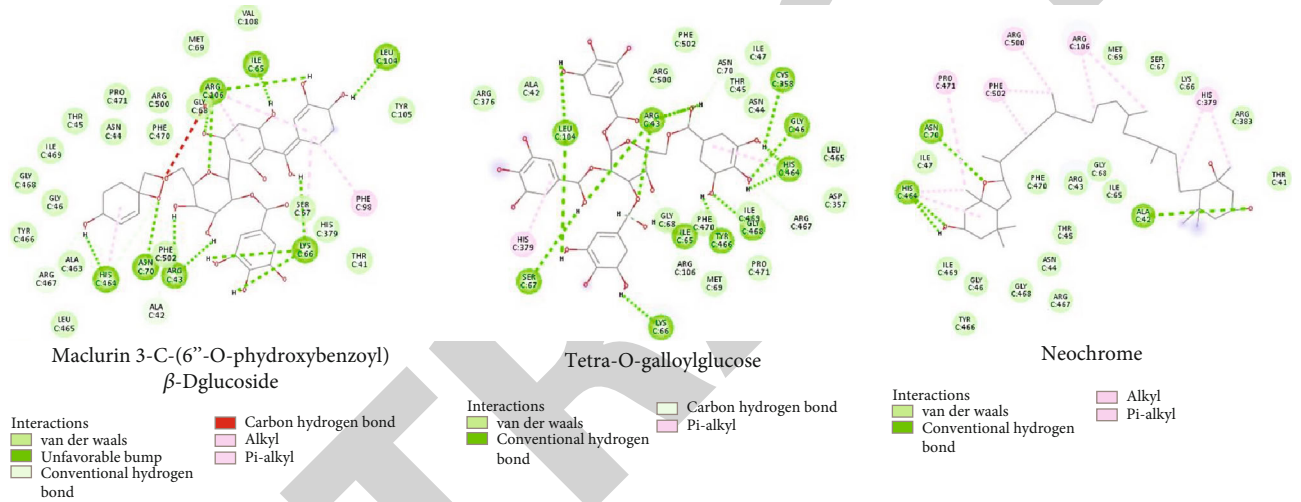

Figure 5: Representation of docking complexes of top three ligands into the AA binding site of PKM2.

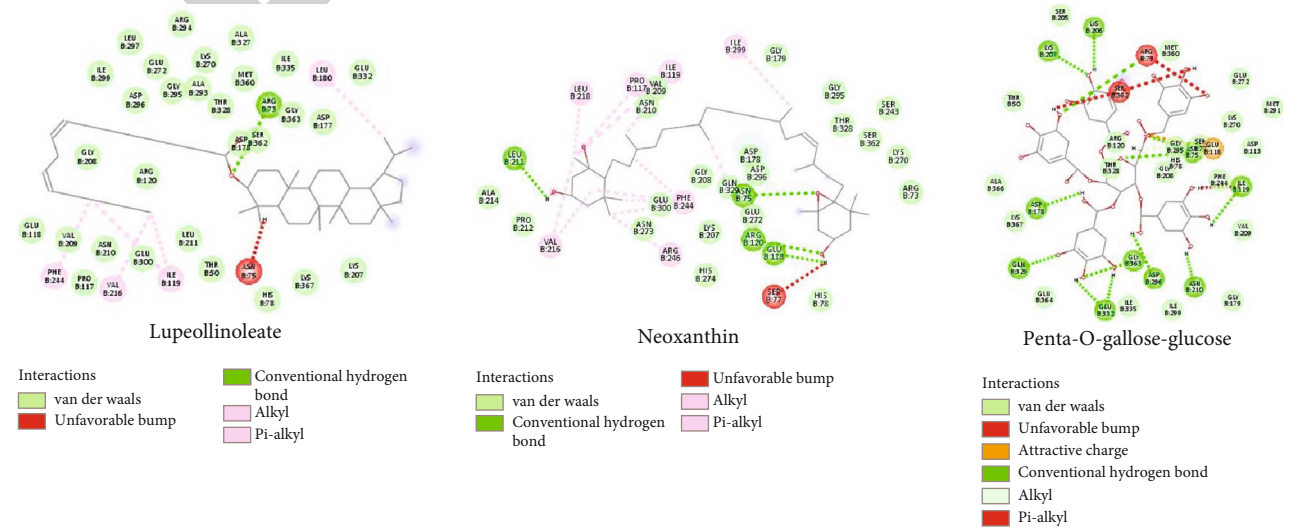

Figure 6: Interaction of hit compounds with amino acid residues at the PEP binding site of PKM2.

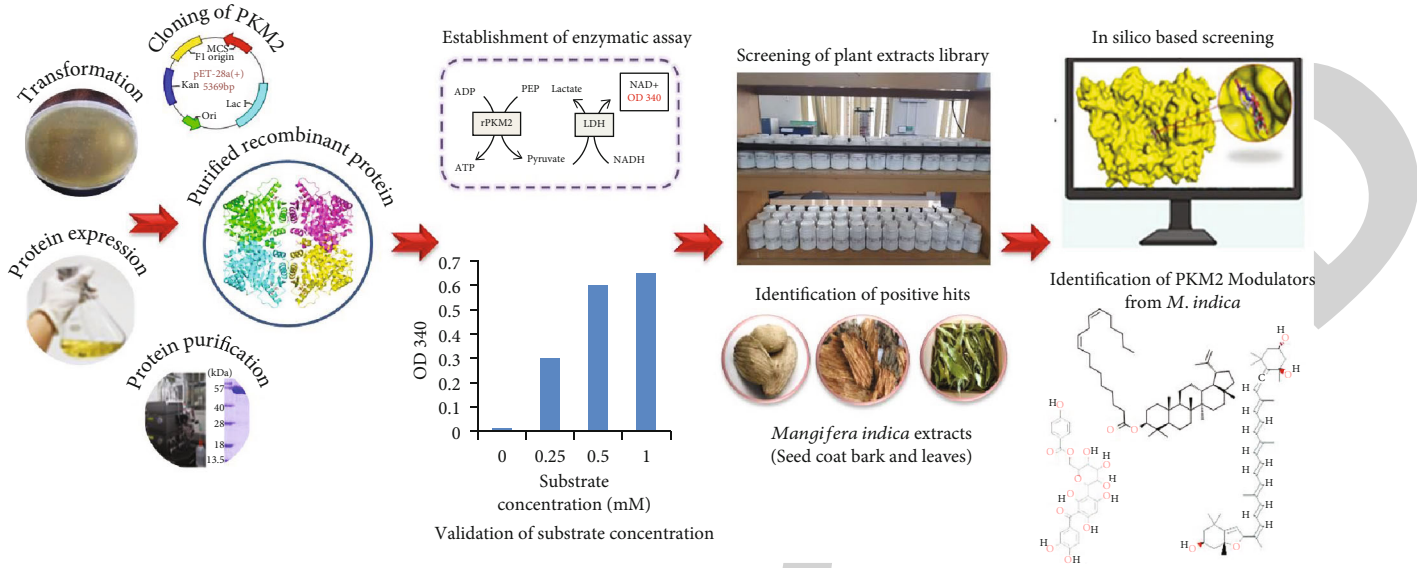

Figure 7: Summary of target protein-based screening of plant extract library and *in silico* based screening of *M. indica*-derived compounds against PKM2.

[22], indicating that blocking PKM2 activity by natural products has potential to halt the proliferation in tumor cells.

M. indica (leaf, bark, and seed coat) extracts also found to possess anticancer potential against highly aggressive breast cancer, TNBC. Our results are found to be concordant with the previous studies reporting anticancer potential of *M. indica* L. extracts against liver, colon, cervical, and gastric cancers [23, 24]. In order to explore new natural scaffolds from *M. indica* and provide further opportunities for anticancer drug discovery, we have screened *M. indica*-derived compounds against PKM2 by molecular docking. *In silico* based screening has identified several modulators of PKM2 which have potential to bind with AA, FBP, and PEP binding site of PKM2. From identified hits, neoxanthin has been previously known to inhibit chemically induced carcinogenesis in an *in vivo* hamster model [25]. Another hit compound, neochrome, is metabolite of neoxanthin which possess antiproliferative potential against prostate cancer cells [26]. Thus, the comparison of our results with existing literature suggests the potential of neoxanthin and neochrome as anticancer agents which might be due to PKM2 inhibition.

5. Conclusions

Conclusively, enzymatic assay-based screening was performed to identify the plant extracts having potential to inhibit PKM2. This screen identified *M. indica* extracts as potential inhibitors of PKM2. Further *in silico* based screening identified various PKM2 modulators from *M. indica*. Although *M. indica* (bark and seed) extracts have been previously reported to possess significant anticancer potential, however, the underlying mechanism remains enigmatic. To the best of our knowledge, this is the first study which discloses that the *M. indica* exerts anticancer effects against TNBC via PKM2 inhibition. This study laid the foundation for further investigations to validate the efficacy of identified compounds against PKM2 via enzymatic activity assay. Although these findings suggest *M. indica* extracts as PKM2 inhibitors, however, further research is also recommended to test their potential in *in vivo* studies.

Data Availability

The data used to support the findings of this study are included within the article.

Conflicts of Interest

The authors declare that they have no conflicts of interest.

Acknowledgments

This study was supported by grants from the Ministry of Science and Technology (2021YFE0108000 and 2016YFE0128500), Science and Technology Department of Jilin Province (20200201025JC), National Natural Science Foundation of China (31870758), Department of Finance of Jilin Province (jsz2018170-3), NRPU Research Grant (8381/Punjab/NRPU/R&D/HEC/2017), and International Foundation for Science (Project No. 1I3_F_041125).

References

[1] N. N. Pavlova and C. B. Thompson, "The emerging hallmarks of cancer metabolism," *Cell Metabolism*, vol. 23, no. 1, pp. 27–47, 2016.

[2] I. Sarfraz, A. Rasul, G. Hussain et al., "Malic enzyme 2 as a potential therapeutic drug target for cancer," *IUBMB Life*, vol. 70, no. 11, pp. 1076–1083, 2018.

[3] F. Sharif, A. Rasul, A. Ashraf et al., "Phosphoglycerate mutase 1 in cancer: a promising target for diagnosis and therapy," *IUBMB Life*, vol. 71, no. 10, pp. 1418–1427, 2019.

Hindawi
BioMed Research International
Volume 2024, Article ID 9834546, 1 page
https://doi.org/10.1155/2024/9834546

Retraction

Retracted: *In Silico* Structural, Functional, and Phylogenetic Analysis of Cytochrome (CYPD) Protein Family

BioMed Research International

Received 12 March 2024; Accepted 12 March 2024; Published 20 March 2024

This article has been retracted by Hindawi following an investigation undertaken by the publisher [1]. This investigation has uncovered evidence of one or more of the following indicators of systematic manipulation of the publication process:

(1) Discrepancies in scope

(2) Discrepancies in the description of the research reported

(3) Discrepancies between the availability of data and the research described

(4) Inappropriate citations

(5) Incoherent, meaningless and/or irrelevant content included in the article

(6) Manipulated or compromised peer review

The presence of these indicators undermines our confidence in the integrity of the article's content and we cannot, therefore, vouch for its reliability. Please note that this notice is intended solely to alert readers that the content of this article is unreliable. We have not investigated whether authors were aware of or involved in the systematic manipulation of the publication process.

Wiley and Hindawi regrets that the usual quality checks did not identify these issues before publication and have since put additional measures in place to safeguard research integrity.

We wish to credit our own Research Integrity and Research Publishing teams and anonymous and named external researchers and research integrity experts for contributing to this investigation.

The corresponding author, as the representative of all authors, has been given the opportunity to register their agreement or disagreement to this retraction. We have kept a record of any response received.

References

[1] H. I. Ahmad, G. Afzal, A. Jamal et al., "*In Silico* Structural, Functional, and Phylogenetic Analysis of Cytochrome (CYPD) Protein Family," *BioMed Research International*, vol. 2021, Article ID 5574789, 13 pages, 2021.

Hindawi
BioMed Research International
Volume 2021, Article ID 5574789, 13 pages
https://doi.org/10.1155/2021/5574789

Research Article

In Silico Structural, Functional, and Phylogenetic Analysis of Cytochrome (CYPD) Protein Family

Hafiz Ishfaq Ahmad,[1] **Gulnaz Afzal**,[2] **Adil Jamal**,[3] **Shumaila Kiran**,[4] **Musarrat Abbas Khan**,[5] **Khalid Mehmood**,[6] **Zahid Kamran**,[7] **Irfan Ahmed**,[7] **Shakeel Ahmad**,[8] **Asmar Ahmad**,[2] **Javed Hussain**,[2] **and Sadaf Almas**[9]

[1]*Department of Animal Breeding and Genetics, University of Veterinary and Animal Sciences, Lahore, Pakistan*
[2]*Department of Zoology, The Islamia University, Bahawalpur, Pakistan*
[3]*Sciences and Research, College of Nursing, Umm Al Qura University, Makkah, 715, Saudi Arabia*
[4]*Department of Applied Chemistry, Government College University, Faisalabad, Pakistan*
[5]*Department of Animal Breeding and Genetics, Faculty of Veterinary & Animal Sciences, The Islamia University of Bahawalpur, Pakistan*
[6]*Department of Clinical Medicine and Surgery, Faculty of Veterinary and Animal Science, The Islamia University, Bahawalpur, Pakistan*
[7]*Department of Animal Nutrition, Faculty of Veterinary & Animal Sciences, The Islamia University of Bahawalpur, Pakistan*
[8]*Department of Poultry Science, Faculty of Veterinary & Animal Sciences, The Islamia University of Bahawalpur, Pakistan*
[9]*Department of Microbiology, University of Veterinary and Animal Sciences, Lahore, Pakistan*

Correspondence should be addressed to Hafiz Ishfaq Ahmad; hafizishfaq93@gmail.com and Khalid Mehmood; khalid.mehmood@iub.edu.pk

Received 10 February 2021; Accepted 23 April 2021; Published 10 May 2021

Academic Editor: Sibtain Ahmed

Cytochrome (CYP) enzymes catalyze the metabolic reactions of endogenous and exogenous compounds. The superfamily of enzymes is found across many organisms, regardless of type, except for plants. Information was gathered about CYP2D enzymes through protein sequences of humans and other organisms. The secondary structure was predicted using the SOPMA. The structural and functional study of human CYP2D was conducted using ProtParam, SOPMA, Predotar 1.03, SignalP, TMHMM 2.0, and ExPASy. Most animals shared five central motifs according to motif analysis results. The tertiary structure of human CYP2D, as well as other animal species, was predicted by Phyre2. Human CYP2D proteins are heavily conserved across organisms, according to the findings. This indicates that they are descended from a single ancestor. They calculate the ratio of alpha-helices to extended strands to beta sheets to random coils. Most of the enzymes are alpha-helix, but small amounts of the random coil were also found. The data were obtained to provide us with a better understanding of mammalian proteins' functions and evolutionary relationships.

1. Introduction

Cytochrome P450 (*CYP*) is a unique heme-containing protein that has always been proven as a centrepiece of the organisms' defense system against toxicants [1, 2]. Various compounds, such as medications, steroid hormones, carcinogens, and environmental toxins, are metabolized by these enzymes. [3]. The CYPs are thought to be active in xenobiotic detoxification processes and the biosynthesis of a variety of endogenous compounds [4, 5]. CYPs are classified primarily into two distinct forms: membrane-bound forms found in eukaryotes and soluble forms found

Figure 1: *CYP2D* gene tree showing minimum evolution among organisms.

in prokaryotes [6, 7]. CYPs are most functional in the liver, where the levels of metabolites, systemic drug alteration, and metabolic rate are excessive [8]. However, it has been reported that the level of drugs in plasma never correlates with therapeutic effect, especially when centrally acting drugs are involved [9].

Among different P450 subfamilies in humans, one of them is the Cytochrome P450 2D (*CYP2D*) located on human chromosome 22 [10], comprised of one functional gene (*CYP2D6*) and two pseudogenes (*CYP2D7*P and *CYP2D8*P) [11, 12]. The CYP2D family of mammalian enzymes is involved in the synthesis of 20–25 percent of structurally distinct common medications such as dextromethorphan, bufuralol, and antiarrhythmic blockers and antidepressants [13] and accounts for about 2–4% of hepatic CYPs. Moreover, the *CYP2D6* proteins in humans have great affinity with alkaloids [14]. Both pseudogenes have similar nucleotide sequences with the *CYP2D6* gene. However, presence at the first exon *CYP2D7P* is due to a single mutational frameshift, responsible for an immature downstream of stop codons. From these pseudogenes, alternative mRNAs have been monitored in the breast, lungs, and brain of humans [15, 16]. Though a functional transcript of *CYP2D7*P has been investigated in few members of the Indian population, no evidence of mRNA from *CYP2D8*P was observed [17]. Despite this, the organization of the CYP2D subfamily genes has been discovered in nonhuman primates such as the rhesus monkey, chimp, white tufted ear marmoset, and Sumatran orangutan. They found that CYP2D7 originated from CYP2D6 in a stem lineage of great apes and humans [5]. As a result, the CYP2D6 and CYP2D8P genes in the human genome originated from the Catarrhine and New World monkeys' stem lineage. [12].

The relationship among different human *CYPs* is scarce and cannot be generalized easily. The human *CYP* subtype homology modeling based on the crystal structure can provide valuable information about their structural and functional association [18]. A high degree of protein sequence similarities is not enough to evaluate these enzymes' different indistinctive activities. According to their respective substrates and inhibitors, various studies regarding the classification of these enzymes based on structural and pharmacophoric characteristics have been done [19, 20]. Substrate recognition sites (SRSs) in the *CYP2* family are vital for the catalysis of target substrates; various functional sites can be monitored with a 3D structure modeling approach in humans and compared with the homology of bacterial *CYPs* [21–23].

Due to the clinical importance, human *CYP2D6* proteins have been studied in various disciplines like structure biology, medicine, and pharmaco-genetics. Therefore, the genetic variability of *CYP2D6* in human populations was investigated extensively [24, 25]. Hence, due to its complex structure and single-nucleotide polymorphism (SNP), *CYP2D6* structural, functional, and evolutionary analyses have yet to be explored more to enhance the clinical implications. To meet this requirement, this study was designed to explore more insights into *CYP2D*s through various bioinformatics tools, which would help in a rational drug design in the future.

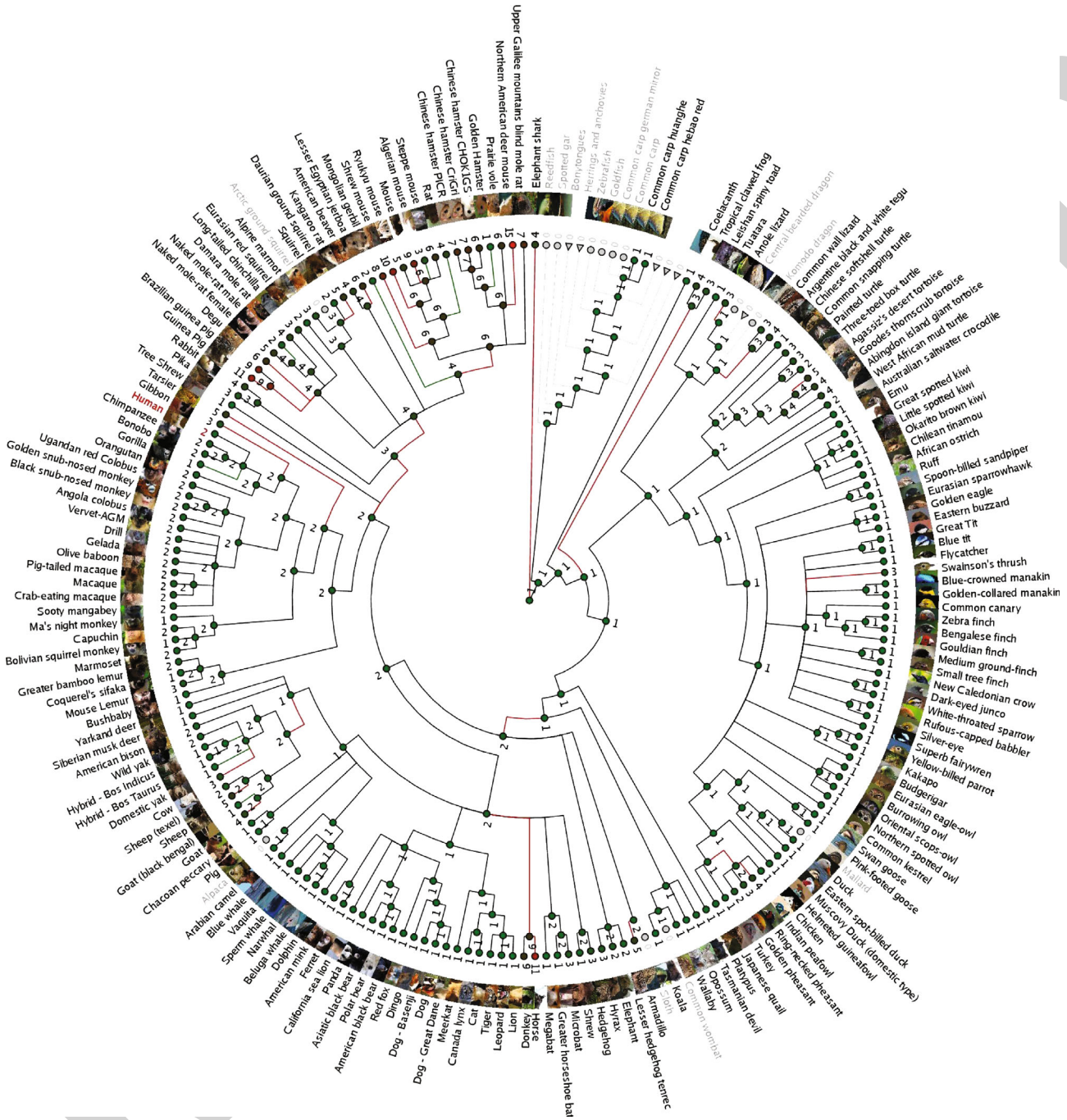

Figure 2: The Gene Gain/Loss Tree depicts the CYP2D gene family's phylogenetic history by showing new gene additions and deletions.

2. Materials and Methods

2.1. Exploration and Mining of Human and Mouse CYP2D Structure and Sequences. The human CYP2D gene family's amino acid sequence was searched from the Public Database of the National Center for Biotechnology Information (NCBI) https://www.ncbi.nlm.nih.gov, and the protein crystal structure was obtained from the Public Database of Protein Data Bank (PDB) http://www.rcsb.org. Further, we also searched the PubChem database for some structural proteins and ligands available at https://pubchem.ncbi.nlm.nih.gov/search/search.cgi.

2.2. 3D Structure Prediction and Validation of Human CYP2D Genes. The solved crystal structure of human and mouse protein *CYP2D* is not available in the PDB. Thus, the three-dimensional (3D) structures of *CYP2D* were predicted by homology modeling approaches. To prepare or predict precise 3D modeled structure of the target proteins, we employed several software programs, including Phyre2 [26], Swiss model [27], and iterative Threading assembly Refinement (I-TASSER) [28, 29], which works by multiple threading approaches through identifying the template from PDB. The 3D modeled target proteins were minimized by

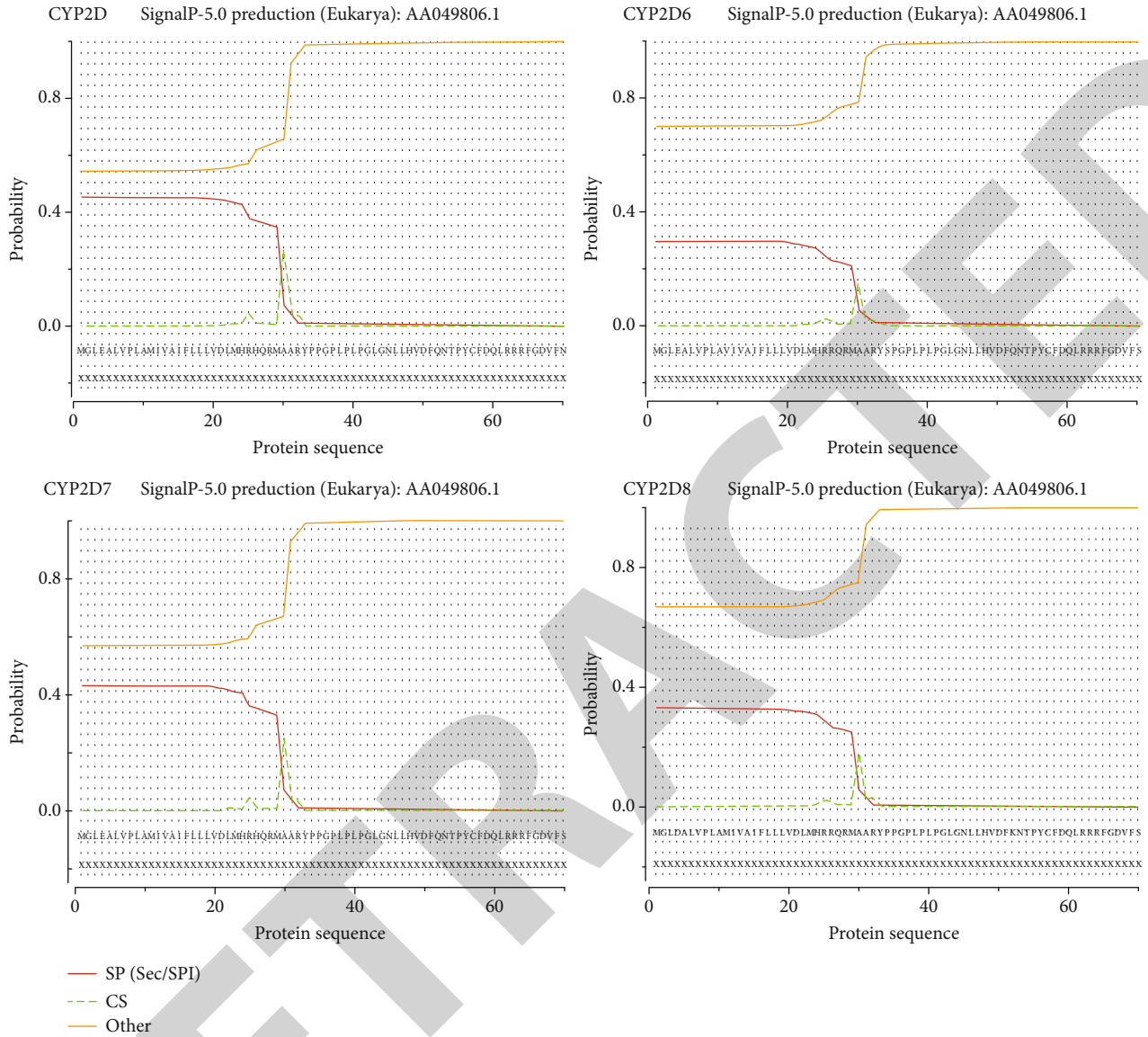

Figure 3: Signal peptide cleavage prediction by the SignalP 4.1 server. The signal peptide score and cleavage site score, cleavage site score, and cleavage site score are shown as combined scores (raw cleavage site score).

employing the conjugate gradient algorithm and the Amber force field in UCSF Chimera 1.10.1 [30]. Validation of the predicted protein structure remained bottlenecked problems. In our analysis, following 3D structure modeling, we used several protein structure validation tools, including protein structure analysis (ProSA), to identify errors in experimental and theoretical protein structure [31, 32]. The ProSA program language is intended to validate from the predicted atomic structure coordinates, and the results are evaluated by *z*-score value.

2.3. Disordered Analysis of Human CYP2D Proteins. Following the 3D homology modeling of the human and mouse *CYP2D* protein, we sought to identify the disordered protein segment or unstructured regions [33]. It is believed that these regions contribute to protein instability, thereby causing pathological conditions. To have precisely predicted unstructured protein segment of amino acid residues positions, we employed Cspritz version 1.2, http://protein.bio.unipd.it/cspritz/ [34].

2.4. Analysis of Human and Mouse CYP2D Protein Ligands and Domain. In proteomics, understanding the structural property of the functional unit of protein is worthwhile. Thus, the protein-ligand, ligand-binding residue, ligand-binding regions, and domains of *CYP2D* were predicted by using several bioinformatics tools. Further, the protein ligands were clustered based on their functional similarity. RapotorX predicted ligand-binding residues of the protein structures, a template-based robust 3D modeling web tool [35, 36] RapotorX is known for its high-quality structural modeling output multiple targets by using one remote template. Other additional programs were used to crosscheck and validate the reliability and the accuracy of the predicted

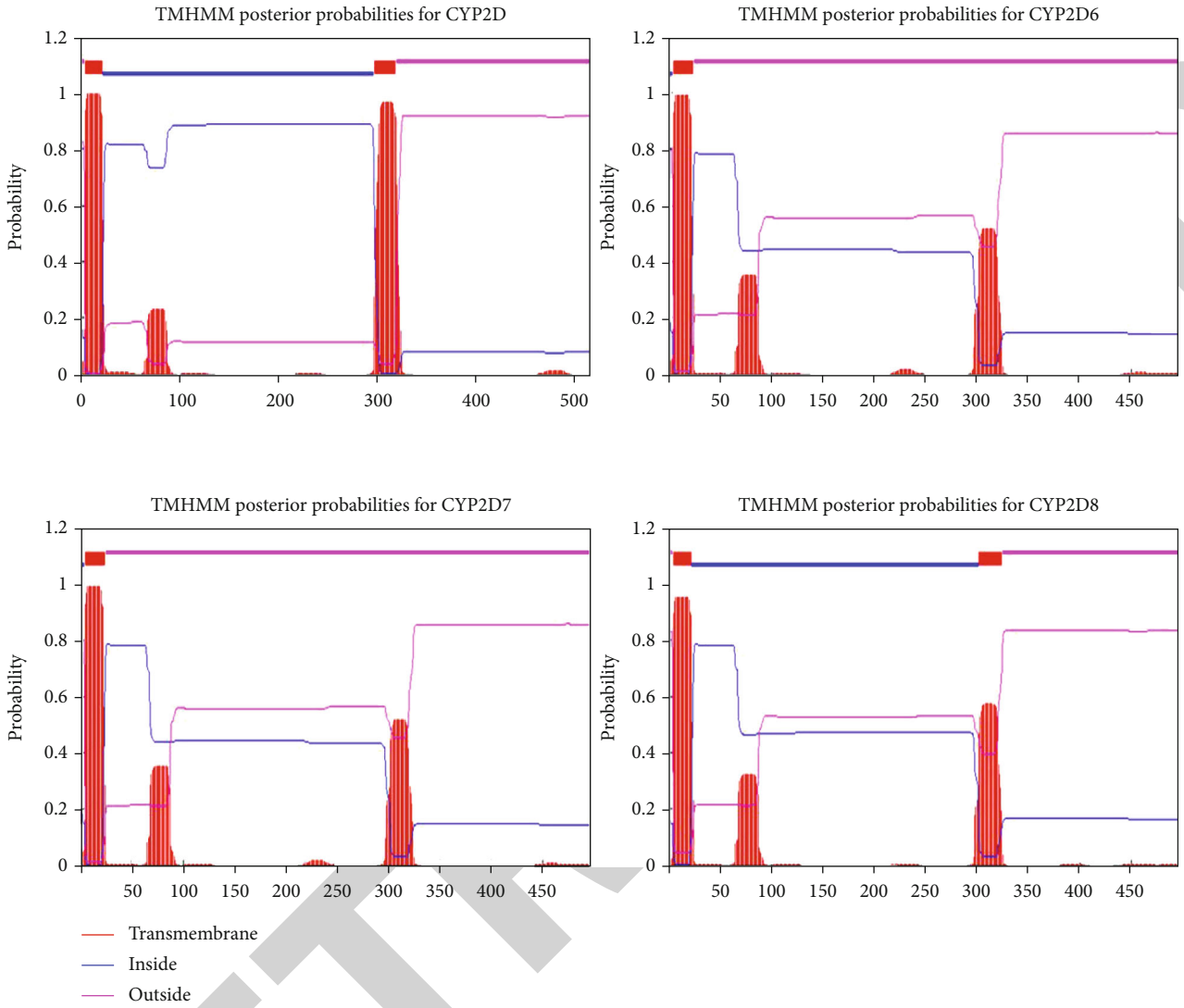

Figure 4: The prediction of transmembrane helices in *Phytophthora infestans* and other organisms by the TMHMM 2.0 server.

result, including COACH server [37], I-TASSER was used to determine the number of binding sites and their positions [28]. COACH is a metaserver approach for predicting ligand-binding targets through two comparative methods TM-SITE [28] and S-SITE. The BioLiP protein function database is used in these methods to recognize ligand-binding sites [38]. To understand the ligand-binding surface on nonbound of freely existing protein structure, we applied FTSite server ligand-binding prediction tools [39]. Its accuracy is reported to be comparable with experimental results [40]. The prediction principle of FTSite is template evolutionary-based; instead, it is based on evidence obtained from experiments [41]. Presumably, the prediction algorithm is designed for the mapping of protein regions [41]. To further understand the interaction between target protein's ligands and amino acids, ligand module clustering was done by LPIcom' web server [42] found at http://crdd.osdd.net/raghava/lpicom. Amino acid residues and ligand interactions were predicted using the LPIcom web server to classify residues' desired interaction and binding motif for a given ligand [43].

2.5. Protein Interactions and Coexpression Analysis. Protein-protein interaction analysis of human and mouse *CYP2D* was undertaken to assess the functional relationship and information flow networks among CYP2D and its neighbouring genes and other proteins. Protein-protein interactions are one of the physiological settings known to affect a multitude of biological functions. The interaction analysis was performed by STRING software [44] and visualized by commercial Cytoscape software [45]. The STRING software program considers both functional and physical interactions among proteins. The software algorithm was developed to capture the protein-protein interactions based on existing literature, experimental output, text mining, and cooccurrence [46].

2.6. Predicting Consensus Sequence Alignment and Secondary Structure. To understand the structural alignment of *CYP2D*, we employed ENDscript 2 open-access tool, which enables us to visualize multiple biochemical and structural alignments [47]. The web tool has been designed to recognize simple to

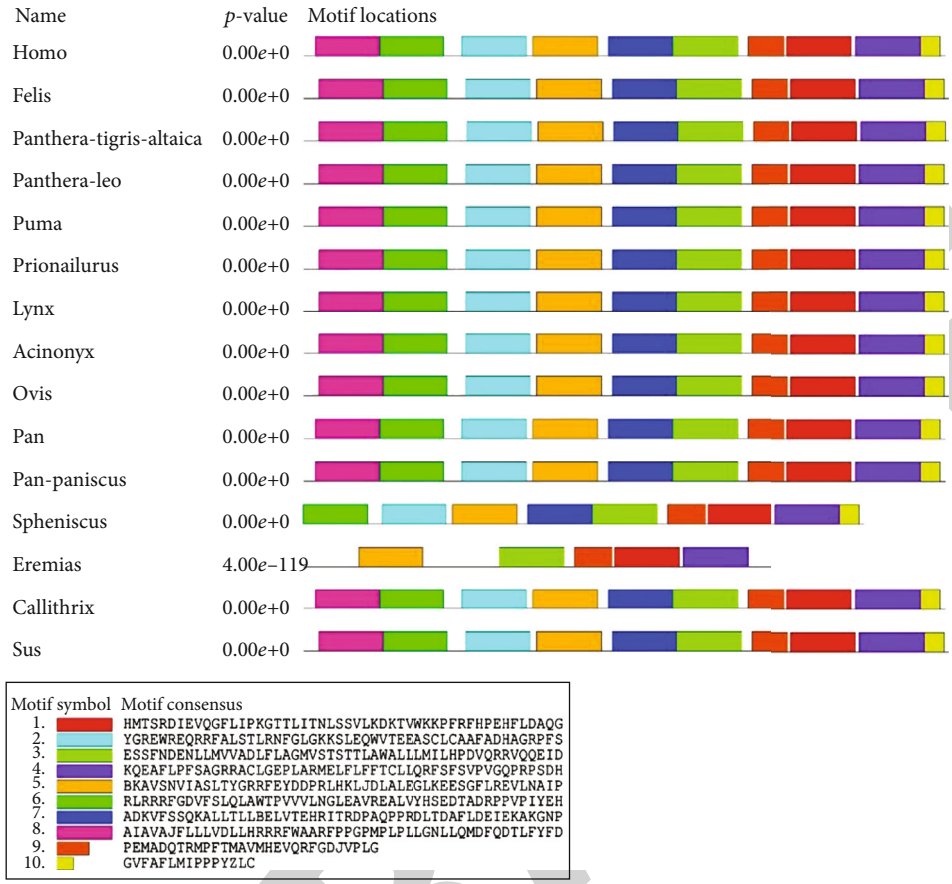

Figure 5: CYP2D motif distribution in the vertebrate species. Motifs of these genes from representatives of different species are predicted using the MEME suite based on amino acid sequences. Some conserved animal motifs have been found. The motifs are marked as grey boxes.

complex structures, i.e., primary to quaternary. Additionally, it utilizes the PDB input format and processes into several categories of outcomes that can be visualized in many structural interface tools. Further, the secondary structure of all target proteins was determined by online server PSIPRED version 3.3 [48], a web tool that combines protein sequences and structural analysis into one platform. Initially, the software utilizes protein sequence input data and performs PSI-BLAST [49].

3. Results

3.1. Gene Cooccurrence and Evolutionary History. Gene trees represent the evolutionary history of gene families that evolved from a common ancestor. Reconciliation of the gene tree with the species' tree enables us to ascertain speciation events by comparing their sequences' similarities and differences. In the case of unique orthologous genes, concordance between the best reciprocal best methods is quite evident. The Gene Tree pipeline can analyze the relationships between more complex gene trees that combine one-to-many and many-to-many. This greatly raises the number of Fly/Mammal and Worm/Mammal orthologues compared to the number of Mammal orthologues and has a much more drastic impact on the Fly/Mammal and Worm/Mammal orthologues. By determining the most recent ancestry of a given internal tree node, we may also use this approach to "time" duplications of events (Figure 1). The tree merging algorithm is used to assemble a single consensus tree from the five trees. This enables TreeBeST to take advantage of the fact that DNA-based trees are often more accurate in determining relationships between distant parts of trees. Under some circumstances, a group of algorithms may outperform others.

The algorithm combines the output of the five models into a single model. The topology of consensus includes clades found in any input trees, minimizing the number of inferred losses and duplications and having the best bootstrap values. Because of the DNA alignment, branch lengths have been estimated according to the HKY model. The Gene Gain/Loss Tree depicts a gene family's phylogenetic history by showing new gene additions and deletions. A red branch on the tree represents a significant expansion of a gene's history, a green branch denotes a contraction, and a grey branch denotes no change (Figure 2). The numbers above each ancestral species refer to the number of distinct genes it once had. The color of each node reflects the gene's size, based on the number of people who have the gene. The species names are colored red, black, and grey to show the current genes of interest and the genes present in Ensembl (species with no current genes in this tree). Only a selected tree of humans, chimps, marmosets, mice, zebrafish, and zebra finches is

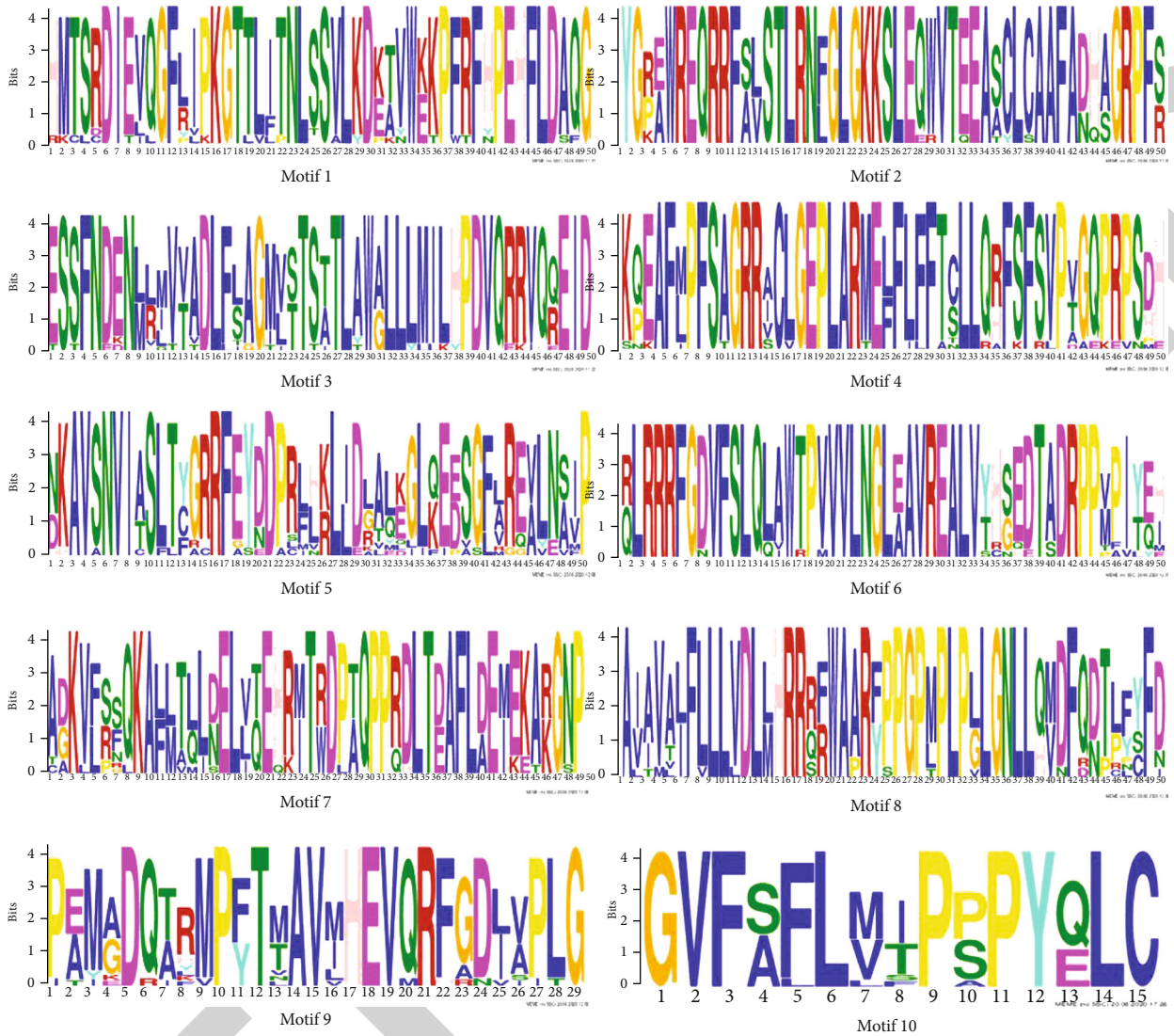

Figure 6: Sequence-specific MEME conserved motifs for *CYP2D* proteins.

displayed on this site. Be warned that the species of interest in these trees may not be included (Figure 2).

The SignalP 4.1 program was used to analyze the protein dataset, which revealed that the protein sequences are enzymatic proteins (Figure 3). Analysis of the cytochrome protein suggests that the amino acids from 1 to 26 have a *D*-score of 0.735 and an upper limit of 0.642 at the position. It is essential to note the *D*-score used in this study as it is used to measure the dissimilarity between signal and nonsignal peptides. In principle, N-terminal or amino-terminal signal peptides are known as short sequences that target and guide secretory proteins to the translocator and the ER. We used protein sequence representations according to the groups of amino acids and amino acids' properties with the TMHMM algorithm. We utilized the publicly available genome annotation parameters of TMHMM and compared them to our selected protein sequences. The possible observations in each state are collapsed into three possible states for polarity (nonpolar, polar, and neutral), three for the charge, three for aromaticity, three for size, and five for electronic properties. Once the body absorbs unwanted proteins, they could be cleaved off from their original passenger protein sequence. Many proteins lacking the N-terminal signal peptide exist outside of cells. It can be exported from the cell without the use of a signal sequence. However, the other proteins analyzed were not found to have N-terminal signal peptides, which continued to pose a mystery on the matter (Figure 4).

3.2. Motif Analysis. The MEME (Multiple Em for Motif Elicitation) algorithms have been used to perform DNA and protein motif analysis. The sequences were compared, and similar sequence motifs were calculated (Figure 5). MEME tool identified the distribution of the motif in protein sequences. This combined high conservation patterns with motifs from one to five (Figure 6). All patterns in protein sequences of animal species have been observed. The homology of motifs in different species means that the structural gene characteristics differ concerning exon-intron relationships. These analyses showed that the variances in the sharing of motifs in these animal species'

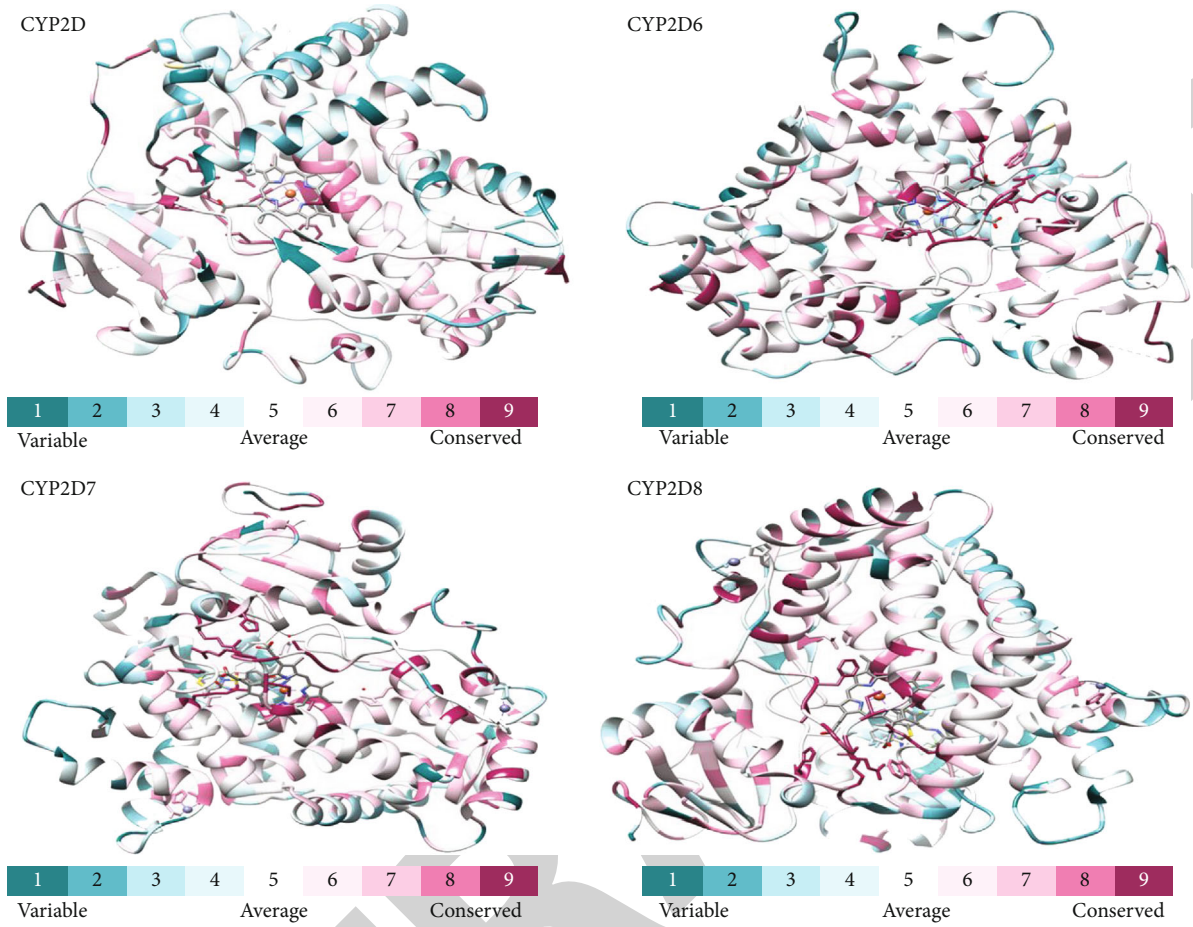

Figure 7: The crystal structure was determined using human protein as a reference species. The amino acids were predicted based on the value of conservation ranging from 1 to 9, with a value between 1 and 4 considered variable, a value of 5 and 6 average conservation, and a value between 7 and 9 highly conserved.

proteins might have deviated from those genes' functions during adaptive evolution.

The crystal protein structure was predicted by powerful online webserver I-TASSER (ahttps://zhanglab.ccmb.med.umich.edu/I-TASSER), which usually utilizes the PDB template. The 3D protein structure of human cytochromes was predicted. After 3D modeling, UCSF Chimera was used in protein-energy by applying the Amber force field principle's conjugate gradient algorithm. We used the ConSurf server to predict nucleic acids' position and the level of evolutionary conservation of amino acids in these proteins to determine the degree of evolutionary conservation between bacterial strains in these two genes (Figure 7). The vast majority of sites positively selected throughout evolution have been maintained across the mammalian branches of evolution. Many amino acids were found to have residues visible or hidden in these proteins regarding the NNA (neural network algorithm).

Protein-protein interactions are a central part of the cellular network and are known to have various impacts. The information flow networks between all targeted proteins were analyzed to determine how much information flows between the cytochrome proteins and other proteins. A molecular-genetic interaction network was created using online STRING software and visualized using Cytoscape software. Nodes, lines, and colors justify the interactive network. (Figure 8). Proteins whose genes are observed to be correlated in expression across a large number of experiments. The STRING performed a coexpression analysis database that showed coexpression scores based on RNA expression patterns and protein coregulation provided by ProteomeHD. Analysis of proteins signaling intensities was analyzed for cytochrome proteins. The result showed that more protein residues are involved in signal receiving as compared to signal communicating residues. The results are described by colors displayed on the predicted structures (Figure 9).

4. Discussion

Bioinformatics can be instrumental in analyzing and interpreting the data of proteomics and genomics. It uses mathematical, statistical, computational, biological, and medical methods and technologies. It is a vital sophisticated tool for interpreting the protein functions from its amino acids sequence and has revolutionized organisms' metabolism. The P450 forms of humans and rats have always been considerable information for the best comparison of its structures

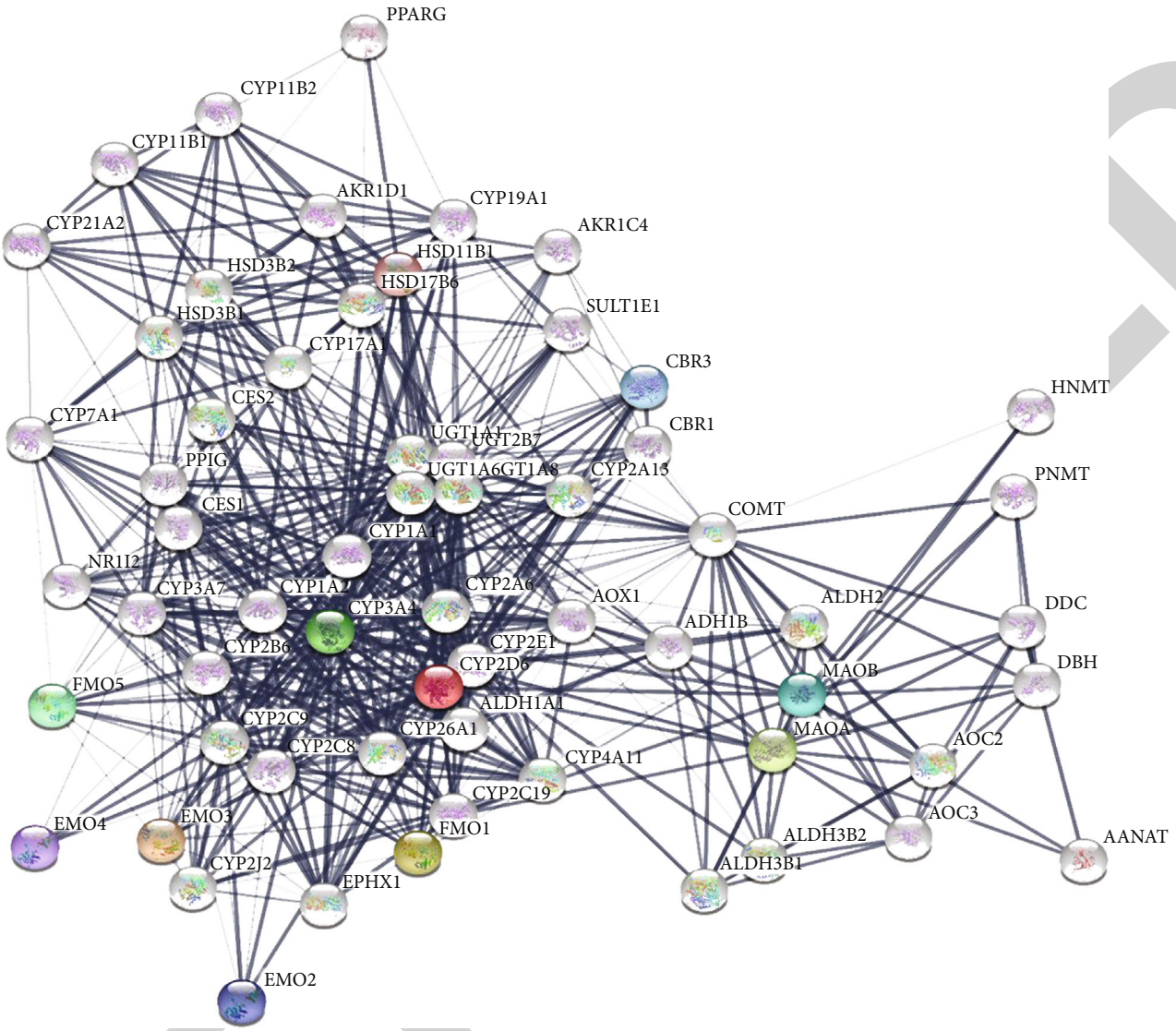

Figure 8: The putative protein-protein interaction of CYP2D protein analysis. Based on protein-protein interaction, it is a solid argument. The length of a connector indicates the distance between the sender and the receiver. Red nodes represent known and unknown proteins, while filled nodes represent known proteins and predicted proteins. Black lines indicate biological interactions between proteins.

and function in both species. However, human conditions have been less extensively studied. *CYP2D6* makes a unique polymorphic enzyme, which is considered more appropriate for the metabolism of all kinds of drugs [13]. In this present study, the study of gene cooccurrence and an evolutionary tree constructed to determine families' histories. According to the results, *CYP2D* proteins of different species were found highly similar in humans and other organisms, so it is stated that they are evolved from a common ancestor (Figure 1). These findings are very similar to McArthur et al. [46]. They reported that the CYP3A gene sequence identity among different species like snake, fish, chicken, and mammalian CYP3A had been found well conserved during vertebrate evolution. However, the multiple copies of that gene within the species showed highly present among paralogues.

Similarly, in another report, the construction of a phylogenetic tree provides the best understanding of the function and diversity of *CYP2* genes. The topology of most species was lineage-specific. However, a few belong to ancestral subfamilies since the *CYP2* gene family has been found diversified among all vertebrates and presented its multiplicity within particular subfamilies like *CYP2X*, *CYP2K*, *CYP2AA*, and zebrafish [13].

In this study, to analyze gene structure and function prediction, the ProtParam server was used to analyze the primary structure of selected CYPs and various physicochemical properties determined from protein sequences. Theoretical pI (isoelectric point), molecular weight, atomic composition, the composition of amino acids, estimated half-life, extinction coefficient, instability index, high hydropathicity, and aliphatic index. SOPMA (Self-Optimized Predictive Method with Alignment) server performed secondary structure prediction. This server calculated the percentage of protein sequences in random coil, alpha-helix, beta-sheet, and extended strands

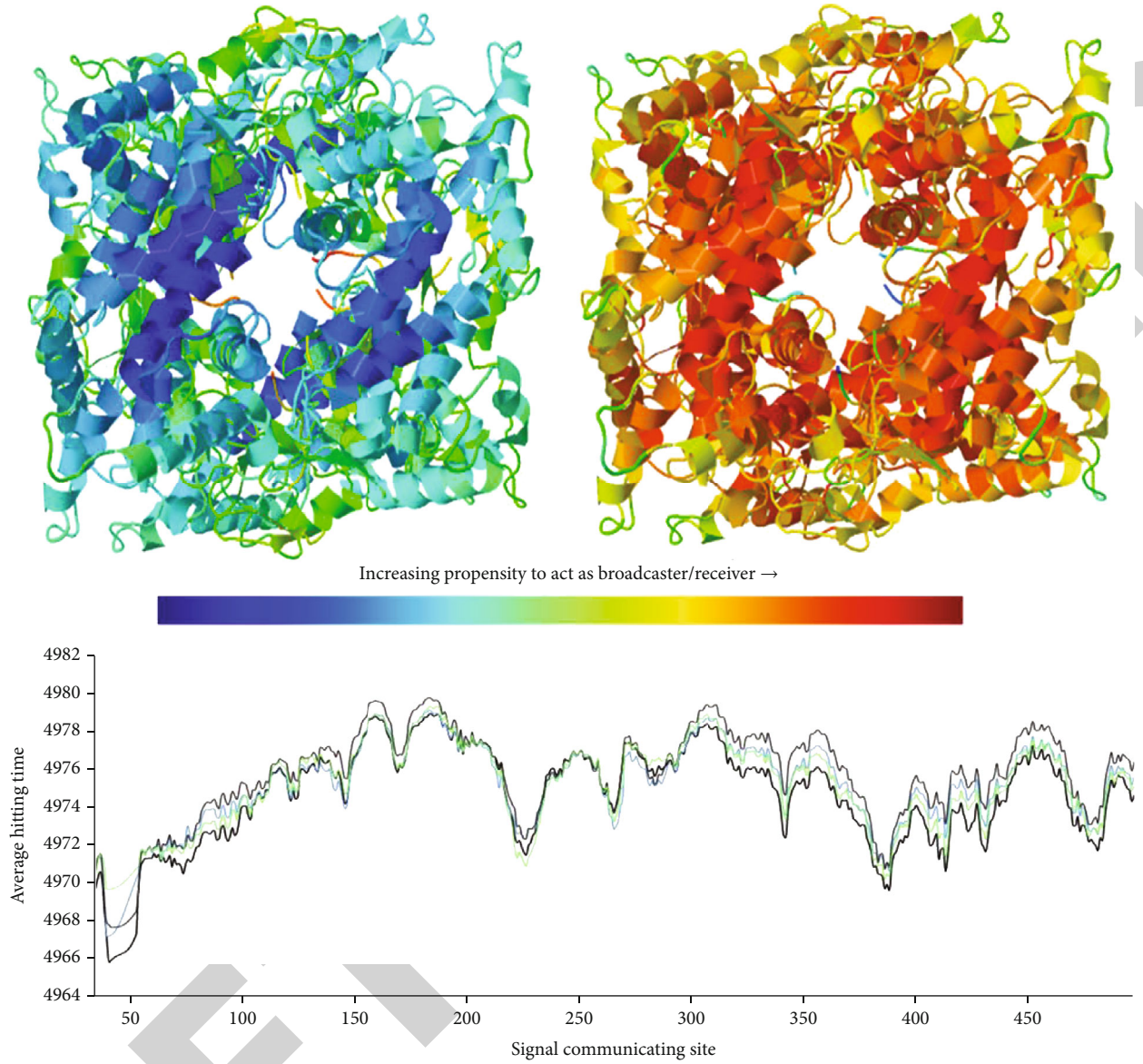

Figure 9: Predicted signal communication of *CYP2D* proteins. Signal communicating residue structure justified by blue color having less residue. The signal receiving residue structure is represented by the orange color with more reside. Signal communicating residue structure is explained by the blue color having less residue and signal receiving residue structure represented by the orange color with more residue.

(Figures 2 and 3). Most parts of the *CYPs* are alpha-helix and random coil, according to the results. Phyre2 server has predicted the tertiary structures of human *CYP2D* as a sample of other organisms. These findings have been very similar and supportive when *CYPs* were analyzed in different species like seed plants and other animal's protein sequences reported previously [50].

Substrate recognition sites (SRSs) in the *CYP2* family are necessary for the catalysis of substrates targeted. Various functional sites can be monitored with a 3D structure modeling approach in humans and compared with the homology of bacterial *CYPs* [1, 22]. Spectroscopic experiments showed that P450 active sites are variable in their flexibility and stability. According to one review report [3, 51, 52], all *CYPs* were different with different activities, and their functional properties were substrate-dependent. The user can swap the active sites to get the desired function from *CYPs* [53]. Rowland et al. [54] reported the crystal structure of *CYP2D*6 at the resolution of 3A° and noted that the primary structure of the *CYP2D*6 is resampled with other *CYPs*.

Similarly, according to the previous study [22], they reported the reaction site centre for *CYP2D*6 substrates based on the ligand-bound *CYP2*C5 model. Besides, it was reported that the substrates of CYP2D6 presented the essential nitrogen at a distance of about 5 to 7A° from the oxidation site and were also found interacting with Glu-216 Asp-301 [55]. The Rabbit *CYP2*C5 crystal structure was used in *CYP2D*6 homology modelling, which was present as Arg440 near the protein surface (Figure 4). Docking the FMN structure of

P450 reductase to the *CYP2D*6 model, it was evident that Arg440 is a central cluster of amino acids basic residues [56].

According to one study, the ligand-binding characteristics of *CYP2D* isoforms *CYP2D*1–4 in rats and *CYP2D*6 in humans were investigated. They measured IC50 values of already known 11 *CYP2D*6 ligands by using 7-methoxy-4-(aminomethyl) coumarin (MAMC) as substrate [57]. The crystallized rabbit *CYP2C*5 based homology model was generated, and its capacity to reproduce binding sequences related to the substrates' metabolic orientation was maintained during direct molecular dynamics simulations [58]. The electrostatic potential of *CYP2D* and *CYP2D*1-4 actives binding sites showed affinities towards ligands. Whereas the active sites residues and their binding pattern differences could help renationalize the IC50 values of every ligand [59]. They concluded that *CYP2D*2 was the most critical rat isoform (resembled with the human) in binding through IC50 values of ligand [18]. According to Hasemann et al. [60], three enzymes, like the hemoprotein domain of $P450_{BM\text{-}3}$ and crystal structures of $P450_{terp}$ and $P450_{cam}$, were compared. They reported that all enzymes' topology was quite similar; however, the substrate-binding region was highly variable. Similarly, compared to local differences in I helices, the heme-binding core structure was conserved well (Figure 7).

In this present study, five motifs were found in most mammalian species according to the conserved motifs obtained by MEME and MAST tools (Figures 5 and 6). Similar findings were reported previously [61]; they made a comparison among six major P450s in humans (CYP3A4, *CYP2D*6, *CYP2C*9, *CYP2C*19, CYP1A2, and *CYP2E*1) to monitor its structural, functional, and evolutionary relationships [50]. According to motif analysis, they suggested eight motifs across these six *CYPs* identified by MEME and interpreted by MAST tools. Among the six *CYPs*, the cytochromes 2C9, 2C19, and 2E1 possessed all eight motifs. However, *CYP2D*6 was found lacking with the 8^{th} number motif. Similarly, CYP1A2 and CYP3A4 were found lacking with 3^{rd}, 6^{th}, and 8^{th} motifs (Figure 5). They concluded that *CYPs* (2C19, 2C9, 2E1, and 2D6) were similar and different from CYP3A4 and CYP1A2. In this connection, Darabi et al. [50] analyzed CYP proteins to find conserved motif patterns using MEME and MAST tools. In a total of 39 different species, ten motifs were found highly conserved. However, motifs (1, 3, 4, and 7) were reported common in 35 species, and no common conserved motif was present in all, according to their results.

5. Conclusion

This study shows the mechanistic insights obtained from a comprehensive computational framework focused on evolutionary details and structure prediction. Bioinformatics methods used across fields such as computer science, mathematics, statistics, genetics, physics, and medicine can forecast and analyze genomic and proteomic results. It could be a novel way of interpreting protein structure, and it could revolutionize knowledge about an organism's metabolism. In humans and other mammals, these bioinformatics experiments have shown the structural-functional and evolutionary understanding of CYP2D. Our findings suggest that the animal species' cytochrome protein family is very diverse, encompassing all species studied. Differences in cytochrome subunits are expected to be critical in deciding the unique substrates that allow this functional diversity.

Data Availability

The data of this study will be available openly to readers, and data the data supporting the conclusions of the study can be accessible.

Conflicts of Interest

There is no conflict of interest in the conduction of this study.

Authors' Contributions

HIA, GA, and KM are responsible for the conceptualization; HIA and GA for the data curation; HIA and GA for the formal analysis; HIA, IA, SA, AA, and JH for the methodology; HIA, GA, SA, and KM for the software; MAK and ZK for the supervision; AJ, SK, AJ, and SK for the validation; HIA, GA, AA, and JH for the writing and original draft; and MAK, ZK, IA, SA, and SK for the writing, review, and editing.

References

[1] U. M. Zanger and M. Schwab, "Cytochrome P450 enzymes in drug metabolism: regulation of gene expression, enzyme activities, and impact of genetic variation," *Pharmacology & Therapeutics*, vol. 138, no. 1, pp. 103–141, 2013.

[2] F. P. Guengerich, M. R. Waterman, and M. Egli, "Recent structural insights into cytochrome P450 function," *Trends in Pharmacological Sciences*, vol. 37, no. 8, pp. 625–640, 2016.

[3] P. Anzenbacher and E. Anzenbacherova, "Cytochromes P450 and metabolism of xenobiotics," *Cellular and Molecular Life Sciences CMLS*, vol. 58, no. 5, pp. 737–747, 2001.

[4] H. Lee, E. Park, H. Ji et al., "Identification of cytochrome P450 enzymes responsible for N-dealkylation of a new oral erectogenic, mirodenafil," *Xenobiotica*, vol. 38, no. 1, pp. 21–33, 2008.

[5] H. Wang and L. M. Tompkins, "CYP2B6: new insights into a historically overlooked cytochrome P450 isozyme," *Current Drug Metabolism*, vol. 9, no. 7, pp. 598–610, 2008.

[6] T. Porter and M. Coon, "Cytochrome P-450. Multiplicity of isoforms, substrates, and catalytic and regulatory mechanisms," *Journal of Biological Chemistry*, vol. 266, no. 21, pp. 13469–13472, 1991.

[7] F. P. Guengerich, "Human cytochrome P450 enzymes," in *Cytochrome P450*, pp. 377–530, Springer, 2005.

[8] S. A. Wrighton and J. C. Stevens, "The human hepatic cytochromes P450 involved in drug metabolism," *Critical Reviews in Toxicology*, vol. 22, no. 1, pp. 1–21, 1992.

[9] X. Ding and L. S. Kaminsky, "Human extrahepatic cytochromes P450: function in xenobiotic metabolism and tissue-selective chemical toxicity in the respiratory and gastrointestinal tracts," *Annual Review of Pharmacology and Toxicology*, vol. 43, no. 1, pp. 149–173, 2003.

[10] S. Kimura, M. Umeno, R. Skoda, U. Meyer, and F. Gonzalez, "The human debrisoquine 4-hydroxylase (CYP2D) locus:

sequence and identification of the polymorphic CYP2D6 gene, a related gene, and a pseudogene," *American Journal of Human Genetics*, vol. 45, no. 6, pp. 889–904, 1989.

[11] D. R. Nelson, "Comparison of P450s from human and fugu: 420 million years of vertebrate P450 evolution," *Archives of Biochemistry and Biophysics*, vol. 409, no. 1, pp. 18–24, 2003.

[12] Y. Yasukochi and Y. Satta, "Evolution of the CYP2D gene cluster in humans and four non-human primates," *Genes & Genetic Systems*, vol. 86, no. 2, pp. 109–116, 2011.

[13] M. Ingelman-Sundberg, "Genetic polymorphisms of cytochrome P 450 2D6 (CYP2D6): clinical consequences, evolutionary aspects and functional diversity," *The Pharmacogenomics Journal*, vol. 5, no. 1, pp. 6–13, 2005.

[14] R. Fonne-Pfister and U. A. Meyer, "Xenobiotic and endobiotic inhibitors of cytochrome p-450dbl function, the target of the debrisoouine/sparteine type polymorphism," *Biochemical Pharmacology*, vol. 37, no. 20, pp. 3829–3835, 1988.

[15] Z. Huang, M. J. Fasco, and L. S. Kaminsky, "Alternative splicing of CYP2D mRNA in human breast tissue," *Archives of Biochemistry and Biophysics*, vol. 343, no. 1, pp. 101–108, 1997.

[16] A. Gaedigk, R. Gaedigk, and J. S. Leeder, "CYP2D7 splice variants in human liver and brain: does CYP2D7 encode functional protein?," *Biochemical and Biophysical Research Communications*, vol. 336, no. 4, pp. 1241–1250, 2005.

[17] H. V. Pai, R. P. Kommaddi, S. J. Chinta, T. Mori, M. R. Boyd, and V. Ravindranath, "A frameshift mutation and alternate splicing in human brain generate a functional form of the pseudogene cytochrome P4502D7 that demethylates codeine to morphine," *Journal of Biological Chemistry*, vol. 279, no. 26, pp. 27383–27389, 2004.

[18] J. Venhorst, A. M. ter Laak, J. N. Commandeur, Y. Funae, T. Hiroi, and N. P. Vermeulen, "Homology modeling of rat and human cytochrome P450 2D (CYP2D) isoforms and computational rationalization of experimental ligand-binding specificities," *Journal of Medicinal Chemistry*, vol. 46, no. 1, pp. 74–86, 2003.

[19] T. Wolff, L. M. Distlerath, M. T. Worthington et al., "Substrate specificity of human liver cytochrome P-450 debrisoquine 4-hydroxylase probed using immunochemical inhibition and chemical modeling," *Cancer Research*, vol. 45, no. 5, pp. 2116–2122, 1985.

[20] O. Gotoh, "Substrate recognition sites in cytochrome P450 family 2 (CYP2) proteins inferred from comparative analyses of amino acid and coding nucleotide sequences," *Journal of Biological Chemistry*, vol. 267, no. 1, pp. 83–90, 1992.

[21] P. Rowland, F. E. Blaney, M. G. Smyth et al., "Crystal Structure of Human Cytochrome P450 2D6," *Journal of Biological Chemistry*, vol. 281, no. 11, pp. 7614–7622, 2006.

[22] R. J. Unwalla, J. B. Cross, S. Salaniwal et al., "Using a homology model of cytochrome P450 2D6 to predict substrate site of metabolism," *Journal of Computer-Aided Molecular Design*, vol. 24, no. 3, pp. 237–256, 2010.

[23] H. Cai, J. Jiang, Q. Yang, Q. Chen, and Y. Deng, "Functional characterization of a first avian cytochrome P450 of the CYP2D subfamily (CYP2D49)," *PLoS One*, vol. 7, no. 6, article e38395, 2012.

[24] S. Raimundo, C. Toscano, K. Klein et al., "A novel intronic mutation, 2988G> A, with high predictivity for impaired dunction of cytochrome P450 2D6 in white subjects," *Clinical Pharmacology & Therapeutics*, vol. 76, no. 2, pp. 128–138, 2004.

[25] A. Fohner, L. I. Muzquiz, M. A. Austin et al., "Pharmacogenetics in American Indian populations: analysis of CYP2D6, CYP3A4, CYP3A5, and CYP2C9 in the Confederated Salish and Kootenai Tribes," *Pharmacogenetics and Genomics*, vol. 23, no. 8, pp. 403–414, 2013.

[26] L. A. Kelley, S. Mezulis, C. M. Yates, M. N. Wass, and M. J. Sternberg, "The Phyre2 web portal for protein modeling, prediction and analysis," *Nature Protocols*, vol. 10, no. 6, pp. 845–858, 2015.

[27] L. A. Kelley and M. J. Sternberg, "Protein structure prediction on the Web: a case study using the Phyre server," *Nature Protocols*, vol. 4, no. 3, pp. 363–371, 2009.

[28] J. Yang, R. Yan, A. Roy, D. Xu, J. Poisson, and Y. Zhang, "The I-TASSER Suite: protein structure and function prediction," *Nature Methods*, vol. 12, no. 1, pp. 7-8, 2015.

[29] Y. Zhang, "I-TASSER: fully automated protein structure prediction in CASP8," *Proteins: Structure, Function, and Bioinformatics*, vol. 77, no. S9, pp. 100–113, 2009.

[30] E. F. Pettersen, T. D. Goddard, C. C. Huang et al., "UCSF Chimera—a visualization system for exploratory research and analysis," *Journal of Computational Chemistry*, vol. 25, no. 13, pp. 1605–1612, 2004.

[31] M. Wiederstein and M. J. Sippl, "ProSA-web: interactive web service for the recognition of errors in three-dimensional structures of proteins," *Nucleic Acids Research*, vol. 35, no. Web Server, pp. W407–W410, 2007.

[32] H. I. Ahmad, A. R. Asif, M. J. Ahmad et al., "Adaptive evolution of peptidoglycan recognition protein family regulates the innate signaling against microbial pathogens in vertebrates," *Microbial Pathogenesis*, vol. 147, p. 104361, 2020.

[33] H. I. Ahmad, M. B. Bin Majeed, M. Z. Ahmad et al., "Comparative analysis of the mitochondrial proteins reveals complex structural and functional relationships in _Fasciola_ species," *Microbial Pathogenesis*, vol. 152, p. 104754, 2021.

[34] J. Cheng, Y. Zhen, S. Miksys et al., "Potential role of CYP2D6 in the central nervous system," *Xenobiotica*, vol. 43, no. 11, pp. 973–984, 2013.

[35] M. Källberg, G. Margaryan, S. Wang, J. Ma, and J. Xu, "RaptorX server: a resource for template-based protein structure modeling," in *Protein structure prediction*, pp. 17–27, Springer, 2014.

[36] Q. Yousafi, H. A. ALI, H. Rashid, and M. S. Khan, "In silico comparative proteomic analysis of enzymes involved in fatty acid biosynthesis in castor bean (Ricinus communis) and soybean (Glycine max)," *Turkish Journal of Botany*, vol. 43, no. 1, pp. 1–26, 2019.

[37] Q. Wu, Z. Peng, Y. Zhang, and J. Yang, "COACH-D: improved protein–ligand binding sites prediction with refined ligand-binding poses through molecular docking," *Nucleic Acids Research*, vol. 46, no. W1, pp. W438–W442, 2018.

[38] J. Yang, A. Roy, and Y. Zhang, "BioLiP: a semi-manually curated database for biologically relevant ligand–protein interactions," *Nucleic Acids Research*, vol. 41, no. D1, pp. D1096–D1103, 2012.

[39] C.-H. Ngan, D. R. Hall, B. Zerbe, L. E. Grove, D. Kozakov, and S. Vajda, "FTSite: high accuracy detection of ligand binding sites on unbound protein structures," *Bioinformatics*, vol. 28, no. 2, pp. 286-287, 2012.

[40] B. K. Dukka, "Structure-based methods for computational protein functional site prediction," *Computational and Structural Biotechnology Journal*, vol. 8, no. 11, article e201308005, 2013.

Hindawi
BioMed Research International
Volume 2024, Article ID 9876404, 1 page
https://doi.org/10.1155/2024/9876404

Retraction

Retracted: Use of Medicinal Plants for Respiratory Diseases in Bahawalpur, Pakistan

BioMed Research International

Received 12 March 2024; Accepted 12 March 2024; Published 20 March 2024

This article has been retracted by Hindawi following an investigation undertaken by the publisher [1]. This investigation has uncovered evidence of one or more of the following indicators of systematic manipulation of the publication process:

(1) Discrepancies in scope

(2) Discrepancies in the description of the research reported

(3) Discrepancies between the availability of data and the research described

(4) Inappropriate citations

(5) Incoherent, meaningless and/or irrelevant content included in the article

(6) Manipulated or compromised peer review

The presence of these indicators undermines our confidence in the integrity of the article's content and we cannot, therefore, vouch for its reliability. Please note that this notice is intended solely to alert readers that the content of this article is unreliable. We have not investigated whether authors were aware of or involved in the systematic manipulation of the publication process.

Wiley and Hindawi regrets that the usual quality checks did not identify these issues before publication and have since put additional measures in place to safeguard research integrity.

We wish to credit our own Research Integrity and Research Publishing teams and anonymous and named external researchers and research integrity experts for contributing to this investigation.

The corresponding author, as the representative of all authors, has been given the opportunity to register their agreement or disagreement to this retraction. We have kept a record of any response received.

References

[1] S. Afzal, H. I. Ahmad, A. Jabbar et al., "Use of Medicinal Plants for Respiratory Diseases in Bahawalpur, Pakistan," *BioMed Research International*, vol. 2021, Article ID 5578914, 10 pages, 2021.

Hindawi
BioMed Research International
Volume 2021, Article ID 5578914, 10 pages
https://doi.org/10.1155/2021/5578914

Research Article

Use of Medicinal Plants for Respiratory Diseases in Bahawalpur, Pakistan

Sadia Afzal,[1] **Hafiz Ishfaq Ahmad**,[2] **Abdul Jabbar**,[3] **Mahmoud M. Tolba**,[4] **Sameh AbouZid**,[5] **Nimra Irm**,[2] **Farheen Zulfiqar**,[6] **Muhammad Zahid Iqbal**,[3] **Shoaib Ahmad**,[7,8] **and Zubair Aslam**[9]

[1]*Department of Botany, Faculty of Life Science, Women University Multan, Punjab, Pakistan*
[2]*Department of Animal Breeding and Genetics, University of Veterinary and Animal Science, Ravi Campus Pattoki Punjab, Pakistan*
[3]*Department of Clinical Medicine, Faculty of Veterinary Science, University of Veterinary and Animal Sciences, Lahore Punjab, Pakistan*
[4]*Pharmaceutical Division, Ministry of Health and Population, Faiyum, Egypt*
[5]*Department of Pharmacognosy, Faculty of Pharmacy, Heliopolis University for Sustainable Development, Egypt*
[6]*Department of Food Science and Human Nutrition, Faculty of Biosciences, University of Veterinary and Animal Sciences, Lahore Punjab, Pakistan*
[7]*Faisalabad Medical University, Faisalabad, Pakistan*
[8]*Punjab Medical College, Faisalabad, Pakistan*
[9]*Department of Agronomy, University of Agriculture, Faisalabad, Pakistan*

Correspondence should be addressed to Hafiz Ishfaq Ahmad; ishfaq.ahmad@uvas.edu.pk

Received 29 January 2021; Revised 14 March 2021; Accepted 20 March 2021; Published 5 April 2021

Academic Editor: Sibtain Ahmed

The most common ethnomedicinal plants being effective in respiratory disorders were studied for the first time in Bahawalpur District. The herbal medication represents a low-cost treatment for the local community. There is a need for documenting the traditional uses of plants for further investigation of bioactive compounds. Using a qualitative approach, the ethnobotanical data was collected from the district of Bahawalpur, Pakistan, from February 2018 to February 2020 through semistructured interviews with the local people and traditional healers. The quantitative analysis included use value, informant consensus factor, family importance value, and relative frequency citation. A total of 20 indigenous plants belonging to 17 families were documented from 185 informants. These plants were claimed to be used for the treatment of 10 respiratory ailments. The plant habit, part of the plant used, and mode of preparation were standardized for authentication. The herbs are the most used life form (55%), while trees and shrubs are also used. Leaves dominate with high use value (47.62%) followed by fruit, stem, flower, and other parts of plants. For the preparation of traditional remedies, decoction (76.19%) and extract (71.43%) are common preparation methods. However, other methods of paste infusion, powder juice, and ash are used to a lower extent. The plants with higher use value are *Glycyrrhiza glabra*, *Acacia arabica*, and *Mentha piperita*; these have significant potential therapeutic activity for respiratory disease. The ethnomedicinal importance of plants against respiratory diseases used by the local population (traditional healers) is the commercial availability of the herbal product. It is a first-time study in this area to fill the gap between traditional practices and synthetic medicine to screen out the phytochemical and pharmacological properties of plants that have a highly futuristic use value to develop antibiotic drug with least side effects by using sustainable methods.

1. Introduction

The ethnobotanical importance of medicinal plants predominantly serves to maintain public health from an era of time in many cultures and traditions around the world [1–3]. It is noteworthy to say that the World Health Organization (WHO) stated that 80% of the global population is nutritionally dependent upon plants as a cure for primary health.

Additionally, about 11% of essential drugs are originated from plants as phytotherapeutic agents [4]. Therefore, to explore the usage of medicinal plants in the treatment of disease, the researchers gained significant knowledge many years ago [5]. The emerging importance of ethnic usage of medical treatment caused the side effects of allopathic medicine and their cost and unavailability of biomedical treatment due to some factors that were seriously urgent to the local community for the indigenous plant [6].

The geographical position of Pakistan makes this region supplemented with a diversity of medicinal plants used by the indigenous people for the medical care of their animals [7, 8]. The majority of the population is living in rural areas, their source of income is based on agriculture, and their low economic livelihood is dependent on ethnomedicinal plants [9]. Therefore, local people use plant-based remedies using different parts of plants in the traditional form of commercially available herbal products [10]. The medicinal plant is locality matter as it is reported that about 90% of plant species are used by the natives [11].

Many significant respiratory diseases contain upper respiratory tract infection and lower respiratory infection causing asthma, bronchitis, common cold, cough, pneumonia, and whooping cough [12]. The respiratory disorder counted to 2.2 million resulting in deaths every year; therefore, in the treatment of acute infection of the respiratory tract, it exceeds a high cost of 20 billion [13]. Bahawalpur is an area with high temperature where a great range of flora exists with dust storm in summer. A high temperature where a great range of flora exists with dust storm in summer is considered a significant factor for ethnobotanical study [14]. The traditional remedies regarding respiratory diseases for human health care are widespread in this area where people rely more on medicinal plants than synthetic medicine [15]. Contextually, many plants from different families are used from one generation to another to cure cough, asthma, respiratory tract infection, and pneumonia by the indigenous population [16]. Due to the reliability of some definite phytochemicals, the plants are exploited for an extended period conventionally go over for curing diverse ailments [17]. Vast medicinal plants have naturally diverse benefits for mankind as they are very useful against respiratory disease worldwide and in other areas of Pakistan [12, 16]. Plants contain external and internal secreting secondary metabolites, such as phenol, tannins, alkaloid, steroid, resins, and gum related to the antimicrobials associated with antimicrobials [17, 18] and antibacterial [19]. Prospectively, the future must satisfy the therapeutic need for more researches on plants to emphasize the use of medicinal plants in primary health needs [20]. Therefore, the objective of this study was to document the most common medicinal plants used for respiratory disorders, which is done for the first time in this region. Furthermore, it is essential to compile indigenous knowledge of the native area by conducting studies on the pharmacological and phytochemical screening of plant species in order to certify their use in treating various ailments, as well as educating rural people about sustainable plant use and conservation.

2. Methods

2.1. Study Area. Southern Punjab is a lower area of Punjab, where Bahawalpur lies at (29°24′0″N, 71°41′0″E) covering an area of 24,830 km^2 [21]. The population of this division is about 11,464,031, which was estimated in the 2017 census [22]. The Bahawalpur District has a large geographical area, which contains six tehsils Bahawalpur Saddar, Bahawalpur City, Khairpur Tamewali, Yazman, Hasilpur, and Ahmedpur East [15] (Figure 1). A river and well-irrigated canal system are the main water sources of this region, while annual rainfall fluctuates from 90 to 200 millimeters. Cholistan Desert is situated in the south of the city, which expands to the Indo Pak border, containing diversified flora and fauna [14]. It is the southeastern part of the Punjab, where the summer is very hot with dust storms in May and June, while the winter is cold. In the desert where the most essential wildlife is a national park away from the richness of wildlife habitat, ethnobotanical studies are the most important for medicinal plant researches [23].

2.2. Data Collection. The ethnomedicinal study of plants for respiratory disorders is undertaken by a structured questionnaire from the population living in the district of Bahawalpur from February 2018 to February 2020, keeping in view the rules of documentation of the ethnobotanical data [24]. For collecting the data of ethnomedicinal plants and the significance of this region, the open-ended and close-ended interviews [25] were conducted on plant locality, the local name of the plant, parts of the plant used, the method used in the preparation, and the plant forms with their usage. To select the informant for indigenous knowledge, a different category was used in which area-wise information was collected from the different age groups in which gender, qualification, income, and experience were considered to analyze the usage of the plant concerning traditional medicine for respiratory diseases. The use of the same species by the informants was characterized and accordingly assessed [26]. On the other side, interviews were also conducted with the 28 traditional healers to peruse medicinal plants as commercial products. All the data obtained from 185 informants and traditional healers were compiled to analyze the locals' use of the medicinal plants.

2.2.1. Demographic Characteristics of Informants. The demographic features of local informants were determined by a questionnaire designed as per the rule of the ethnomedicinal survey. A total of 185 informants were involved in the current study; 139 males were interviewed at their workplace, and 64 females were interviewed at houses through face-to-face conversation. Most of the informants were shopkeepers, farmers, laymen, gardeners, teachers, and housewives. To collect the traditional knowledge regarding medicinal plants, the informants above 60 years were prioritized. The very significant information about the use of medicinal plants in their products was taken from traditional health practitioners through an interview. The questionnaire was also used. Many studies of the ethnomedicinal use of plants have been testified worldwide along with Pakistan [27] and Turkey [28].

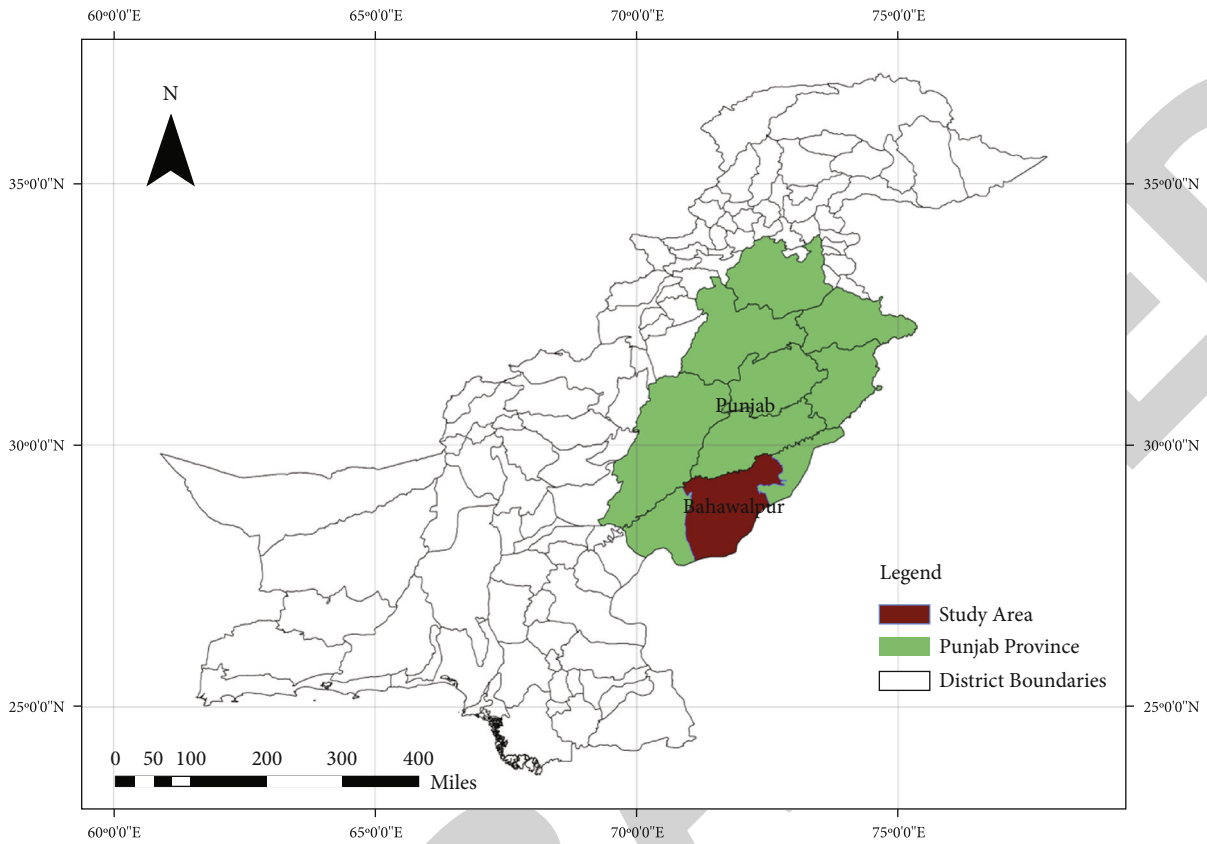

Figure 1: Study area map—Bahawalpur District, Pakistan.

2.2.2. Plant Collection and Identification. The traditionally useful plants in respiratory diseases by the natives of Bahawalpur were collected from the area: dried, pressed, and mounted on the herbarium sheet. For the authentication of the plant name index and the list of the plant, http://www.ipni.org and http://www.theplantlist.org were used, respectively, and for the taxonomic verification of the plant, http://www.ars-grin.gov/cgi-bin/npgs/html/queries.pl was used. All the herbarium plants were accompanied by data such as family, their scientific name, local name, life form, part of the plant used, and the association of disease with the plant. Identification and voucher specimen were according to the Flora of China, Scopus, Flora Iranica, Web of Science, and Google scholar and the flora of Punjab [29] and the flora of West Pakistan and Kashmir for the vascular plants [30].

2.3. The Quantitative Study of Ethnobotanical Plants. To analyze the quantitative research of the ethnobotanical plants, there are different quantitative directories: use value (UV), informant's consensus factor (ICF), relative frequency citation (RFC), and family importance value (FIV).

2.3.1. Use Value (UV). This is a method that shows the relative significance of the medicinal plants used by the locals of the studied area. For the standard approach to evaluate a plant's UV, a specific protocol was given by [31]

$$\mathrm{UV} = \sum \frac{U}{N}, \tag{1}$$

where the informant's numbers are represented by "N" which specifies the use of plant species. Its value shows the user report of a specific plant but does not indicate the multiple benefits of a plant.

2.4. Informant's Consensus Factor (ICF). It is the value that refers to the consumption of medicinal plants and analyzes the disease cured by adapted methods. Therefore, the respiratory disorder is sorted into different categories. To calculate the ICF value, the formula is given as

$$\mathrm{ICF} = \frac{N_{\mathrm{ur}-} N_t}{N_{\mathrm{ur}-} 1}. \tag{2}$$

For each category of diseases, the user report (UR) number is indicated by "N_{ur}" while species of medicinal plant use are represented by "N_{t}" [32]. To prove the authenticity of locals, the data for the use of medicinal plant range from 0 to 1.00 in which the greater value expresses a high consumption of a medical plant, while the low value tells that the informants rarely use the medicinal plant species.

2.4.1. Relative Frequency Citation (RFC). The traditional significant value of a plant species in its native area (RFC value) of each species was calculated by respondents that mention the use of specific medicinal plants (FC) by the whole

Table 1: Demographic knowledge of informants in the current study.

Variable	Demographic variants	Number	Percentage (%)
Gender	Male	139	75
	Female	64	35
Plant species			
Age	30-45	39	21
	46-60	57	30.8
	61-75	65	35.1
	>75	24	12.9
Informants	Locals	157	84.8
	Traditional healers	28	15.1
Education	Illiterate	50	27
	Elementary	28	15.1
	Secondary	20	10.8
	Undergraduate	48	25.9
	Graduate	39	21
Experience of TH	2-5 years	18	65
	5-10 years	10	35

number of informants (N) in the survey. The formula is given as [33]

$$\mathrm{RFC} = \frac{\mathrm{FC}}{N}. \quad (3)$$

2.4.2. Family Importance Value (FIV). It is the quantitative measure to analyze the important value of the family and is described by the informants. It is calculated by using this formula:

$$\mathrm{FIV} = \frac{\mathrm{fc}}{n} \times 100, \quad (4)$$

where it is the percentage of informant's report for a family of the plant to which it belongs.

3. Results and Discussion

3.1. Medicinal Plant Documentation and Ethnodemography of the Inhabitants. The most common 21 medicinal plants, belonging to 17 families, are used by indigenous people for 11 associated respiratory diseases. A survey was conducted by 185 informants interviewed; it was classified into different classes of demographic characters shown in Table 1.

The medicinal plants are mostly used to cure respiratory diseases giving designated information as presented in Table 2. The males—75% informants—were interviewed, and 25% of females were included in the survey. The demographic characters are designed in such a way that it showed the experience of the informant with plant species so that traditional healers were also included in studies where 65% have 2–5-year experience; those having 5-10-year experience are 35%, while the most reported locals are under the age of 61-75 (35.1%) followed by the age of 46-60 (30.8%) and 30-45 (21%), and the least are those with age above 75 years. In this study, it is clearer that respiratory disorders prevail more in illiterate people, which is 27%.

3.2. Medicinal Plant and Indigenous Experience. The 21 species of medicinal plants that were most recorded have been used for different respiratory diseases (Table 2). These plants belong to 17 different families: *Lamiaceae* (3 species), *Boraginaceae*, and *Zingiberaceae* (2 species), while others reported only one species used by indigenous people. The life form of the plant is very significant because it specifies the environmental condition of the region (Bahawalpur). Figure 2 shows that herbaceous plants (52.38%) are more common and trees (23.8%) are followed by shrubs (19.10%). The parts of the plants were leaves (47.62%), fruits (33.33), and stem, roots, flower, seed, and bark which were also used to some extent (Figure 3). In ethnobotanical preparation, the leaves were used, so their collection does not impact the life cycle of plants [34]. The leaves are more tolerable for the local plants regarding other life forms of plants or entire plants. The plant's mode of usage depends upon the part of plant use that is delicate, soft, and hard [12]. According to the life form and plant part used in the crude preparation for respiratory disease, many traditional recipes are made with or without a subsidiary substance: decoction (71.4%), extract (66.7%), infusion, paste (38.1%), and powder (33.3%), and least mode of preparations that are made contains juice and ash (14.3%) (Figure 2). The traditional healer role for practice is that they use two or more plant mixes with some other ingredients: water, milk, essential oils, honey, and butter. The most used preparation is a decoction; it is prepared by boiling the plant part in water so that the required amount is obtained. Mostly, the administered dose is internal in this disease, but its external use is also preferred in the form of a paste. The dose and mode of administration to each patient are according to the physical condition and stage of the disease.

Table 2: Most common medicinal plant species of Bahawalpur District with their use values, relative frequency citation, and family importance value.

Name of plant	Family name	Common name	Plant part used	Preparation method	Life form	Therapeutic effects	UR	FC	UV	RFC	FIV
Justicia adhatoda BP01	*Acanthaceae*	Malabar nut	Leaves	Extract, paste, ash, powder, decoction	Shrub	Asthma, cough, sore throat, tuberculosis	2	9	0.67	0.05	4.86
Achyranthes aspera BP02	*Amaranthaceae*	Puthkanda	Root	Decoction, powder, extract, paste, ash	Herb	Asthma, bronchitis, cold, cough, pneumonia	4	1	0.7	0.01	0.54
Mangifera indica BP03	*Anacardiaceae*	Mango	Bark, leaves	Juice, paste infusion, extract	Tree	Sore throat	1	11	0.86	0.06	5.95
Foeniculum vulgare BP04	*Apiaceae*	Fennel	Seeds and leaves, flower	Decoction, powder, extract, paste, ash	Herb	Respiratory disorder cold, cough	4	12	0.65	0.06	6.49
Phoenix dactylifera BP05	*Arecaceae*	Date palm	Fruit	Decoction, extract, powder	Tree	Bronchial infection	2	7	0.59	0.04	3.78
Cordia obliqua BP06	*Boraginaceae*	Lasora	Fruit, leaves	Powder, extract	Tree	Dry cough, tuberculosis	3	7	0.61	0.04	3.78
Onosma bracteatum BP07	*Boraginaceae*	Gaozaban	Fruit, leaves	Extract, decoction, infusion	Herb	Respiratory tract infection, influenza	4	9	0.32	0.05	4.86
Glycyrrhiza glabra BP08	*Fabaceae*	Liquorice	Roots	Decoction, extract, paste	Herb	Asthma, cough, pneumonia	2	12	0.89	0.06	6.49
Thymus vulgaris BP09	*Lamiaceae*	Thyme	Leaves, flower	Decoction, powder, extract, paste, ash	Shrub	Bronchitis, whooping cough	3	8	0.54	0.04	4.32
Mentha piperita BP10	*Lamiaceae*	Peppermint	Leaves, stem	Juice, paste infusion, extract	Herb	Cough, sore throat, influenza	2	14	0.9	0.08	7.57
Hyssopus officinalis BP11	*Lamiaceae*	Zoofa	Herb	Decoction, extract, powder	Shrub	Cough	2	5	0.5	0.03	2.7
Abelmoschus esculentus L. BP12	*Malvaceae*	Okra	Seed fruit	Powder	Herb	Asthma	2	8	0.63	0.04	4.32
Acacia arabica BP13	*Mimosaceae*	Kiker	Fruit and leaves	Decoction, extract, powder	Tree	Bronchitis, cold tonsillitis	4	10	0.91	0.05	5.41
Ficus religiosa BP14	*Papilionaceae*	Peepal	Fruit, leaves	Extract, paste, ash	Tree	Asthma, tuberculosis	1	9	0.68	0.05	4.86
Ziziphus vulgaris BP15	*Rhamnaceae*	Anab	Fruit, leaves	Extract, decoction, infusion	Shrub	Cough and cold, influenza	3	3	0.29	0.02	1.62
Withania somnifera BP16	*Solanaceae*	Ashwagandha	Roots	Decoction extract	Herb	Asthma, bronchitis	4	14	0.87	0.08	7.57
Phyla nodiflora BP17	*Verbenaceae*	Cape weed	Whole plant	Infusion	Herb	Asthma, influenza	2	6	0.57	0.03	3.24
Viola odorata BP18	*Violaceae*	Banafsha	Stem, root	Extract, decoction, infusion	Herb	Respiratory disorders	3	12	0.85	0.06	6.49
Curcuma longa BP19	*Zingiberaceae*	Turmeric	Underground stem	Extract, decoction, infusion	Herb	Pulmonary infection, tuberculosis	4	6	0.57	0.03	3.24
Zingiber officinale BP20	*Zingiberaceae*	Ginger	Stem	Juice, paste infusion, extract	Herb	Cold, cough and throat infection, influenza	2	15	0.91	0.08	8.11

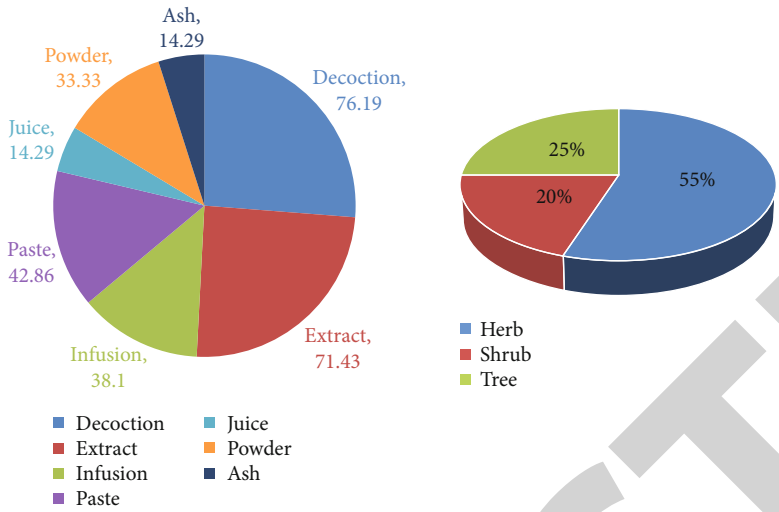

Figure 2: Mode of preparation used in the respiratory treatment and life form of a plant.

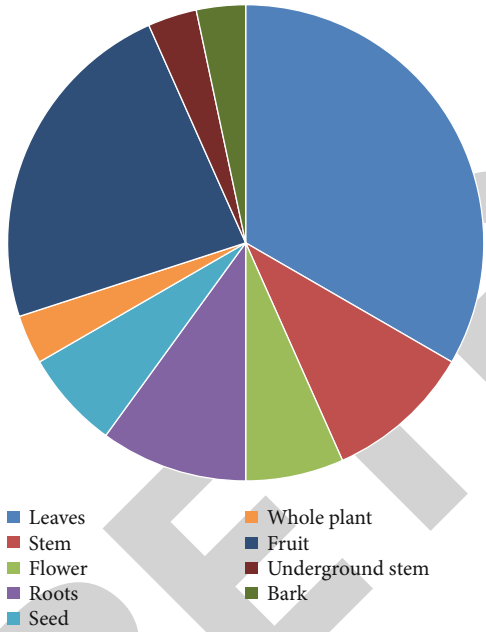

Figure 3: Plant part used for respiratory disease.

3.3. Therapeutic Significance. According to the survey from the region of Bahawalpur, the respiratory disease is categorized into 10 disorders (Figure 4). In this region, the most reported diseases in regard to plants are cough (10 species), asthma (8 species), bronchitis (5 species), influenza (4 species), sore throat and respiratory disorder (3 species), and pneumonia and tuberculosis (2 species). Other species are also significant in dry and whooping cough.

3.4. The Quantitative Study of Ethnorespiratory Information

3.4.1. The Family Importance Value (FIV). The family importance value (FIV) indicates the family significance in the region used by the informants, in which the reported dominant family is *Zingiberaceae* with FIV (8.11), followed by *Lamiaceae* (10.27), *Solanaceae* (7.7), *Violaceae and Apiaceae* (6.5), *Anacardiaceae* (5.9), and *Mimosaceae* (5.4), and the families with least FIV are *Acanthaceae and Boraginaceae* (4.86), *Malvaceae* (4.3), and *Arecaceae* (3.78), followed by *Rhamnaceae* (1.6) and *Amaranthaceae* (0.54). This result is shown in Figure 5.

3.4.2. Relative Frequency Citation (RFC). From different localities of Bahawalpur, the most used medicinal plant for respiratory ailments by the informants shows the RFC value. The highest value shows the highest consumption of medicinal plants including *Zingiber officinale*, *Mentha piperita* and *Withania somnifera* (0.08), and *Mangifera indica*, *Glycyrrhiza glabra*, *Viola odorata*, and *Foeniculum vulgare* (0.06), while the medicinal plant with regard to respiratory disease has low RFC, but their other therapeutic indication has significant value. These are *Justicia adhatoda*, *Ficus religiosa*, *Acacia arabica*, and *Onosma bracteatum* having an RFC value of 0.05.

Zingiber officinale is a herb used for cold, cough, throat infection, and influenza where an underground stem is used to make juice and a paste is made by grinding, infusion, and extraction. *Mentha piperita* is a common plant in which leaves and the stem are used to make juice, paste infusion, and extract in water. It is mainly helpful to treat cough, sore throat, and influenza. *Withania somnifera* is a small plant, commonly known as Ashwagandha; its delicate roots make decoction and extracts to treat asthma and bronchitis. Its use in a commercial product for these diseases indicates its significance. *Mangifera indica* is a perennial tree whose bark and leaves are used to treat the sore throat by making juice and paste by crushing the leaves, infusion; bark extract is also made for crude preparation. *Glycyrrhiza glabra* is a small herb plant where the plant's roots are used to make the decoction, paste, and extract helpful in curing asthma, cough, and pneumonia. *Viola odorata* is a common herb commonly known as *Banafsha.* This region is used in traditional remedies for cough and other respiratory disorders by making

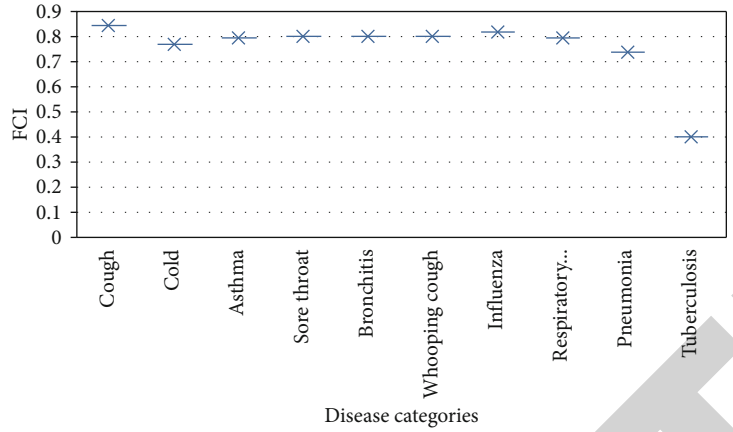

Figure 4: FCI value of plant against respiratory diseases.

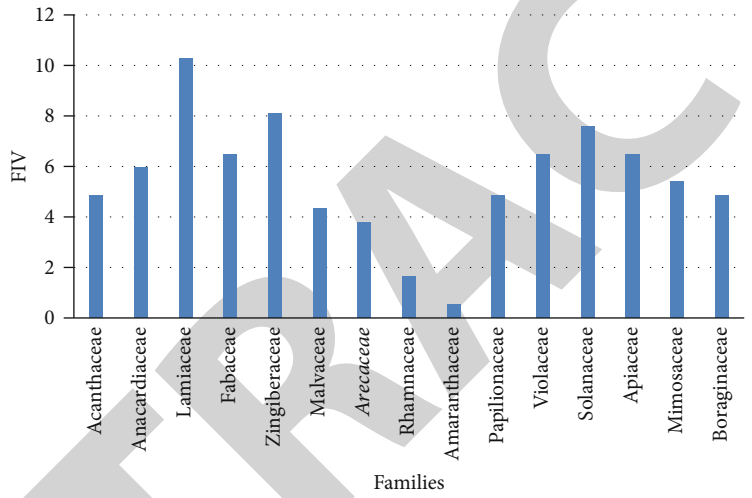

Figure 5: Family importance value of plants.

decoction and extract of stem and root. The decoction, the seeds of *Foeniculum vulgare*, is used to treat cold and cough, while extract and paste of the stem and leaves are consumed for respiratory disorders. *Justicia adhatoda* is a shrub plant that is considered important to cure asthma and cough by preparing extract, paste, powder, decoction, and ash, which is also prepared for tuberculosis and sore throat.

3.4.3. User Value (UV). The relative importance of medicinal plants by quantitative analysis in a population is known as the plant's user value (UV). The plants with high UV are *Acacia Arabica* (0.91), *Mentha piperita* (0.9), which is contrary to the study conducted in Gujranwala Pakistan, *Glycyrrhiza glabra* (0.89), *Withania somnifera* (0.87), *Mangifera indica* (0.86), *Viola odorata* (0.85), and *Achyranthes aspera* (0.7) [35]. The plants with the highest UV are popular among the indigenous people of Bahawalpur District for respiratory diseases. *Acacia arabica* has antibacterial properties [36], which effectively treats the association of bronchitis, colds, and tonsillitis with respiratory diseases by using pods and leaves to make a decoction and a paste of leaves. *Achyranthes aspera* with a high UV value indicates its extensive use for asthma, bronchitis, cold, cough, and pneumonia in the Bahawalpur. It has been used by making decoction, powder, and extract for asthma. In addition, paste and ash are also used. The plants show their less use by the population due to minimum knowledge and exposure of plant with the natives of the region Bahawalpur. The medicinal plant with lower user value is *Ficus religiosa* (0.68), *Phoenix dactylifera* (0.59), *Curcuma longa* (0.57), *Hyssopus officinalis* (0.5), and *Onosma bracteatum* (0.32). The plant's availability makes a medicinal plant achieving its highest and low user value.

3.4.4. Informant Consensus Factor (ICF). To analyze medicinal plants important for a disease used by the informant, the usage report is valuable to categorize respiratory disease into ten diseases. The cough is reported for 95.24% plant species by 66 users, followed by cold. Around 85.71% of medicinal plants have been used for asthma, and after that, plants recorded for sore throat (76.19%), bronchitis (66.67%), whooping cough (61.9%), influenza (52.38%), respiratory disorder (47.62%), pneumonia (42.86%), and tuberculosis (33.33%). The study shows that cough and cold are the most prevailing diseases in this area. The same results for disease regarding plants have been described in northern Pakistan [16].

Table 3: Commercial availability of plants in herbal products.

Commercial products	Treatment associated	Major plants included in the herbal product	References
Suduri	Bronchitis	*Ocimum basilicum*, *Adhatoda vasica*	[45]
Infuza	Asthma	*Glycyrrhiza glabra*	[45]
Joshina	Bronchitis	*Ziziphus sativa*, *Viola odorata*, *Adhatoda vasica*	[45]
Sharbat Banafsha	Cough	*Viola odorata*	[46]
Shaafi Joshanda	Cough	*Adhatoda vasica*, *Viola odorata*, *Foeniculum vulgare*	[45]
Linkus	Cough	*Adhatoda vasica*, *Foeniculum vulgare*, *Viola odorata*	[45]
Joshinda	Bronchitis	*Ocimum basilicum*, *Onosma bracteatum*, *Ziziphus sativa*, *Viola odorata*	[45]
Johar Joshanda	Cough	*Ocimum basilicum*, *Viola odorata*	[46]
Corezcol	Expectorant	*Mentha arvensis*, *Adhatoda vasica*	[46]

Table 4: Comparison of similarities and differences between the study area and neighboring regions.

Area	References	No. of species	Plants with similar use	Plants with different use	Similarity ratio
Urmia	[12]	20	1	0	0
Turkey	[45]	137	1	2	1.46
Bahawalpur, Pakistan	[46]	123	7	0	0
Gallies, Northern Pakistan	[16]	120	5	0	0
Hafizabad, Pakistan	[27]	85	4	2	2.35
Uganda	[37]	88	2	0	0
Pakistan	[38]	384	8	0	0
Lahore, Pakistan	[39]	129	4	2	1.55
Uttar Pradesh, India	[40]	57	4	3	5.26
Swat, Pakistan	[41]	100	0	3	3

3.5. The Medicinal Plant Available in Commercial Products. To confirm the ethnorespiratory plant significance, the market survey of herbal medicine as drugs for the usage of plants was conducted to treat respiratory disease. It is reported that five plants among the 20 plants belong to commercial treatment as respiratory disease drugs; local healers used these plants with other substituents in commercially available plants with a great source of income for the local community and traditional healer. The data of plants used commercially is shown in (Table 3).

3.6. Comparative Study of Plants in Respiratory Disease. The ethnorespiratory plant analysis was compared in other studies in many regions of Pakistan and our neighboring countries to conform to the stated data. The comparison of this study showed that the plants reported in the Bahawalpur region were also used for respiratory diseases in another region (Table 4).

The study at west Azerbaijan shows the respiratory disease cured by traditional medicinal plants showing a similar study. Some 20 plants used in treating disease, the species of *Mentha*, have the same uses as our study [12]. The study of ethnobotanical plants in *manisia* where the plant has similar uses and modes of preparation through *Glycyrrhiza glabra*, but there is a contrast in the use of plants *Mentha x piperita* L and *Foeniculum vulgare* Mill. So, there is the novelty of the use of plants against respiratory disorder [37].

The area of Bahawalpur, Pakistan, was reported with 123 plants out of these 7 species, which uses *Achyranthes aspera*, *Mangifera indica*, *Phoenix dactylifera*, *Mentha longifolia*, *Acacia nilotica*, *Withania somnifera*, and *Phyla nodiflora*, with properties to cure respiratory diseases [38].

A similar study in the Northern region shows 120 plants with 5 plants having comparable uses and modes of preparation including *Acacia nilotica* (L.), *Glycyrrhiza glabra* L. *Justicia adhatoda*, *Achyranthes aspera*, *Abelmoschus esculentus* (L.) [27] studied 85 medicinal plants *Mentha longifolia*, *Achyranthes aspera*, *Withania somnifera*, and *Ficus religiosa* tally with plants used in the present study while some plants having dissimilar use are *Mangifera indica* and *Acacia arabica* [16, 39]. A study in Uganda, 2 plants out of 88 plants, *Mangifera indica L* and *Achyranthes* aspera L, are used for respiratory disease, but its use in tuberculosis is more emphasized [40].

A previous study contains 129 plants in which 4 plants with have same use including *Justicia adhatoda*, *Achyranthes aspera*, *Withania somnifera*, and *Ficus religiosa* are included, but 2 plants have dissimilar use and these plants are *Mangifera indica* and *Acacia nilotica* [41]. 384 medicinal plants from which 8 plants have been studied with similar use. The plant's similar use for respiratory diseases is *Glycyrrhiza glabra*, *Onosma bracteatum*, *Zingiber officinalis*, *Viola odorata* L., *Mangifera indica*, *Ficus religiosa* L, *Phoenix dactylifera*, and *Phyla nodiflora* [42].

It was reported, in India, that 57 medicinal plants belong to 37 families and 53 genera [43]. The plants, used for respiratory disease, are *Acacia nilotica (L.) Curcuma longa*, *Withania somnifera*, and *Zingiber officinale* while the plants *Achyranthes aspera*, *Ficus religiosa*, and *Mangifera indica*

have dissimilar use with the present study. 100 plants were studied and no one has similar uses, but these plants have other expectorant and diuretic viz. *Acacia nilotica*, *Achyranthes aspera*, and *Mentha longifolia* [44].

4. Conclusion

This survey examines the most common uses of medicinal plants against respiratory diseases in the district of Bahawalpur, Pakistan. The indigenous people of this region use the native plants to cure their respiratory diseases because of synergistic and preventive causes. The most common plants belong to different families like *Lamiaceae*, *Fabaceae*, *Papilionaceae*, *Anacardiaceae*, *Zingiberaceae*, *Solanaceae*, and *Arecaceae*, which can cause associated respiratory symptoms: cough, asthma, bronchitis, and pulmonary infection. Traditional healers also use the plants, but the commercial manufacturer's used plants and other plants in herbal medication help ease the dilemmas of respiratory disorders. The exploration of ethnomedicinal information is necessary to value the traditional use of medicinal plants by the local community. Thus, bioassay and frequency of plant-related drugs can be executed relationally. The present study is an enduring survey supporting the prospect by documenting the traditional knowledge of indigenous plants of this area and raising the significance of old practices for treatment. As a contextual recommendation, the need for an hour is to establish research to screen out the important phytochemicals in plants and develop the antibiotics by using these plants, which have resistance against bacteria and have the least side effect on the human body. Contextually, this survey is to fill up the gaps between the traditional usage of plants and pharmacological studies of respiratory disorders to document ethnomedicinal data in a meaningful way. A conventional method of collecting the parts of plants is recommended so that its life cycle is not disturbed as well as the survival of endangered species of plants is not affected.

Data Availability

The numerical data used to support the findings of this study are available from the corresponding author upon request.

Conflicts of Interest

The authors declare that they have no competing interests.

Authors' Contributions

Hafiz Ishfaq Ahmad and Abdul Jabbar designed the project. Sadia Afzal, Muhammad Zahid Iqbal, Farheen Zulfiqar, Nimra Irm, Shoaib Ahmad, Zubair Aslam, and Abdul Jabbar conducted the research and wrote the primary draft. Mahmoud M. Tolba designed the map. Sameh AbouZid edited the manuscript. All authors read and approved the final draft.

Acknowledgments

The authors highly acknowledge HebaT Allah Nasser (Microbiology and Public Health Department, Faculty of Pharmacy and Drug Technology, Heliopolis University, Egypt) for the moral support.

References

[1] M. Bahmani and Z. Eftekhari, "An ethnoveterinary study of medicinal plants in treatment of diseases and syndromes of herd dog in southern regions of Ilam province, Iran," *Comparative Clinical Pathology*, vol. 22, no. 3, pp. 403–407, 2013.

[2] P. A. Ghasemi, M. Momeni, and M. Bahmani, "Ethnobotanical study of medicinal plants used by Kurd tribe in Dehloran and Abdanan districts, Ilam Province, Iran," *African Journal of Traditional, Complementary, and Alternative Medicines*, vol. 10, no. 2, pp. 368–385, 2013.

[3] S. Asgary, A. Sahebkar, M. R. Afshani, M. Keshvari, S. Haghjooyjavanmard, and M. J. P. R. Rafieian-Kopaei, "Clinical evaluation of blood pressure lowering, endothelial function improving, hypolipidemic and anti-inflammatory effects of pomegranate juice in hypertensive subjects," *Phytotherapy Research*, vol. 28, no. 2, pp. 193–199, 2014.

[4] I. Haq, "Safety of medicinal plants," *Pakistan Journal of Medical Research*, vol. 43, no. 4, pp. 203–210, 2004.

[5] M. Heinrich, "Ethnobotany and its role in drug development," *Phytotherapy Research*, vol. 14, no. 7, pp. 479–488, 2000.

[6] M. Heinrich, *Herbal and symbolic forms of treatment in the medicine of the lowland Mixe (Oaxaca, Mexico)*, Bergin & Garvey, 1997.

[7] S. Ismail and M. F. J. B. Nisar, "Ethnomedicinal survey for important plants of district Lodhran, Punjab, Pakistan," *BIOL (E-Journal of Life Sciences)*, vol. 1, no. 3, pp. 52–58, 2010.

[8] A. Rashid and M. Arshad, "Medicinal plant diversity, threat imposition and interaction of a mountain people community," in *Proceeding of Workshop on Curriculum Development in Applied Ethnobotany*, pp. 84–90, Ethnobotany Project, WWF Pakistan, 2002.

[9] H. M. Said and A. Saeed, *Medicinal Herbal: A Textbook for Medical Students and Doctors*, Hamdard Foundation Pakistan, 1996.

[10] P. Ramesh and R. N. Okigbo, "Effects of plants and medicinal plant combinations as anti-infectives," *African Journal of Pharmacy and Pharmacology*, vol. 2, no. 7, pp. 130–135, 2008.

[11] J. Oteo, E. Lázaro, F. J. de Abajo, F. Baquero, J. Campos, and Spanish members of EARSS, "Antimicrobial-resistant invasive Escherichia coli, Spain," *Journal List Emerging Infectious Diseases*, vol. 11, no. 4, pp. 546–553, 2005.

[12] A. A. Khan, S. Arshad, and M. Mohsin, "Population growth and its impact on urban expansion: a case study of Bahawalpur, Pakistan," *Universal Journal of Geoscience*, vol. 2, no. 8, pp. 229–241, 2014.

[13] S. Kayani, M. Ahmad, M. Zafar et al., "Ethnobotanical uses of medicinal plants for respiratory disorders among the inhabitants of Gallies - Abbottabad, Northern Pakistan," *Journal of Ethnopharmacology*, vol. 156, pp. 47–60, 2014.

[14] B. Joshi, S. Lekhak, and A. Sharma, "Antibacterial property of different medicinal plants: Ocimum sanctum, Cinnamomum zeylanicum, Xanthoxylum armatum and Origanum

Hindawi
BioMed Research International
Volume 2021, Article ID 5550180, 8 pages
https://doi.org/10.1155/2021/5550180

Research Article

Investigation of Hypoglycemic Peptides Derived from Conserved Regions of adMc1 to Reveal Their Antidiabetic Activities

Hafiza Salaha Mahrosh,[1] Rizwan Mehmood,[1] Shazia Anwer Bukhari,[1] Gulnaz Afzal,[2] and Rawaba Arif[1]

[1]*Department of Biochemistry, Government College University Faisalabad, Pakistan*
[2]*Department of Zoology, The Islamia University of Bahawalpur, Bahawalpur, Pakistan*

Correspondence should be addressed to Rawaba Arif; ruwaibaa@gmail.com

Received 1 February 2021; Revised 12 February 2021; Accepted 1 March 2021; Published 9 March 2021

Academic Editor: Andrea Scribante

Diabetes mellitus is the most common chronic disorder and leading cause of renal, neurological, and gastrointestinal manifestations in developed and developing countries. Despite of many drugs and combinational therapies, the complications of diabetes are still listed due to severe consequences of those drugs. In past few years, plant-derived drugs draw special attention due to their higher efficacy and fewer side-effects. *Momordica charantia* also known as bitter melon is referred as an antidiabetic and hypoglycemic plant in native populations of Asia and East Africa. In current study, an in silico approach was used to evaluate the interactions and binding patterns of plant-derived peptides devised from a hypoglycemic protein adMc1 of *M. charantia* as potential inhibitor of DPP-IV, SGLT1, and GLUT2 receptor proteins. The study has described a novel approach to investigate hypoglycemic peptides to cure diabetes. A total of eighty tetra-, penta-, and hexapeptides were devised from conserved regions of adMc1 homologs. The molecular docking approach using MOE software was employed to reveal inhibiting potentials of devised peptides against three selected proteins. Out of 30 shortlisted ligands six peptides (i.e. SMCG, DECC, TTIT, RTTI, ARNL and TVEV) accomplished the criteria of being good drug candidates against selected receptor proteins following the drugability assessment test. The overall results are acceptable on the basis of ADMET profiling for being good drug candidates against selected proteins.

1. Introduction

Diabetes mellitus (DM) is a heterogenous group of chronic metabolic disorders associated with irregular glucose homeostasis and results in elevated level of blood glucose and insulin resistance [1]. The rapid increase in diabetes cases is estimated to increase 4.4% in 2030 among all age groups [2]. Currently, there are many synthetic hypoglycemic drugs available in market including sulfonylureas, incretins, α-glucosidase inhibitors, dipeptidyl peptidase-IV (DPP-IV) inhibitors, sodium-dependent glucose transport proteins (SGLTs) inhibitors, and thiazolidinediones but they result in severe consequences. Therefore, owing to severe side-effects of these drugs, there is a need of new class of drugs with much potency and efficacy [3].

The potential target proteins in diabetes include DPP-IV, SGLTs, glucose transporters (GLUT), α-glucosidase inhibitors, and peroxisome proliferator-activated receptors [4]. DPP-IV or adenosine deaminase binding protein is a serine exopeptidase predominantly expressed on surface of cells. DPP-IV selectively involves in N-terminal dipeptide cleavage from a variety of substrates including cytokines, growth factors, and incretin hormones [5]. Since the approval of DPP-IV inhibitors, their importance has been raised clinically to cure DM [6]. DPP-IV inhibitors are a class of oral diabetic drugs commonly used as stable drug candidates which have prospectively been designed using therapeutic agent's strategy focused on deep study on mode of action of incretin peptides [7].

In type 2 diabetes mellitus (T2DM) patients, the insulin resistance leads towards elevated level of glucose and the activation of incretins. Incretins are group of metabolic gut peptides secreted from enteroendocrine cells into the blood after intake of nutrients. Incretins lower the glucose level by

stimulating the induction of insulin from islets of Langerhans and also inhibits the glucagon production. Glucagon-like peptide-1 (GLP-1), glucagon-like peptide-2 (GLP-2), and glucose dependent insulinotropic peptide/gastric inhibitory polypeptide (GIP) are two examples of incretin hormones [8].

SGLTs are glucose transporters found in six isoforms (i.e., SGLT1, SGLT2, SGLT3, SGLT4, SGLT5, and SGLT6) and have been found to be scattered across the human body. Among these six isoforms, SGLT1 and SGLT2 are well known and extensively investigated in diabetes. Studies have showed that selective inhibition of SGLT1 can slow postprandial gut uptake of glucose and increase plasma levels of GLP-1 and GIP in healthy volunteers [9]. Glucose transporters are proteins widely distributed in body cells and facilitate in the maintenance of blood glucose level in the human body [2]. Among all the glucose transporters, GLUT2 plays a bidirectional role in specific transportation of glucose in the hepatocytes and absorption and reabsorption of glucose from the enterocytes and the renal tubule particularly [10]. GLUT2 is a sugar carrier that sustains power generation in the cell but can also serve as a receptor for extracellular glucose. GLUT2 is regarded as a competent target in treatment of DM due to its major role in glucose homeostasis.

In developing countries, the plant-based compounds have been used as drugs in 75-80% population to cure various diseases [11–13]. Peptides are generated from specific proteins and then consumed as food ingredients. The bioavailability of these peptides depends on absorption, distribution, metabolism, excretion, and toxicity- (ADMET-) based parameters to reach the target organ [14]. Currently, there are many hypoglycemic drugs in the market but these are correlated with multiple gastrointestinal and renal disorders. In silico targeting of different glucose transporters explores new ways in the management of type 2 diabetes mellitus. In this study, the adMc1 protein of medical plant *Momordica charantia* was used to prepare ready-to-dock library of 80 ligands. This includes the in silico approach to target DPP-IV, SGLT1, and GLUT2 to gain the structural insight of binding patterns of different ligands with receptor proteins. The main objective of this study was to evaluate the insulin-like activity of *Momordica charantia* derived peptides using in silico methods and to explore the best inhibitors of DPP-IV, SGLT1, and GLUT2 receptor proteins among prepared ligands.

2. Materials and Methods

2.1. Retrieval of the 3D Structures of Receptor Proteins. In this study, the 3D structures of three target molecules were employed to reveal hypoglycemic activities of different peptides which were companionable with the properties of the target binding site in the molecular docking study. The three-dimensional structures of human dipeptidyl peptidase-IV (PDB ID: 4A5S) and sodium-dependent glucose cotransporter (PDB ID: 3DH4) were retrieved from the RCSB Protein Data Bank (https://www.rcsb.org/).The protein sequence of GLUT2 was retrieved from the protein database of NCBI (accession number: P11168.1). The 3D structure of GLUT1 (PDB ID: 5EQG) was used as a template to predict the 3D structure of the GLUT2 protein. MODELLER 9.21 was used for homology modeling, and the best model was selected as a receptor protein for further analysis [15, 16].

2.2. Ligand Selection and Receptor Optimization. The protein sequence of the adMc1 protein from *Momordica charantia* was retrieved from the protein database of NCBI (accession No: CDG50933.1). MEME Suite was used to predict motifs from the selected protein homologs [17, 18]. Tetra-, penta-, and hexapeptides were devised from the predicted motifs, and their 3D structures were obtained using ChemSketch in MOL format [19]. Optimization of receptor was done by removing water molecules, addition of hydrogen atoms, energy minimization, and 3D protonation for the perfect and accurate docking. The minimized structures were then docked against devised peptides.

2.3. Molecular Docking. The prediction of the active site is the most crucial step in in silico drug discovery as it has a direct impact on the reliability of the results. Molecular docking of 80 ligands was performed at the active site of DPP-IV, SGLT1, and GLUT2 receptor proteins separately. Site finder tool of Molecular Operating Environment (MOE) was used to predict active sites in the selected receptor proteins. The parameters (i.e., rescoring 1: London dG, retain: 10, refinement: force field and rescoring 1: London dG, retain: 10) were set to their default to calculate the interactions of ligands with the binding residues of receptor proteins. All devised peptides were docked against the receptor proteins using MOE. Most appropriate interactions and bindings between ligands and receptor proteins were selected on the basis of the best *S*-score, root mean squared deviation (RMSD), and energy validation rankings.

2.4. Drug Scan and ADMET Profiling. The drug-likeness properties were determined following the Lipinski's rule of five using SwissADME [20]. The Lipinski's rule of five is based on five parameters (i.e., molecular mass: ≤500 Dalton, molar refractive index: 40-130, partition coefficient (log *P*): ≤5, hydrogen bond donors: <5, and hydrogen bond acceptors: <10). Only the molecules that accomplish all these parameters could be accepted as potential drug candidates. The online bioinformatic server admetSAR was used for ADMET-based chemical screening of selected drug candidates [21].

3. Results

3.1. Devising Tetra-, Penta-, and Hexapeptides from adMc1. The MEME Suite was used to explore five motifs in ten selected homologs of the adMc1 protein. The motifs were used to devise tetra-, penta-, and hexapeptides to be docked as ligands against DPP-IV, SGLT1, and GLUT2.

3.2. Molecular Docking. Molecular docking provides discernment into structural interactions of inhibitors with the receptor proteins. The prepared library of 80 peptides devised from the adMc1 protein of *M. charantia* was docked against

Table 1: The interactions of top ten devised peptides with DPP-IV as the receptor protein.

Sr. no.	Peptide	*S*-score	Interacting residues
1	MRGID	-17.8389	Glu206, Tyr547, Arg356, Pro550
2	TTVEV	-15.8132	Glu206, Tyr662, Ser209, Arg669
3	LRQQSR	-15.7212	Glu206, Tyr547, Arg356, Ser209, Arg358
4	TVEV	-15.0490	Glu205, Tyr662, Asn710, His126
5	FDECC	-14.6527	Glu206, Tyr547
6	ECCRE	-14.3605	Tyr547, Tyr662, Tyr666, Pro550, Arg358, Ser209
7	MRGIEN	-14.3088	Glu206, Tyr662
8	RCRQ	-13.5417	Tyr547, Val207
9	TTIT	-13.5247	Glu205, Ser209
10	EECR	-13.3807	Tyr662, Ser209

Table 2: The interactions of top ten devised peptides with SGLT1 as receptor protein.

Sr. no.	Peptide	*S*-score	Interacting residues
1	EEQRQA	-21.0223	Ser372, Ser368
2	FDEC	-21.0722	Ser372, Ser368, Ser365, Ser364, Tyr138, Tyr263, Asp189, Ala63, Gln268
3	ITTVE	-20.0948	Ser368, Ser365, Ser364, Asn267, Asp189
4	AREEQR	-19.3288	Ser368, Ser365, Tyr138, Ala361, Ala63, Asp189
5	YAYRTT	-18.9325	Ser368, Tyr263, Asn142, Asn267
6	EEQR	-18.5788	Ser372, Ser368, Ser364, Tyr138, Tyr176
7	SMCG	-17.4970	Ser372, Tyr138, Tyr269, Gln428
8	DECC	-17.3894	Ser368, Ser365, Asn267
9	ERCR	-17.1217	Ser368, Asn142, Thr375
10	TTIT	-16.9639	Ser372, Ser368, Tyr138, Asn142

DPP-IV, SGLT1, and GLUT2 receptor proteins using the docking algorithm of MOE software. MOE aligned the suitable confirmations and ranked the ligands based on four factors (i.e., the binding pocket with minimum energy structure, strength of hydrogen bond, root mean squared deviation value, and *S*-score). The results of computational docking showed the potency of adMc1 peptides as good inhibitors of DPP-IV, SGLT1, and GLUT2. In this study, three different receptor proteins were selected due to their major roles in diabetes and upregulation of glucose homeostasis. Top 10 conformations were selected in each analysis based on binding patterns and energy validations.

3.3. Interaction Analysis. For the receptor protein DPP-IV, top 10 conformations have been selected based on their structural interactions and *S*-scores. In literature, Glu205, Glu206, Tyr547, and Tyr662 have been reported as major amino acids of catalytic pocket of DPP-IV [22]. In this study, the selected top 10 peptides also showed interactions with these reported amino acids (Table 1). The peptide MRGID showed the best interaction (binding score: -17.8389) with the receptor protein, and Glu206, Tyr547, Arg356, and Pro550 were found to be the leading interactive residues in these interactions. All the remaining ligands also showed strong interactions with Glu205, Glu206, Tyr547, and Tyr662 which are also the active amino acid residues of DPP-IV. These ligands have been revealed as maximum pocket shareholders by interacting with the active amino acids of catalytic triad.

The protein sodium-dependent glucose cotransporter 1 (SGLT1) is a major contributor in the reabsorption of glucose in proximal tubules of nephrons. The binding pocket of the SGLT1 receptor protein contains Ser372 and Ser368 as main interacting amino acids. Out of 80 prepared ligands in this study, the top 10 ligands with best *S*-scores and interactions with these active amino acids were selected (Table 2). The peptides EEQRQA, FDEC, and ITTVE with docking scores of -21.0223, -21.0722, and -20.0948 showed strong interactions with Ser372 and Ser368.

Glucose transporters play major role in renal and intestinal glucose absorption and reabsorption. In current study, the Lys288 showed strong interactions with the GLUT2 protein and revealed as a major interacting amino acid. Among the selected ligands, the peptide REEQR with *S*-score of -17.4161 exhibited potential of being a good drug candidate with the best binding affinity with Lys288, Glu286, Ser284, Arg124, and Ser112. The remaining ligands could also be foremost inhibitors of GLUT2 with the best binding affinity and *S*-scores and could be potential drug candidates (Table 3).

3.4. Drugability and ADMET Profiling. The Lipinski's rule of five evaluates the drug-like properties of proposed drug candidates based on five parameters. The rule illustrates the

Table 3: The interactions of top ten devised peptides with GLUT2 as the receptor protein.

Sr. no.	Peptide	*S*-score	Interacting residues
1	REEQR	-17.4161	Lys288, Glu286, Ser284, Arg124, Ser112
2	YAYRTT	-17.1186	Lys288, Glu282, Arg124
3	ITTVEV	-16.9540	Lys288, Glu286, Ala283, Ser169
4	LEEIA	-15.8995	Lys288, Ser169
5	YLRQ	-14.8063	Lys288
6	RCRQ	-13.5942	Lys288
7	RTTI	-13.5003	Lys288, Phe113, Val289
8	ARNL	-12.9365	Lys288
9	FDEC	-12.8992	Lys288
10	TITTVE	-15.6597	Ser169, Ser112

Table 4: Pharmacokinetic parameters important for bioavailability of compounds drug-likeness properties of selected peptides.

Peptides	Target	Molecular properties[†]						
		MW	HBD	HBA	Nrotb	Log *P*	*A*	Violations
SMCG	SGLT1	396.48	6	7	15	-1.86	94.77	1
DECC		468.50	7	10	17	-2.39	107.10	1
TTIT	GLUT2	434.48	8	9	15	-2.06	105.61	1
RTTI		489.57	10	9	19	-2.17	123.16	1
ARNL		472.54	9	8	19	-2.38	118.94	1
TVEV	DPP-IV	446.50	7	9	16	-0.93	109.86	1
FDEC		512.53	7	10	18	-1.40	123.66	2

[†]Molecular properties were calculated using SwissADME an online tool. MW: molecular weight; HBD: number of hydrogen bond donors; HBA: number of hydrogen bond acceptors; nrotb: number of rotatable bonds; log *P*: the logarithm of octanol/water partition coefficient; *A*: molar refractivity.

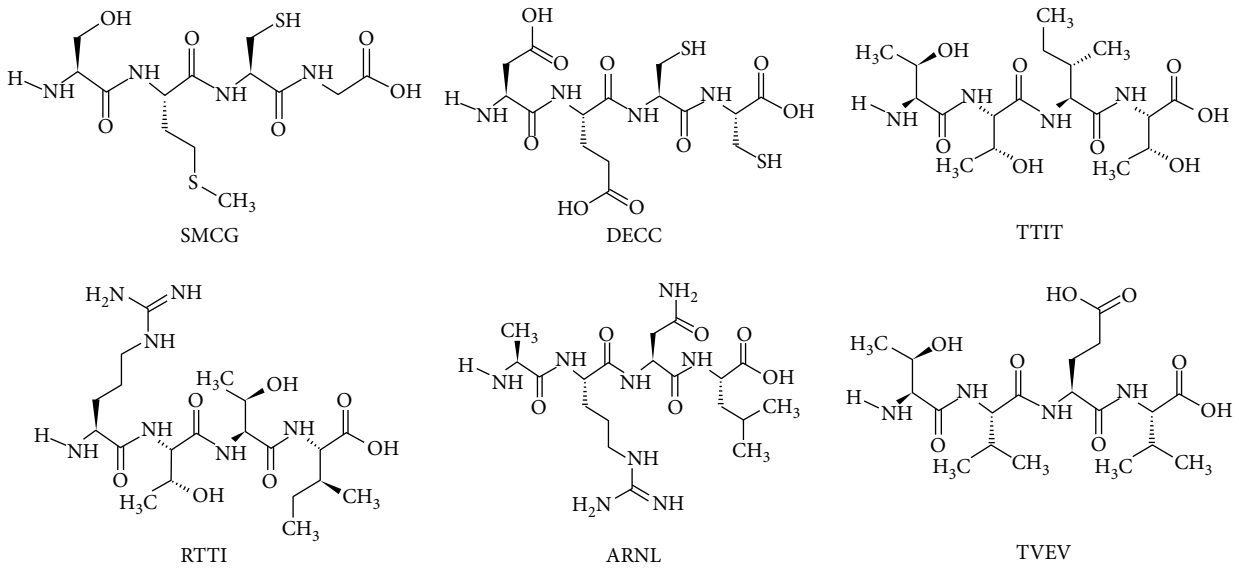

Figure 1: Structures of best selected peptides.

drugability and behavior of selected drug candidate as it distinguishes the drug-like and nondrug-like nature of biologically active ligands. Only the molecules that accomplish all these parameters could be accepted as potential drug candidates. In this study, total 30 ligands have been shortlisted on the bases of their best interactions with active amino acids, *S*-scores, and energy validations. Out of 30 selected ligands used in this study, three tetrapeptides (SMCG, DECC, and TTIT) were found to be effective inhibitors of SGLT1, two tetrapeptides (RTTI and ARNL) were found effective inhibitors of GLUT2, and one tetrapeptide (TVEV) was found to be an efficient inhibitor of DPPI-IV as all these peptides only

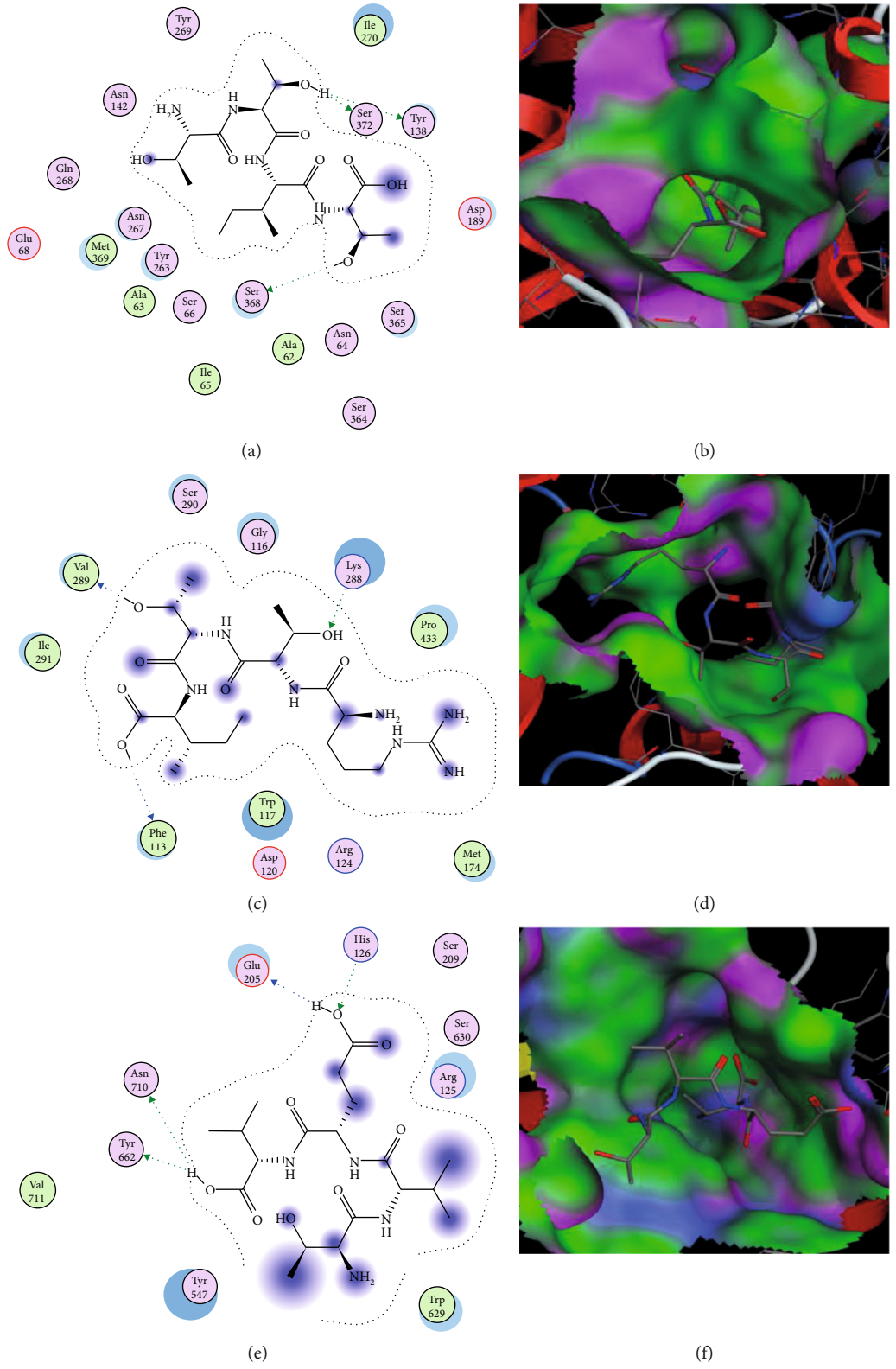

FIGURE 2: Interactions (on left) and binding patterns (on right) of best selected peptides. (a, b) Interactions and binding patterns of TTIT with SGLT1. (c, d) Interactions and binding pattern of RTTI with GLUT2. (e, f) Interaction and binding pattern of TVEV with DPP-IV, respectively.

Table 5: ADMET profiling of best selected peptides.

	SMCG	DECC	TTIT	RTTI	ARNL	TVEV
Absorption						
Blood-brain barrier	BBB+	BBB+	BBB+	BBB+	BBB+	BBB+
Human intestinal absorption	HIA-	HIA-	HIA-	HIA-	HIA+	HIA-
Caco-2 permeability	Caco-2-	Caco-2-	Caco-2-	Caco-2-	Caco-2-	Caco-2-
P-Glycoprotein substrate	Substrate	Nonsubstrate	Nonsubstrate	Nonsubstrate	Substrate	Nonsubstrate
P-Glycoprotein inhibitor	Noninhibitor	Noninhibitor	Noninhibitor	Noninhibitor	Noninhibitor	Noninhibitor
Renal organic Cation transporter	Noninhibitor	Noninhibitor	Noninhibitor	Noninhibitor	Noninhibitor	Noninhibitor
Metabolism						
CYP3A4 substrate	Substrate	Nonsubstrate	Nonsubstrate	Nonsubstrate	Substrate	Nonsubstrate
CYP2C9 substrate	Nonsubstrate	Nonsubstrate	Nonsubstrate	Nonsubstrate	Substrate	Nonsubstrate
CYP2D6 substrate	Nonsubstrate	Nonsubstrate	Nonsubstrate	Nonsubstrate	Nonsubstrate	Nonsubstrate
CYP3A4 inhibition	Noninhibitor	Noninhibitor	Noninhibitor	Noninhibitor	Noninhibitor	Noninhibitor
CYP2C9 inhibition	Noninhibitor	Noninhibitor	Noninhibitor	Noninhibitor	Noninhibitor	Noninhibitor
CYP2C19 inhibition	Noninhibitor	Noninhibitor	Noninhibitor	Noninhibitor	Noninhibitor	Noninhibitor
CYP2D6 inhibition	Noninhibitor	Noninhibitor	Noninhibitor	Noninhibitor	Noninhibitor	Noninhibitor
CYP1A2 inhibition	Noninhibitor	Noninhibitor	Noninhibitor	Noninhibitor	Noninhibitor	Noninhibitor
Toxicity						
AMES toxicity	Non-AMES toxic	Non-AMES toxic	Non-AMES toxic	Non-AMES toxic	Non-AMES toxic	Non-AMES toxic
Carcinogens	Noncarcinogens	Noncarcinogens	Noncarcinogens	Noncarcinogens	Noncarcinogens	Noncarcinogens

violated one parameter of Lipinski's rule of five (Table 4). The structures of these six peptides are given in Figure 1. On the basis of Lipinski's rule, these peptides are expected for having reasonable oral bioavailability. The interactions and binding patterns of best peptides each against SGLT1 (i.e., TTIT), GLUT2 (i.e., RTTI), and DPP-IV (i.e., TVEV) have been shown in Figure 2.

For further validations of drug-like behavior of selected ligands, all six ligands were subjected to admetSAR server for assessment of five parameters of ADMET profiling (absorption, distribution, metabolism, excretion, and toxicity). From the results, it has been revealed that all the selected peptides are non-AMES toxic and noncarcinogens (Table 5). The overall results of ADMET drug scanning of these lead ligands were tolerable, and these peptides could be accepted as efficient drug candidates against selected receptor proteins.

4. Discussion

Diabetes mellitus is a heterogeneous group of diseases characterized by irregular glucose homeostasis and chronic hyperglycemia due to flaw in insulin secretion and activity [23]. Type 1 diabetes mellitus (insulin dependent) and type 2 diabetes mellitus (noninsulin dependent) are referred as two peculiar forms of diabetes. Type 1 or insulin dependent DM is characterized by total destruction of pancreatic β-cells and shutting down the glucose metabolism. The type 2 or noninsulin-dependent diabetes is reported as the most common form due to abnormal insulin secretion and insulin resistance. In type 2 DM, the continuous exposure of body to glucose causes the severity of the disease leading to neurological, gastrointestinal, renal, and cardiovascular syndromes [24]. A vast variety of natural compounds have been reported with medicinal perspectives for the treatment of various diseases [25]. In this study, tetra-, penta-, and hexapeptides (80 in total) were devised from the adMc1 protein of *Momordica charantia*, and their interactions with different receptor proteins that play role in glucose homeostasis were checked through the molecular docking approach. Molecular docking is an elaborative method to evaluate the best possibilities of ligand interactions against different targets for in silico drug designing [26].

The balancing of glucose homeostasis, maintenance of hyperglycemic state to normal level, and shutting of the enzymes that cause irregular glucose homeostasis are the possible ways to control diabetes. Over the past few years, many conventional drug therapies have been in practice but the outcomes are undesirable due to poor efficacy and different side-effects [27]. Thus, scientists are moving towards the use of natural bioactive compounds as antidiabetic agents. The extensive literature survey reveals a large set of targets such as DPP-IV, sodium glucose transporters (SGLTs), α-glucosidase, protein tyrosine phosphatase 1B (PTP1B), glucose transporters (GLUT), and G protein-coupled receptors [28–30].

In this study, DPP-IV, SGLT1, and GLUT2 have been listed as target receptor proteins due to their major roles in glucose homeostasis. DPP-IV is a serine exopeptidase that is associated with incretin deficiency in type 2 DM. Current combinational drug therapies include oral hypoglycemic

agents including metformin, komboglyze, janumet, and juvisync but these drugs result in unsustainable outcomes. Therefore, the need of new drugs with more efficacies and less side-effects is urgent in order to treat DM [27]. Citrus flavonoids were taken as ligands against different target proteins (e.g., glycogen synthase kinases 3β, DPP-IV, and glucokinase) [29]. Shen and Lu [29] have reported that the binding pocket of DPP-IV contains Glu205, Glu206, Tyr662, and Ser209 as active amino acids. In this study, Glu205, Ser209, and Tyr662 were also found as active amino acids as they exhibited strong interactions with DPPI-IV with energy validations.

Sodium glucose transporter-1 (SGLT1) is a glucose transporter expressed at the striated border of intestine. In diabetic patients, the overwhelming glucose concentration might be controlled by SGLT1 inhibition [31]. The 3D structure of human SGLT1 was not available; therefore, the 3D structure of SGLT2 from *Vibrio parahaemolyticus* was taken as a template in this study for the homology modeling of human SGLT1. Both isoforms of sodium glucose transporters share about 60% sequence identity and are highly expressed in S1 segment of border brush membrane [31]. In previous studies, Ser372, Ser50, Asn51, Gly53, Ser54, Gly55, His56, Gln271, Ser368, Ser369, Gln433, and Ser368 of SGLTs have been reported as polar active amino acids [32]. In current study, Ser372 and Ser368 were also found among the interacting residues of SGLT1 that showed strong interactions with the selected ligands.

On the bases of drug-likeness, only 6 peptides have been shortlisted (i.e., SMCG, DECC, TTIT, RTTI, ARNL, and TVEV) followed by Lipinski's rule of five. The remaining 24 ligands violated two or more parameters of Lipinski rule of five. The further assessment of these ligands included ADMET drug scanning to prognosticate the probability of success and failure of potential drug candidates. All the selected ligands passed the criteria of drugability. The efforts and purpose of this study were to target the proteins that play roles in glucose homeostasis to overcome the diabetes mellitus. The mutational changes in certain receptor proteins which are involved in the metabolism and regulation of glucose lead towards severe consequences including the onset of prediabetes and diabetes mellitus. Diabetes mellitus is a group of chronic metabolic diseases that leads towards the onset of many other leading disorders. In the market, many hypoglycemic agents have been in practice to cure diabetes and hyperglycemia but the unsustainable results of these agents lead towards their failure. So, the current need of time is to explore the insulin-like peptides from natural sources with maximum potential and less side-effects.

5. Conclusion

The current study offers conversational and comprehensive computational study towards the discovery of insulin-like hit ligands, screened from ready-to-dock library of peptides as ligand molecules against the DPP-IV, SGLT1, and GLUT2 receptor proteins. In this study, 80 highly conserved tetra-, penta-, and hexapeptides as leading ligands were devised from the adMc1 protein of *Momordica charantia*, and the in silico approach was applied to check their molecular dynamic validations and ultimately, to explore their antidiabetic potentials. The peptides SMCG, DECC, TTIT, RTTI, ARNL, and TVEV provided valuable results in drug assessment and ADMET drug scanning. Among the 30 ligands selected on the basis of molecular docking studies, these six tetrapeptides passed the drug assessment tests with great ability to be recognized as drug candidates with potential of inhibiting the DPP-IV, SGLT1, and GLUT2 receptor proteins.

Data Availability

The data used to support the findings of this study are available from the corresponding author upon request.

Conflicts of Interest

The authors declares that they have no conflicts of interest.

Acknowledgments

The authors would like to gratefully acknowledge the Department of Biochemistry, Government College University Faisalabad for providing space and facilities to accomplish this study.

References

[1] A. Yasmin, S. A. Bukhari, M. K. Zahoor, G. Mustafa, and A. Rasul, "Screening of novel phytochemicals as secreted frizzled-related protein 4 inhibitors: an early stage biomarker of type 2 diabetes," *Pakistan Journal of Pharmaceutical Sciences*, vol. 33, no. 3, pp. 1245–1250, 2020.

[2] S. Duddela, P. Nataraj Sekhar, G. Padmavati, A. K. Banerjee, and U. Murty, "Probing the structure of human glucose transporter 2 and analysis of protein ligand interactions," *Medicinal Chemistry Research*, vol. 19, no. 8, article 9234, pp. 836–853, 2010.

[3] S. Q. Pantaleão, V. G. Maltarollo, S. C. Araujo, J. C. Gertrudes, and K. M. Honorio, "Molecular docking studies and 2D analyses of DPP-4 inhibitors as candidates in the treatment of diabetes," *Molecular BioSystems*, vol. 11, no. 11, pp. 3188–3193, 2015.

[4] N. D. Trang Nguyen and L. T. le, "Targeted proteins for diabetes drug design," *Advances in Natural Sciences: Nanoscience and Nanotechnology*, vol. 3, no. 1, article 013001, 2012.

[5] D. Röhrborn, N. Wronkowitz, and J. Eckel, "DPP4 in diabetes," *Frontiers in Immunology*, vol. 6, p. 386, 2015.

[6] D. Lamers, S. Famulla, N. Wronkowitz et al., "Dipeptidyl peptidase 4 is a novel adipokine potentially linking obesity to the metabolic syndrome," *Diabetes*, vol. 60, no. 7, pp. 1917–1925, 2011.

[7] C. F. Deacon, "Peptide degradation and the role of DPP-4 inhibitors in the treatment of type 2 diabetes," *Peptides*, vol. 100, pp. 150–157, 2018.

[8] S. Gupta and U. Sen, "More than just an enzyme: Dipeptidyl peptidase-4 (DPP-4) and its association with diabetic kidney remodelling," *Pharmacological Research*, vol. 147, article 104391, 2019.

[9] R. L. Dobbins, F. L. Greenway, L. Chen et al., "Selective sodium-dependent glucose transporter 1 inhibitors block glucose absorption and impair glucose-dependent insulinotropic peptide release," *American Journal of Physiology-Gastrointestinal and Liver Physiology*, vol. 308, no. 11, pp. G946–G954, 2015.

[10] M. Vani, N. Ritesh Siddhartha Reddy, and P. Uma Maheswari Devi, "In silico analysis for detection of glucose transport-2 inhibitors from seagrass," in *Advances in Computational and Bio-Engineering: Proceeding of the International Conference on Computational and Bio Engineering, 2019, Volume 1*, vol. 15 of Learning and Analytics in Intelligent Systems, , pp. 491–498, Springer, 2020.

[11] G. Mustafa, R. Arif, A. Atta, S. Sharif, and A. Jamil, "Bioactive compounds from medicinal plants and their importance in drug discovery in Pakistan," *Matrix Science Pharma*, vol. 1, no. 1, pp. 17–26, 2017.

[12] S. Sharif, M. Shahid, A. Atta, M. Abbas, and G. Mustafa, "Comparative evaluation of antioxidant and DNA protective potentials of fifteen selected medicinal plants native to Pakistan," *Oxidation Communications*, vol. 40, no. 2, pp. 657–674, 2017.

[13] S. A. Bukhari, M. Qasim, M. Masoud, H. Anwar, A. Waqas, and G. Mustafa, "Evaluation of medicinally important constituents of Cotoneaster afghanicus G. Klotz collected from baluchistan region of Pakistan," *Indian Journal of Pharmaceutical Sciences*, vol. 81, no. 2, pp. 259–265, 2019.

[14] L. Mojica, M. Berhow, and E. Gonzalez de Mejia, "Black bean anthocyanin-rich extracts as food colorants: physicochemical stability and antidiabetes potential," *Food Chemistry*, vol. 229, pp. 628–639, 2017.

[15] A. Mushtaq, T. M. Ansari, G. Mustafa, M. A. Shad, J. Cruz-Reyes, and A. Jamil, "Isolation and characterization of nprB, a novel protease from Streptomyces thermovulgaris," *Pakistan Journal of Pharmaceutical Sciences*, vol. 33, no. 5, pp. 2361–2369, 2020.

[16] B. Webb and A. Sali, "Comparative protein structure modeling using MODELLER," *Current protocols in bioinformatics*, vol. 54, no. 1, 2016.

[17] T. L. Bailey, M. Boden, F. A. Buske et al., "MEME SUITE: tools for motif discovery and searching," *Nucleic acids research*, vol. 37, no. Web Server, pp. W202–W208, 2009.

[18] A. Mushtaq, G. Mustafa, T. M. Ansari, M. A. Shad, J. Cruz-Reyes, and A. Jamil, "Antiviral activity of hexapeptides derived from conserved regions of bacterial proteases against HCV NS3 protease," *Pakistan Journal of Pharmaceutical Sciences*, vol. 34, no. 1, pp. 215–223, 2021.

[19] Z. Li, H. Wan, Y. Shi, and P. Ouyang, "Personal experience with four kinds of chemical structure drawing software: review on ChemDraw, ChemWindow, ISIS/draw, and ChemSketch," *Journal of Chemical Information and Computer Sciences*, vol. 44, no. 5, pp. 1886–1890, 2004.

[20] A. Daina, O. Michielin, and V. Zoete, "SwissADME: a free web tool to evaluate pharmacokinetics, drug-likeness and medicinal chemistry friendliness of small molecules," *Scientific Reports*, vol. 7, no. 1, pp. 1–13, 2017.

[21] F. Cheng, W. Li, Y. Zhou et al., *admetSAR: a comprehensive source and free tool for assessment of chemical ADMET properties*, ACS Publications, 2012.

[22] H. Meduru, Y.-T. Wang, J. J. Tsai, and Y.-C. Chen, "Finding a potential dipeptidyl peptidase-4 (DPP-4) inhibitor for type-2 diabetes treatment based on molecular docking, pharmacophore generation, and molecular dynamics simulation," *International journal of molecular sciences*, vol. 17, no. 6, p. 920, 2016.

[23] S. A. Bukhari, A. Yasmin, M. A. Zahoor, G. Mustafa, I. Sarfraz, and A. Rasul, "Secreted frizzled-related protein 4 and its implication in obesity and type-2 diabetes," *IUBMB Life*, vol. 71, no. 11, pp. 1701–1710, 2019.

[24] M. Kumar and D. Verma, "Antidiabetic and antihyperlipidemic effect of Morinda citrofolia and Coccinia indica in alloxan induced diabetic rats," *Pharmacology*, vol. 2, pp. 307–311, 2011.

[25] G. Mustafa, S. Ahmed, N. Ahmed, and A. Jamil, "Phytochemical and antibacterial activity of some unexplored medicinal plants of Cholistan desert," *Pakistan Journal of Botany*, vol. 48, no. 5, pp. 2057–2062, 2016.

[26] G. Mustafa, M. Majid, A. Ghaffar, M. Yameen, H. A. Samad, and H. S. Mahrosh, "Screening and molecular docking of selected phytochemicals against NS5B polymerase of hepatitis C virus," *Pakistan Journal of Pharmaceutical Sciences*, vol. 33, no. 5, pp. 2317–2322, 2020.

[27] N. Kerru, A. Singh-Pillay, P. Awolade, and P. Singh, "Current anti-diabetic agents and their molecular targets: a review," *European Journal of Medicinal Chemistry*, vol. 152, pp. 436–488, 2018.

[28] R. Balamurugan, A. Stalin, and S. Ignacimuthu, "Molecular docking of γ-sitosterol with some targets related to diabetes," *European Journal of Medicinal Chemistry*, vol. 47, no. 1, pp. 38–43, 2012.

[29] W. Shen and Y. H. Lu, "Molecular docking of citrus flavonoids with some targets related to diabetes," *Bangladesh Journal of Pharmacology*, vol. 8, no. 2, pp. 156–170, 2013.

[30] P. Kaushik, S. Lal Khokra, A. Rana, and D. Kaushik, "Pharmacophore modeling and molecular docking studies on Pinus roxburghii as a target for diabetes mellitus," *Advances in bioinformatics*, vol. 2014, Article ID 903246, 8 pages, 2014.

[31] N. Harada and N. Inagaki, "Role of sodium-glucose transporters in glucose uptake of the intestine and kidney," *Journal of diabetes investigation*, vol. 3, no. 4, pp. 352-353, 2012.

[32] R. Feng, L. Dong, L. Wang, Y. Xu, H. Lu, and J. Zhang, "Development of sodium glucose co-transporter 2 (SGLT2) inhibitors with novel structure by molecular docking and dynamics simulation," *Journal of Molecular Modeling*, vol. 25, no. 6, article 4067, pp. 1–11, 2019.